Computational studies of relativistic effects on NMR shieldings using perturbative approaches for spin-orbit coupling

---

Master Thesis

to obtain the Master's degree
from the Faculty of Mathematics and Natural Scince
of the Heinrich-Heine University Düsseldorf
submitted by

Hannah Hagemann

from Hilden

October 26, 2020

Heinrich-Heine Universität in cooperation with the Max-Plack-Insititut für Kohlenforschung

Institut für Theoretische Chemie und Computerchemie
Mathematisch Naturwissenschaftliche Fakultät
der Heinrich-Heine Univeristät

Molekulare Theorie und Spektroskopie
Max-Planck-Institut für Kohlenforschung
Mülheim an der Ruhr

Supervisor: Prof. Dr. Alexander A. Auer

Evaluator : Prof. Dr. Christel M. Marian

Declaration of Independence

I affirm in lieu of oath that I have independently written the present work and have not used any other sources and aids than those indicated. I have not submitted this paper to any other examination office or person in the context of an examination.

Date	Hannah Hagemann

Abstract

Quantum chemistry deals, inter alia, with the determination of NMR parameters for prediction or explanation of physical effects. Most methods use non-relativistic approaches, which lead to errors. Those errors occur not just for heavy elements, but also for the NMR parameters of light nuclei close to heavy elements. The influence of such effects is called, e.g. SO-HALA effect.

In this thesis, NMR parameters of light nuclei in the presence of heavy nuclei are calculated. Different quantum chemistry packages, approaches and implementations are used and compared. For testing, benchmark molecules are assembled from the p-block elements. Central point of this work is the validation of available *ORCA* algorithms. *ORCA*[1] is a modern quantum chemistry package and developed especially for spectroscopic applications. It is found that the ZORA implementation in *ORCA* shows the same results as the ZORA implementation in *NWChem*. A pilot implementation RIZORA provides the same results while eliminating the grid dependency of ZORA. However, a a-posteriori spin-orbit (SO) approach in *ORCA* does not give the same results as two- or four-component calculations in *DIRAC*. Since spin-orbit coupling is essential for the description of the SO-HALA effect, the use of the BSS Hamiltonian in *DIRAC* currently offers a good solution.

In this work, NMR shielding constants of bismuth-aryl compounds with halides are investigated, because NMR experimental spectra showed an Inverse Halogen Dependence (IHD) of these compounds. This means that the chemical shift of the *ortho* proton to the bismuth atom increases with increasing nuclear charge of the halides. This effect has not yet been ex-

plained or simulated in the literature. It is surprisingly found that the IHD is not caused by a HALA effect, while NMR parameters are drastically effected by geometry changes.

Zusammenfassung

Ein Gebiet der Quantenchemie beschäftigt sich mit NMR Parametern zur gezielten Vohersage oder Erklärung von auftretenden physikalischen Effekten. Meist werden dafür nicht-relativistische Ansätze verwendet, welches nicht nur zu Fehlern bei schweren Atomen, sondern auch bei leichten Atomen in der Nähe von schweren Kernen führen kann. Der SO-HALA Effekt beschreibt beispielweise den Einfluss eines schweren Kerns auf die Abschirmung eines leichten Kerns.

In dieser Arbeit wurden NMR Parameter von leichten Kernen in der Anwesenheit schwerer Kerne berechnet. Es wurden verschiedene Quantenchemie Programme, Ansätze und Implementierungen verwendet und verglichen, wofür Benachmark-Moleküle aus p-Block Elementen zusammengestellt wurden. Der zentrale Punkt in dieser Arbeit war die Validierung von verfügbaren *ORCA* Algorithmen. *ORCA*[1] ist ein modernes Quantchemisches Programmpaket, welches speziell für Spektroskopiker entwickelt wurde. Es konnte gezeigt werden, dass die ZORA Implementierung in *ORCA* die gleichen skalar-relativistischen Korrekturen wie die ZORA Implementierung in *NWChem* liefert. In *ORCA* zeigte eine RIZORA Pilot-Implementierung die gleichen Ergebnisse wie die *ORCA* ZORA Implementierung, zusätlich kann mit RIZORA die Grid-Abhängigkeit des ZORA Hamiltonian verringert bzw. aufeghoben werden. Für die Spin-Bahn-Kopplung wurde ein neuer a-posteriori Ansatz in *ORCA* getestet, indem Ergebnisse mit zwei- und vier-Komponentigen *DIRAC* Rechnungen verglichen wurden. Jedoch konnten keine ähnlichen und vergleichbaren Ergebnisse zu den *DIRAC* Rechnungen mit dem a-posteriori Ansatz erzielt werden. Da für die Beschreibung des SO-HALA Effektes die Spin-Bahn-Kopplung unabdingbar ist,

erwies sich von den getesteten Ansätzen die Verwendung des BSS Hamiltonian in *DIRAC* als aktuell beste Lösung.

In dieser Arbeit wurden NMR-Verschiebungen von Bismut-Aryl-Verbindungen mit Halogeniden untersucht, da experimentelle NMR-Spektren dieser Verbindungen einen Inversen Halogen Effekt (IHD) aufwiesen. IHD bedeutet in diesem Fall, dass die chemische Verschiebung des zum Bismutatom *ortho*-ständigen Protons mit steigender Kernladungszahl des benachbarten Halogenids weiter im Tieffeld liegt. Dieser auftretende Effekt konnte in der Literatur nicht erklärt werden. Überraschenderweise wurde in dieser Arbeit herrausgefunden, dass der IHD nicht durch einen HALA Effekt zu erklären ist, sondern die NMR Parameter stark durch eine Geometrie-Änderung beeinflusst werden.

Contents

List of Tables

List of Figures

List of abbreviations

ADF	Amsterdam Density Functional	45
AMFI	Atomic Mean-Field Integral	32
AO	atomic orbital	24
c.c.	complex conjugated	7
CPHF	coupled-perturbed Hartree-Fock	17
DFT	Density functional theory	VIII
DKH	Douglas-Kroll-Hess	1
ECP	effective core potential	42
e.g.	*exempli gratia* for example	
EPR	electron paramagnetic resonance	1
FC	Fermi-contact	34
FORA	first-order regular approximation	31
GGA	generalized gradient approximation	15
GIAO	gauge-including atomic orbitals	1
HALA	heavy-atom effects on the shielding of light atoms	1
HF	Hartree-Fock	5
IHD	inverse halogen dependence	2
IORA	infinite order regular approximation	1
KS	Kohn-Sham	14
LCAO	linear combination of atomic orbitals	9

1. Introduction

ORCA[1] is a modern quantum chemistry package used not only by theoreticians but also by spectroscopists. Since it is mainly used for simulations in spectroscopy and the development is motivated by the application in bioinorganic chemistry, transition metals or heavier elements are often important. Relativistic effects are not negligible for heavy elements. They can be approximated by combining a scalar-relativistic calculation with a spin-orbit coupling (SOC) calculation. Especially for the not so heavy atoms, e.g. for the 4th period, a four-component approach is not always necessary to achieve good results.

In *ORCA*, relativistic Hamiltonians such as Douglas-Kroll-Hess (DKH), zeroth-order regular approximation (ZORA), infinite order regular approximation (IORA) and other Hamiltonians are already available. Thus it is possible to include scalar relativistic effects also in property calculations, simulating e.g. nuclear magnetic resonance (NMR) or electron paramagnetic resonance (EPR) experiments. Already available are SOC Hamiltonians for EPR calculations, but those are not yet available for NMR property calculations.

Experimental NMR spectra are usually recorded for ^{1}H, ^{13}C, ^{15}N, ^{19}F and ^{31}P nuclei, i.e. rather light elements. It could be assumed that SOC effects are uninteresting in NMR calculations. However, heavy-atom effects on the shielding of light atoms (HALA) can occur due to the vicinity of a heavy atom. Therefore it is important to consider SOC of such molecules to predict NMR spectra or coupling constants correctly. Therefore, a new feature was implemented in *ORCA* to consider SOC for NMR chemical shifts (and coupling constants) for the gauge-including atomic orbitals (GIAO) algo-

rithms. The use in MP2, DH-DFT and DLPNO algorithms is currently in progress.

One goal of this thesis was to test the new feature in a series of systematic calculations. Comparisons of combination with existing algorithms in *ORCA* should show which algorithms and approaches are accurate for the description of the NMR shift of light nuclei in heavy element compounds. Furthermore it was investigated whether the already implemented ZORA Hamiltonian for NMR calculations is sufficient for the calculation of scalar-relativistic corrections. A resolution-of-identity (RI) approximated ZORA version was tested to avoid possible grid dependencies.

A possible application of SOC in NMR is the prediction of halogen dependencies in bismuth compounds. Mehring *et al.*[2] experimentally showed an inverse halogen dependence (IHD) of the *ortho* proton to the bismuth atom in some bismuth-aryl compounds. The experimental NMR study was supported by theoretical electronic structure calculations carried out on a non-relativistic and scalar-relativistic basis. In this work additional calculations including SOC effects should be carried out in order to investigate the possible HALA effect.

2. Theory

The main goal of non-relativistic quantum chemistry is to find accurate solutions of the time-independent Schrödinger equation (2.1), which is an eigenvalue equation. The latter can be solved exactly for the simplest case[3], one electron moving in a simple external potential.

$$\mathcal{H}\left|\Psi\right\rangle = \mathcal{E}\left|\Psi\right\rangle \tag{2.1}$$

Thereby, the Hermitian operator $\mathcal{H}$, called the Hamiltonian, acts on a wave function Ψ to obtain the energy $\mathcal{E}$.[3] The Hamiltonian for a system of nuclei and electrons can be written in atomic units for N electrons and M nuclei as in 2.2.

$$\begin{aligned}\mathcal{H} = &-\sum_{i=1}^{N}\frac{1}{2}\nabla_i^2 - \sum_{A=1}^{M}\frac{1}{M_A}\nabla_A^2 \\ &-\sum_{i=1}^{N}\sum_{A=1}^{M}\frac{Z_A}{r_{iA}} + \sum_{i=1}^{N}\sum_{j>i}^{N}\frac{1}{r_{ij}} + \sum_{A=1}^{M}\sum_{B>A}^{M}\frac{Z_A Z_B}{R_{AB}} \\ = &\ \mathcal{T}_e + \mathcal{T}_N + \mathcal{V}_{Ke} + \mathcal{V}_{ee} + \mathcal{V}_{KK}\end{aligned} \tag{2.2}$$

The first term denotes the kinetic energy of the electrons $\mathcal{T}_e$, the second the kinetic energy of the nuclei $\mathcal{T}_K$, the third term the attractive Coulomb interaction between nuclei and electrons $\mathcal{V}_{Ke}$ and the last two terms denote the repulsion interaction between electrons $\mathcal{V}_{ee}$ and between nuclei $\mathcal{V}_{KK}$, respectively.[3] ∇ denotes a further operator representing the derivative with respect to the coordinates of the electrons or nuclei, M_K is the mass of the nuclei K and Z_K the associated charge. r_{iA} denotes the distance between the electron i and the nucleus A and R_{AB} the distance between the nuclei A and B. The wave function Ψ contains coordinates of the electrons

and the nuclei (2.3).

$$\Psi = \Psi(\{vecr_i\}; \{\vec{R}_A\}) \tag{2.3}$$

As a central approximation, the Born-Oppenheimer approximation, is used to solve the Schrödinger equation separately for nuclei and electrons. This is due to the fact that protons are much heavier that electrons and protons consequently have a lower speed of motion.[4] Therefore the kinetic energy of the electrons $\mathcal{T}_e$ and nuclei $\mathcal{T}_K$ (2.2) can be separated and the nuclear repulsion $\mathcal{V}_{KK}$ term can be added later to the electronic energy. This allows to write the electronic Hamiltonian in the following form

$$\mathcal{H}_{elec} = \mathcal{T}_e + \mathcal{V}_{Ke} + \mathcal{V}_{ee} \tag{2.4}$$

and to split the wave function into an electronic Ψ_{elec} and a nuclear wave function Ψ_{nuc} (2.5).

$$\Psi = \Psi_{elec}(\{\vec{r}_i\}; \{\vec{R}_A\})\Psi_{nuc}(\{\vec{R}_A\}) \tag{2.5}$$

The electronic wave function depends on the electronic coordinates and parametrically on the nuclear coordinates.

An electronic Schrödinger equation (2.6) can be established.

$$\mathcal{H}_{elec} \left|\Psi_{elec}\right\rangle = \mathcal{E}_{elec} \left|\Psi_{elec}\right\rangle \tag{2.6}$$

The electronic energy depends, like the electronic wave function, parametrically on the nuclear coordinates (2.7).

$$\mathcal{E}_{elec} = \mathcal{E}_{elec}(\{R_A\}) \tag{2.7}$$

Note that the total energy $\mathcal{E}_{total}$ is composed of the electronic energy $\mathcal{E}_{elec}$

and the nuclear repulsion energy.[3]

$$\mathcal{E}_{total} = \mathcal{E}_{elec} + \sum_{A=1}^{M} \sum_{B>A}^{M} \frac{Z_A Z_B}{R_{AB}} \tag{2.8}$$

The first two sections will present common approaches used to find approximate solutions to 2.6.

2.1. Hartree-Fock Theory

Approximate solutions of the electronic Schrödinger equation (2.6) for a many-electron problem can be found with the Hartree-Fock (HF) approximation. This approach uses the variation principle, which states that the expectation value $\mathcal{E}$ of the Hamiltonian and a trial wave funtion $\tilde{\Psi}$ (2.9) is the upper limit to the exact ground state energy $\mathcal{E}_0$ (2.10).[3]

$$\langle \tilde{\Psi} | \mathcal{H} | \tilde{\Psi} \rangle = \mathcal{E} \tag{2.9}$$

$$\langle \tilde{\Psi} | \mathcal{H} | \tilde{\Psi} \rangle \geq \mathcal{E}_0 \tag{2.10}$$

The trial wave function can, for example, be expanded in an infinite basis $\{\chi_i\}$ (2.11) and the expansion is therefore exact.

$$\tilde{\Psi} = \sum_{i=1}^{\infty} c_i \chi_i \tag{2.11}$$

The parameters c_i are varied until the expectation value reaches a minimum.

In practice, the total wave function is approximated with by Slater de-

terminant ξ.

$$\xi = \frac{1}{\sqrt{n!}} \begin{vmatrix} \phi_i(\vec{x}_1) & \phi_i(\vec{x}_2) & \dots & \phi_i(\vec{x}_2) \\ \phi_j(\vec{x}_1) & \phi_j(\vec{x}_2) & \dots & \phi_j(\vec{x}_2) \\ \vdots & \vdots & \ddots & \vdots \\ \phi_n(\vec{x}_1) & \phi_n(\vec{x}_2) & \dots & \phi_n(\vec{x}_2) \end{vmatrix} \tag{2.12}$$

Thus the many-electron wave function is represented as an antisymmetric linear combination of N one-electron spin functions ϕ_i. Note that the degrees of freedom of the spin orbitals (2.13) are the spatial coordinates r and the spin ω of the electron.

$$\vec{x} = \{\vec{r}, \omega\} \tag{2.13}$$

The Slater determinant changes the sign by electron exchange which fulfills the Pauli exclusion principle stating that "it is impossible for two electrons [...] to have the same values of the four quantum numbers [...]"[5]. A second important idea is that the orbitals are chosen to be orthonormal.

$$\langle \phi_i | \phi_j \rangle = \delta_{ij} \tag{2.14}$$

The Schrödinger equation to be solved with a Slater determinant can be written as 2.15.

$$\mathcal{H} \left| \xi \right\rangle = \mathcal{E} \left| \xi \right\rangle \tag{2.15}$$

Minimizing of the energy expectation value $\mathcal{E}$ of a closed-shell Slater determinant requires the condition 2.16.

$$\delta \mathcal{E} = 0 \tag{2.16}$$

The approach to minimize the expectation value is to use the method of Langrange's undetermined multipliers. A function is constructed contain-

ing the boundary condition 2.14. Therefore, the boundary condition is set to zero and added to the expectation value with a further variable, called multiplier λ. Note that the physical meaning of the multipliers are the orbital energies. The stationary point of the expectation value is determined via the stationary point of the Lagrange's function 2.17

$$\delta\mathcal{L}(c_1, c_2, ..., c_n, \lambda) = \delta\Big(\mathcal{E} - \sum_{i=i}^{n/2}\sum_{j=1}^{n/2} \lambda_{ij}\big(\langle\phi_i|\phi_j\rangle - \delta_{ij}\big)\Big) = 0 \tag{2.17}$$

λ is a set of Lagrange multipliers. Inserting the Hamiltonian 2.18 into 2.17 and collecting terms yields 2.19.

$$\mathcal{H} = \widehat{h}_1 + \widehat{g}_{12} \tag{2.18}$$

$$\begin{aligned}\delta\mathcal{L}(c_1, c_2, ..., c_n, \lambda) &= 2\sum_{i}^{n/2}\langle\delta\phi_i|\widehat{h}_1|\phi_i\rangle + \sum_{i}^{n/2}\sum_{j}^{n/2}\Big(4\langle\delta\phi_i\phi_j|\widehat{g}_{12}|\phi_i\phi_j\rangle \\ &\quad - 2\langle\delta\phi_i\phi_j|\widehat{g}_{12}|\phi_j\phi_i\rangle - \lambda\langle\delta\phi_i|\phi_j\rangle\Big) \\ &\quad + \text{c.c.} \\ &= 0\end{aligned} \tag{2.19}$$

The Hamiltonian is split into two parts. The first one $\widehat{h}_1$ contains the one-electron part, the kinetic energy and the nuclear-electron interaction. g_{12} denotes the two-electron interaction. The resulting expression contains the one-electron integral, the Coulomb- and the exchange integral, the added 'zero' (2.14) and the complex conjugated (c.c.).

By introducing a Coulomb (2.20) and exchange operator (2.21) 2.19 can

be written as 2.22.

$$\mathcal{J}_j(1)\phi_i(1) = \Big(\int dx_2 \phi_j^*(2)\hat{r}_{12}^{-1}\phi_j(2)\Big)\phi_i(1) \tag{2.20}$$

$$\mathcal{K}_j(1)\phi_i(1) = \Big(\int dx_2 \phi_j^*(2)\hat{r}_{12}^{-1}\phi_i(2)\Big)\phi_j(1) \tag{2.21}$$

$$\delta\mathcal{L} = 2\sum_{i=1}^{n/2} \langle\delta\phi_i|\Big[\hat{h}_1 + \sum_{j=1}^{n/2}(2\mathcal{J}_i - \mathcal{K}_j)|\phi_i - \sum_{j=1}^{n/2}\lambda_{ij}\phi_j\rangle\Big] + \text{c.c.} = 0 \tag{2.22}$$

To fulfill 2.22 the square brackets must be set to zero, which is the HF equation (2.24) with the Fock operator $\hat{f}_1$ (2.23).

$$\hat{f}_1 = \hat{h}_1 + \sum_{j=1}^{n/2}\Big(2\mathcal{J}_j(1) - \mathcal{K}_j(1)\Big) \tag{2.23}$$

$$\hat{f}_1\,|\phi_i(1)\rangle = \sum_{j=1}^{n/2}\frac{1}{2}\lambda_{ij}\,|\phi_j(2)\rangle \tag{2.24}$$

The left and right side contain different orbitals so here still off-diagonal terms are coupled integro-differentially and cannot be solved directly. Since the Fock operator depends intrinsically on the solutions of the orbitals it can be solved iteratively in a self-consistent field (SCF) procedure and forms a pseudo-eigenvalue equation.

Diagonalization of the Lagrange multipliers ((2.25) with a transformation matrix $\mathbf{X}$ yields the eigenvalue matrix $\mathbf{E}$.

$$\mathbf{X}^\dagger\frac{1}{2}\lambda\mathbf{X} = \mathbf{E} \tag{2.25}$$

Inserting the eigenvalue matrix $\mathbf{E}$ into the HF equation (2.24) and multiplying with $\mathbf{X}$ from the right side (2.26) yields the canonical closed-shell HF equation in matrix notation (2.27). Note that no spin-adaption has been performed, the closed shell is defined by the total spin, which is zero

and can therefore be neglected.

$$\hat{f}\phi\mathbf{X} = \phi\mathbf{X}\mathbf{X}^{\dagger}\frac{1}{2}\lambda\mathbf{X} \tag{2.26}$$

$$\hat{f}\phi' = \phi'\mathbf{E} \tag{2.27}$$

$\mathcal{J}$ and $\mathcal{K}$ contain the orbitals ϕ, but not the transformation matrix-multiplied orbitals phi'.

So far no statement about the orbitals has been made. The solution strategy is using the linear combination of atomic orbitals (LCAO) approach in which the molecular orbitals (MOs) ϕ_j are expanded in a finite basis of K known and fixed atomic orbitals (AOs) χ with variable molecular coefficients $c_{\mu j}$ (2.28). The coefficients are varied to solve the Fock equation (2.24).

$$\phi_j = \sum_{\mu=1}^{K} c_{\mu j}\chi_\mu \tag{2.28}$$

Note that the finite expansion is an approximation and must be due to to computational costs. This expansion turns the canonical HF equation (2.27) into 2.29.

$$\hat{f}_1 \sum_{\mu=1}^{K} c_{\mu j}\chi_\mu(1) = \epsilon_j \sum_{\mu=1}^{K} c_{\mu j}\chi_\mu(1) \tag{2.29}$$

Multiplying 2.29 with χ_μ^* from the left and integrating over $d\vec{r}_1$ yields the canonical Roothaan-Hall equation (2.30).

$$\sum_{\mu=1}^{K} \int d\vec{r}_1 c_{\mu j}\chi_\mu^* \hat{f}_1 \chi_\mu = \epsilon_j \sum_{\mu=1}^{K} \int d\vec{r}_1 c_{\mu j}\chi_\mu^* \chi_\mu \tag{2.30}$$

In matrix notation the coefficients can be collected into a matrix $\mathbf{C}$. Note that the AOs at different centers are not orthonormal, so an overlap matrix $\mathbf{S}$ is introduced.

$$S_{\mu\nu} = \int d\vec{r}_1 \chi_\mu \chi_\nu \tag{2.31}$$

The definition of the Fock matrix **F**

$$\begin{aligned} F_{\mu\nu} &= \int d\vec{r}_1 \chi_\mu^* \hat{f}_1 \chi_\nu \\ &= \int d\vec{r}_1 \chi_\mu^* \hat{h}_1 \chi_\nu + \sum_{\alpha=1}^{n/2} \int d\vec{r}_1 \chi_\mu^* \Big[2\mathcal{J}_\alpha - \mathcal{K}_\alpha \Big] \chi_\nu \\ &= h_{\mu\nu}^{Core} + G_{\mu\nu} \end{aligned} \tag{2.32}$$

contains an one-electron integral $h_{\mu\nu}^{Core}$ of the $\hat{h}_1$ operator, which has to be calculated once in the later described SCF procedure (does not depend on the coefficients), and two electron part $G_{\mu\nu}$ of the Coulomb and exchange operator. With these definitions the solvable Roothaan-Hall equation for a closed-shell system can be written as 2.33 or in matrix notation (2.34).

$$\sum_\mu F_{\mu\nu} c_{\mu j} = \epsilon_j \sum_\mu S_{\mu\nu} c_{\mu j} \tag{2.33}$$

$$\mathbf{FC} = \mathbf{SCE} \tag{2.34}$$

$G_{\mu\nu}$ of the Fock matrix (2.35) contains the Coulomb and exchange operator. This can be transformed and the resulting expression containing the density matrix in the form of 2.36, the resulting expression can be written

as in 2.37.

$$
\begin{aligned}
G_{\mu\nu} &= \sum_{j=1}^{n/2} 2 \int d\vec{r}_1 d\vec{r}_2 \chi_\mu^*(1) \underbrace{\sum_\lambda c_{\lambda j}^* \chi_\lambda^*(2) \hat{r}_{12}^{-1} \sum_\sigma c_{\sigma j} \chi_\sigma(2)}_{\text{Coulomb operator}} \chi_\nu(1) \\
&\quad \sum_{j=1}^{n/2} \int d\vec{r}_1 d\vec{r}_2 \chi_\mu^*(1) \underbrace{\sum_\lambda c_{\lambda j}^* \chi_\lambda^*(2) \hat{r}_{12}^{-1} \sum_\sigma c_{\sigma j} \chi_\nu(2)}_{\text{exchange operator}} \chi_\sigma(1) \\
&= \sum_{j=1}^{n/2} \sum_\lambda \sum_\sigma c_{\sigma j} c_{\lambda j}^* 2 \int d\vec{r}_1 d\vec{r}_2 \chi_\mu^* \chi_\lambda^* \hat{r}_{12}^{-1} \chi_\sigma \chi_\nu \\
&\quad - \sum_{j=1}^{n/2} \sum_\lambda \sum_\sigma c_{\sigma j} c_{\lambda j}^* \int d\vec{r}_1 d\vec{r}_2 \chi_\mu^* \chi_\lambda^* \hat{r}_{12}^{-1} \chi_\nu \chi_\sigma
\end{aligned}
\tag{2.35}
$$

$$
\text{with } P_{\lambda\sigma} = 2 \sum_{j=1}^{n/2} c_{\sigma j} c_{\lambda j}^* \tag{2.36}
$$

$$
G_{\mu\nu} = \sum_\lambda \sum_\sigma P_{\lambda\sigma} \Big[(\mu\nu|\lambda\sigma) - \frac{1}{2} (\mu\sigma|\lambda\nu) \Big] \tag{2.37}
$$

Because $\mathbf{S}$ is not a unit matrix the Roothaan-Hall equation (2.33) is to be solved as a nonorthogonal matrix eigenvalue equation. This can be transformed into usual matrix eigenvalue equation by a matrix transformation (2.38) of the overlap matrix $\mathbf{S}$ into a unit matrix $\mathbf{1}$.

$$
\mathbf{X}^\dagger \mathbf{S} \mathbf{X} = \mathbf{1} \tag{2.38}
$$

Multiplying from the left with $\mathbf{X}^\dagger$ and inserting $\mathbf{X}\mathbf{X}^\dagger$ into the Roothaan-Hall equation (2.33) the Fock matrix $\mathbf{F}$, coefficient matrix $\mathbf{C}$ are transformed (marks) and the overlap matrix is eliminated.

$$
\mathbf{F}' = \mathbf{X}^\dagger \mathbf{F} \mathbf{X} \quad \text{and} \quad \mathbf{C}' = \mathbf{X}^\dagger \mathbf{C} \tag{2.39}
$$

$$
\begin{aligned}
\mathbf{X}^\dagger \mathbf{F} \mathbf{X} \mathbf{X}^\dagger \mathbf{C} &= \mathbf{X}^\dagger \mathbf{S} \mathbf{X} \mathbf{X}^\dagger \mathbf{C} \mathbf{E} \\
\mathbf{F}' \mathbf{C}' &= \mathbf{C}' \mathbf{E}
\end{aligned}
\tag{2.40}
$$

This yields an orthogonal eigenvalue equation.

The whole SCF procedure is performed by the following steps[3]:

1. Specification of a molecule and a basis set $\{\chi_\mu\}$
2. Calculation of $S_{\mu\nu}$, $H^{core}_{\mu\nu}$ and $(\mu\nu|\lambda\sigma) - \frac{1}{2}(\mu\sigma|\lambda\nu)$ of the $\mathbf{G}$ matrix
3. Diagonalization of the overlap matrix $\mathbf{S}$ to obtain the transformation matrix $\mathbf{X}$
4. Guess for the density matrix $\mathbf{P}$
5. Obtaining the $\mathbf{G}$ matrix from the density matrix $\mathbf{P}$ and the two electron integrals from step 2
6. Collecting $\mathbf{H}^{core}$ and $\mathbf{G}$ matrices for the Fock matrix $\mathbf{F} = \mathbf{H}^{core} + \mathbf{G}$
7. Transformation of the Fock matrix $\mathbf{F}'$ with the obtained $\mathbf{X}$ matrix from step 3
8. Diagonalization of $\mathbf{F}'$ and obtaining $\mathbf{C}'$ and $\mathbf{E}$
9. Calculation of the coefficients from $\mathbf{C} = \mathbf{X}\mathbf{C}'$
10. Building of a new density matrix $\mathbf{P}$ by using $\mathbf{C}$
11. Restarting from step 5 if the calculation is not converged. The procedure is converged e.g. the density matrix $\mathbf{P}$ is the same as in the previous step and/or the change of energy is below a defined threshold.

2.2. Density Functional Theory

The HF method described above is a mean-field approximation. This method does not capture the total non-relativistic energy, this error is called correlation energy. The DFT approach allows the correction of e.g. Coulomb correlation[6, 7], depending on the choice of the exchange-correlation functionals, which will be introduced later.

This method finds its early origin in the 1920s through Thomas[8] and Fermi[9], considering the electrons as a homogeneous interacting electron gas.[10] This approach proved to be usefuel for atoms and metals. The idea

was extended by Dirac and Slater, but the theoretical basis for DFT was provided by Hohenberg and Kohn in the mid 1960s. They established two essential theorems for the breakthrough of the theory for use in quantum chemical calculations and formulated a variation approach for the calculation of the ground state energy. The first theorem states that there is a one-to-one correspondence between the electronic density $\rho(\vec{r})$ and the wave function $\Psi(\vec{r})$.[11]

$$\Psi = \Psi(\vec{r}_1, \vec{r}_2, \cdots, \vec{r}_N) \;\leftrightarrow\; \rho(\vec{r}) \tag{2.41}$$

Note that the density depends only on three and the wave function on 3N coordinates. The integration by the electron density provides the total number of electrons N.[12]

$$N = \int \rho(\vec{r}) dr \tag{2.42}$$

When the exact density is known, the solution is equivalent to the solution of the Schrödinger equation.

The second theorem states that there is a variational principle of the density. The total energy of a system can be formulated as a functional of the density $E[\rho]$. A similar relation as for a wave function (2.10) can be set up for the density. The energy $E[\tilde{\rho}]$ of a trial density $\tilde{\rho}$ is larger than the true energy $E[\rho]$ (2.43), if the number of particles is kept constant.[11]

$$E[\tilde{\rho}] \geq E[\rho] \tag{2.43}$$

In the simplest case, the Hamiltonian for N non relativistic , interacting

electrons can be written as 2.44.

$$\mathcal{H} = -\frac{1}{2}\sum_j \nabla_j^2 + \sum_j \nu(r_j) + \frac{1}{2}\sum_{i\neq j}\frac{1}{r_{ij}} \tag{2.44}$$

$\nu(r_j)$ denotes an arbitrary potential in which the electrons are moving, not only the physically relevant nucleus-electron Coulomb interaction. Hohenberg and Kohn[11] postulated that the ground-state density $\rho(\vec{r})$, which is obtained by a parameterized Slater determinant (Kohn-Sham determinant), determines the external potential $\nu(\vec{r})$, the starting point of DFT.[12] By a given $\nu(\vec{r})$ the energy can be written as a functional of the density $\rho(\vec{r})$ as

$$E_{\nu(\vec{r})}[\rho(\vec{r})] = \int \nu(\vec{r})\rho(\vec{r})d\vec{r} + F[\rho(\vec{r})] \tag{2.45}$$

$F[\rho(\vec{r})]$ is a functional of the kinetic energy and the electron repulsion-interaction.

$$F[\rho(\vec{r})] = \Big(\Psi, \big(-\frac{1}{2}\sum_j \nabla_j^2 + \frac{1}{2}\sum_{i\neq j}\frac{1}{r_{ij}}\big)\Psi]\Big) \tag{2.46}$$

A useful approach of Kohn and Sham[7] is to extract the functional $F[\rho(\vec{r})]$ (2.47).

$$F[\rho(r)] = \mathcal{T}_s[\rho(\vec{r})] + \mathcal{J}[\rho(\vec{r})] + E_{XC}[\rho(\vec{r})] \tag{2.47}$$

$$\begin{aligned} \text{with } \mathcal{T}_s[\rho(\vec{r})] &= \sum_{i=1}^{N} \langle \chi_i' | -\frac{1}{2}\nabla_i^2 | \chi_i' \rangle \\ \mathcal{J}[\rho(\vec{r})] &= \frac{1}{2}\int\int \frac{\rho(\vec{r})\rho(\vec{r}')}{|\vec{r}-\vec{r}'|} d\vec{r}d\vec{r}' \end{aligned} \tag{2.48}$$

Thereby $\mathcal{T}_s$ denotes the kinetic energy of a noninteracting system with the density $\rho(\vec{r})$ and $\mathcal{J}[\rho(\vec{r})]$ the interaction. By using 2.45, 2.47 and the Lagrange method it is possible to set up a new self-consistent equation (2.49) as for HF, the Kohn-Sham (KS) equation.

$$\Big(-\frac{1}{2}\nabla^2 + \nu(\vec{r}) + \int \frac{\rho(\vec{r}')}{|\vec{r}-\vec{r}|}d\vec{r}' - \nu_{XC}(\vec{r})\Big)\chi_j' = \epsilon_j \chi_j' \tag{2.49}$$

The equation contains the fictious single-particle orbitals χ'_j comparable to the single-electron orbitals from HF theory and can be solved if 2.50 and 2.51 apply.

$$\rho(r) = \sum_{j=1}^{N} |\chi'_j|^2 \tag{2.50}$$

$$\nu_{XC}(r) = \frac{\delta E_{XC}[\rho(\vec{r})]}{\delta \rho(\vec{r})} \tag{2.51}$$

ν_{XC} is calculated by 2.51 in each iteration with an appropriate approximation of the exchange-correlation functional $E_{XC}[\rho(\vec{r})]$. In principle, the KS approach is exact in the case that an exact $E_{XC}[\rho(r)]$ is used. It depends on the total electron density, which is different at different places in the system.[7] Note that all terms in $E[\rho]$ can be constructed, but not the exchange-correlation functional E_{XC}, therefore parameterized functionals are used to describe the exchange-correlation effect as good as possible.

2.2.1. Functionals

The true exchange-correlation functional is unknown, so users must rely on density functional approximations. As a consequence, hundreds of these functionals have been developed, each with its own advantages and disadvantages.[13]

The simplest approximation is the local density approximation (LDA)[7], which describes the electrons as a uniform interacting electron gas with 2.52.

$$E_{XC}^{LDA} = \int \epsilon_{XC}[\rho(\vec{r})]\rho(\vec{r})d\vec{r} \tag{2.52}$$

$\epsilon_{XC}[\rho(\vec{r})]$ is the exchange-correlation energy of the density $\rho(\vec{r})$. A higher level is the generalized gradient approximation (GGA), which in addition

includes the gradient of the density (2.53).[12]

$$E_{XC}^{GGA} = \int f\big(\rho(\vec{r}), \nabla\rho(\vec{r})\big) d\vec{r} \tag{2.53}$$

The functional E_{XC}^{GGA} contains $\rho(\vec{r})$ and $\nabla\rho(\vec{r})$. High accuracy is obtained by combining GGA and exact exchange (HF). This functionals are called hybrid functionals.

The main functionals that have been used are the hybrid functional B3LYP[14–16] for geometry-optimization calculations and the GGA functional BP86[14, 17]for other calculations.

2.3. Theoretical basics of the NMR Spectroscopy

NMR spectroscopy is a common analysis to determine molecular structures[18] by chemical shifts, coupling constants and a variety of modern NMR techniques. Calculation of such properties could be helpful for predictions or analysis of physical effects.

Molecular properties may be calculated by the derivative of the total energy of a system, which is connected to the derivative of the used Hamiltonian. This arises from the Hellmann-Feynman theorem[19, 20]

$$\frac{\partial E_\lambda}{\partial \lambda} = \langle \Psi_\lambda | \frac{\partial H_\lambda}{\partial \lambda} | \Psi_\lambda \rangle \tag{2.54}$$

which is valid in this form when the wave function is independent of λ in first order or invariant. The first and second derivative with respect to an external electric field can be associated with the electric moments and the polarizability. Magnetic properties e.g. NMR-shieldings, are obtainable by the second derivative with respect to a constant external magentic field B and the nuclear-magentic moment m_K [21–23] at $B = 0$ and $m_K = 0$,

called shielding tensor σ_{st} (2.55).

$$\sigma_{st} = \left.\frac{\partial^2 E^{total}}{\partial B_s \partial m_{K_t}}\right|_{B=0,m_K=0} \tag{2.55}$$

Note that the index s and t denotes the x, y and z coordinates of the magnetic field $\vec{B}$ the nuclei K. The shilding tensor σ is a second-rank tensor.[24] Later in the results section (sec. 4), the focus will be on isotropic shielding values σ^{iso}, which is obtained from the trace of the shielding tensor (2.56).[25]

$$\sigma^{iso} = \frac{1}{3} Tr(\sigma_{st}) \tag{2.56}$$

Before the shielding tensor is presented, the general idea is how to deal with a second derivative of an expectation value. The second derivative of an expectation value E with respect to the parameter x and y can be written as

$$\begin{aligned}\frac{\partial^2 E^{HF}}{\partial x \partial y} &= \sum_{\mu\nu} P_{\mu\nu} \frac{\partial^2 H_{\mu\nu}}{\partial x \partial y} + \frac{1}{2} \sum_{\mu\nu\lambda\sigma} P_{\mu\nu} P_{\lambda\omega} \frac{\partial^2}{\partial x \partial y} (\mu\lambda||\nu\sigma) \\ &+ \frac{\partial^2 V_{nuc}}{\partial x \partial y} - W_{\mu\nu} \frac{\partial^2 S_{\mu\nu}}{\partial x \partial y} \\ &+ \sum_{\mu\nu} \frac{\partial P_{\mu\nu}}{\partial y} \frac{\partial H_{\mu\nu}}{\partial x} + \frac{1}{2} \sum_{\mu\nu\lambda\sigma} \frac{\partial P_{\mu\nu}}{\partial y} P_{\lambda\omega} \frac{\partial}{\partial x} (\mu\lambda||\nu\sigma) \\ &- \frac{\partial W_{\mu\nu}}{\partial y} \frac{\partial S_{\mu\nu}}{\partial x}\end{aligned} \tag{2.57}$$

where W is given through

$$W_{\mu\nu} = \sum_j \epsilon_j c^*_{\mu j} c_{\nu j} = \sum_j \epsilon_j P_{\mu\nu} \tag{2.58}$$

The resulting expression 2.57 includes derivatives of the wave function. The coupled-perturbed Hartree-Fock (CPHF) formalism shows how to deal with those.

2.3.1. CPHF-equation

The first two lines of 2.57 contain the second derivative of the Hamiltonian, which is easy to calculate. The last two lines includes the derivatives of P and W and thus the derivative of the coefficients. In the case of the second derivative, a perturbed wave function or rather a perturbed density must be calculated. Therefore the coefficients of the perturbed density $\frac{\partial P_{\mu\nu}}{\partial y} = P(y)$ can be expand into the unperturbed coefficients c and the using of a transformation perturbation matrix $\mathbf{U}(y)$ 2.59 .

$$c_{\mu p}(y) = \sum_q c_{\mu q} u_p(y) \tag{2.59a}$$

$$\text{in matrix form: } \mathbf{C}(y) = \mathbf{CU}(y) \tag{2.59b}$$

Note that greek letters imply unperturbed while roman letters define perturbed factors. The perturbed spin orbitals $\chi(y)$ are expanded in perturbed basis functions $\omega(y)$ (2.60).

$$\chi_p(y) = \sum_\mu c_{\mu p}(y)\omega_\mu(y) = \sum_\mu \sum_q c_{\mu q} u_p(y)\omega_\mu(y) \tag{2.60}$$

The derivative of u, so $u^{(1)}$, is used, which can be expressed by the central result of the CPHF formalism. Therefore the matrix U is divided into diagonal (2.61) and off-diagonal (2.62) terms.

$$u_{pp}^{(1)} = -\frac{1}{2}\tilde{S}_{pp}^{(1)} \tag{2.61}$$

$$u_{pq}^{(1)} = \frac{\tilde{F}_{pq}^{(1)} - \tilde{S}_{pp}^{(1)}\epsilon_p}{\epsilon_p - \epsilon_q} \tag{2.62}$$

$$\text{with } \epsilon_p^{(1)} = \tilde{F}_{pp}^{(1)} - \tilde{S}_{pp}^{(1)}\epsilon_p \tag{2.63}$$

Note that $\tilde{F}$ and $\tilde{S}$ are given through

$$\tilde{\mathbf{F}}(y) = \mathbf{C}^{\dagger}\mathbf{F}(y)\mathbf{C} \tag{2.64}$$

$$\tilde{\mathbf{S}}(y) = \mathbf{C}^{\dagger}\mathbf{S}(y)\mathbf{C} \tag{2.65}$$

The whole derivation of the central result of the CPHF formalism is shown in the appendix (A.10.1).

2.3.2. $\mathcal{H}$ with magnetic field

After a description of the general derivative procedure for HF-like equations it is now shown which terms result in the shielding tensor.

The expectation value of a Hamiltonian $\mathcal{H}$ can be written as

$$E = \langle \xi | \mathcal{H} | \xi \rangle \tag{2.66}$$

To obtain the shielding tensor (2.67), the second derivative with respect to the external magnetic field B_s and the nuclear magnetic moment $m_{K,t}$ of the expectation value E has to be determined.

$$\begin{aligned} \sigma_{st} = \frac{\partial^2 E}{\partial B_s \partial m_{K_t}} &= \left\langle \xi \middle| \frac{\partial^2 \mathcal{H}}{\partial B_s \partial m_{K,t}} \middle| \xi \right\rangle + 2 \left\langle \frac{\partial \xi}{\partial B_s} \middle| \frac{\partial \mathcal{H}}{\partial m_{K,t}} \middle| \xi \right\rangle \\ &= \sigma^{dia} + \sigma^{para} \end{aligned} \tag{2.67}$$

Note that the index s and t denotes the x, y and z coordinates of the magnetic field $\vec{B}$ the nuclei K. The non-relativistic shielding tensor has diamagnetic σ^{dia} and paramagnetic σ^{para} contributions.

In the following, the derivative of a simple non-relativistic Hamiltonian is worked out. The second derivative with respect to the magnetic field B and the magnetic moment m_K has to be multiplied with the wave function (diamagnetic) and the derivative with respect to the magnetic moment m_K

with the perturbed wave function (paramagnetic). The simple Hamiltonian in atomic units is written as

$$\mathcal{H} = \frac{\vec{p}^2}{2} + V(\vec{r}) \tag{2.68}$$

The kinetic energy operator p has to be extended by a vector potential $A(r)$[22]. This ansatz is called minimal substitution.

$$\vec{p} \rightarrow \vec{\pi} = \vec{p} + \frac{1}{c} \cdot A(\vec{r}) \tag{2.69}$$

c denotes the speed of light.

The minimal substitution introduces the interaction of the electrons with the field into the Hamiltonian. $A(r)$ contains the vector potential of the external magnetic field A^{ext} and the nuclear magnetic moment A^K.

$$A(\vec{r}) = A^{ext} + A^K = \frac{1}{2}\vec{B} \times \vec{r} + \frac{\vec{m}_K \times (\vec{r} - \vec{R}_K)}{|\vec{r} - \vec{R}_K|^3} \tag{2.70}$$

Inserting the vector potential for the external magnetic field A^{ext} into the Hamiltonian 2.68 yields

$$\begin{aligned} \mathcal{H}(\vec{B}) &= \frac{(\vec{p} + \frac{1}{2c}\vec{B} \times \vec{r})^2}{2} + V(r) \\ &= -\frac{1}{2}\vec{\nabla}^2 - \frac{i}{2c} \cdot \vec{B}(\vec{r} \times \vec{\nabla}) \\ &\quad + \frac{1}{c^2} \cdot \Big((\vec{B} \times \vec{r}) \cdot (\vec{B} \times \vec{r})\Big) + V(\vec{r}) \end{aligned} \tag{2.71}$$

and the vector potential of the magnetic moment A^K in 2.68 yields

$$\begin{aligned}\mathcal{H}(\vec{m}_K) &= \frac{1}{2}\Big(\vec{p}+\frac{1}{c}\frac{\vec{m}_K\times(\vec{r}-\vec{R}_K)}{|\vec{r}-\vec{R}_K|^3}\Big)^2+V(\vec{r})\\ &= -\frac{1}{2}\vec{\nabla}^2-\frac{i}{2c}\frac{\vec{m}_K\cdot(\vec{r}-\vec{R}_K)\times\vec{\nabla}}{|\vec{r}-\vec{R}_K|^3}\\ &\quad+\frac{1}{2c^2}\cdot\Big(\frac{\vec{m}_K\times(\vec{r}-\vec{R}_K)}{|\vec{r}-\vec{R}_K|^3}\Big)^2+V(\vec{r})\end{aligned} \tag{2.72}$$

Using of $A(\vec{r})$ (2.70), which contain both the vector potential of the magnetic field A^{ext} and of the magnetic moment A^K in 2.68 the Hamiltonian is obtained.

$$\mathcal{H}(\vec{B},\ \vec{m}_K)=\frac{1}{2}\left(\vec{p}+\frac{1}{c}\left[\frac{1}{2c}\vec{B}\times\vec{r}+\frac{\vec{m}_K\times(\vec{r}-\vec{R}_K)}{|\vec{r}-\vec{R}_K|^3}\right]\right)^2+V(\vec{r}) \tag{2.73}$$

Many terms result from expanding (2.73), but most vanish in the derivative. Only the term necessary to be considered is listed in the Hamiltonian (2.74).

$$\mathcal{H}(\vec{B},\ \vec{m}_K)=\frac{1}{2c^2}\cdot\frac{(B_s\times\vec{r})\cdot(\vec{m}_{K_t}\times(\vec{r}-\vec{R}_K))}{|\vec{r}-\vec{R}_K|^3} \tag{2.74}$$

A simple approach to obtain the second derivative of the Hamiltonian 2.74 is to separate the derivatives with respect to B_s and $m_{K,t}$ and subsequent multiplication of them.

The derivative with respect to the external magnetic field B_s of 2.71 yields

$$\frac{\partial\mathcal{H}(\vec{B})}{\partial B_s}=-\frac{i}{2c}\cdot(\vec{r}\times\vec{\nabla})_s \tag{2.75}$$

and the derivative of 2.72 with respect to the nuclear magnetic moment m_{K_t} is given through

$$\frac{\partial\mathcal{H}(\vec{m}_K)}{\partial m_{K_t}}=-\frac{i}{c}\frac{[(\vec{r}-\vec{R}_K)\times\vec{\nabla}]_t}{|\vec{r}-\vec{R}_K|^3} \tag{2.76}$$

The mixed derivative (2.77) of the Hamiltonian (2.73) is obtained by multiplying 2.75 and 2.76 to obtain 2.78.

$$\frac{\partial^2 \mathcal{H}(\vec{B},\ \vec{m}_K)}{\partial B_s \partial m_{K,t}} = \frac{\partial \mathcal{H}(\vec{B})}{\partial B_s} \cdot \frac{\partial \mathcal{H}(\vec{m}_K)}{\partial m_{K,t}} \tag{2.77}$$

$$= \frac{1}{2c^2} \frac{r \cdot (\vec{r} - \vec{R}_K)\delta_{st} - r_t(\vec{r} - \vec{R}_K)_s}{|\vec{r} - \vec{R}_K|^3} \tag{2.78}$$

Using the second derivative (2.78) in the first term of 2.67 the diamagnetic contribution σ^{dia} of the shielding tensor σ_{st} one obtains (2.79).

$$\sigma^{dia} = \left\langle \xi \middle| \frac{1}{2c^2} \frac{\vec{r} \cdot (\vec{r} - \vec{R}_K)\delta_{st} - r_t(\vec{r} - \vec{R}_K)_s}{|\vec{r} - \vec{R}_K|^3} \middle| \xi \right\rangle \tag{2.79}$$

The paramagnetic contribution σ^{para} of the shielding tensor σ_{st} contains the perturbed wave function and can be obtained by using the central solution of the CPHF equation. In the CPHF formalism, the wave function is expanded in a perturbed basis (2.60). Derivative of the expansion with respect to the external magnetic field and multiplying with the derivative Hamiltonian with respect to the nuclear magnetic moment (2.76) yields the paramagnetic contribution.

$$\begin{aligned}
\sigma^{para} &= \frac{2}{ic} \left\langle \frac{\partial}{\partial B_s} \Big(\sum_p \sum_\mu \sum_q c_{\mu q} u_p(\vec{B}) \omega_\mu(\vec{B}) \Big) \middle| \frac{[(\vec{r} - \vec{R}_K) \times \vec{\nabla}]_t}{|\vec{r} - \vec{R}_K|^3} \middle| \xi \right\rangle \\
&= \frac{2}{ic} \left\langle \sum_p \sum_\mu \sum_q c_{\mu q} \frac{\partial}{\partial B_s} u_p(\vec{B}) \omega_\mu(\vec{B}) \middle| \frac{[(\vec{r} - \vec{R}_K) \times \vec{\nabla}]_t}{|\vec{r} - \vec{R}_K|^3} \middle| \xi \right\rangle \\
&+ \frac{2}{ic} \left\langle \sum_p \sum_\mu \sum_q u_p(\vec{B}) \frac{\partial}{\partial B_s} \omega_\mu(\vec{B}) \middle| \frac{[(\vec{r} - \vec{R}_K) \times \vec{\nabla}]_t}{|\vec{r} - \vec{R}_K|^3} \middle| \xi \right\rangle
\end{aligned} \tag{2.80}$$

How the resulting paramagnetic part looks like depends on ω_μ. A good choice are GIAOs[26], more about this later in section 2.3.3. By using GIAO ω_μ can be written as 2.81[27], where the basis functions χ_μ multiply

by a complex phase factor.

$$\omega_\mu(B,r) = exp\Big(-\frac{i}{2}(\vec{B}\times\vec{R}_{\mu O})\cdot\vec{r}\Big)\cdot\chi_\mu(r_M) \tag{2.81}$$

Using the central results of CPHF the diagonal (2.61) and off-diagonal (2.62) definitions of $u^{(1)}$, and the derivative of 2.81 the paramegentic contribution can be written as shown in 2.82. Note that $R_{\mu O}$ is only written as R_μ for simplicity.

$$\begin{aligned}\sigma^{para} =& \sum_i 2\Bigg\{\sum_{\lambda\nu}\frac{1}{ic}c_{\lambda i}c_{\nu i}\Big\langle\chi_\lambda\Big|\frac{1}{2}\Big(\vec{R}_\lambda\times\vec{R}_\nu\Big)_s\left(\frac{\vec{r}_N}{r_N^3}\times\vec{\nabla}\right)_t\Big|\chi_\nu\Big\rangle\Bigg\}\\ &+\sum_j\frac{1}{ic}S_{ij}^{(1)}\Big\langle\phi_i\Big|\left(\frac{\vec{r}_N}{r_N^3}\times\vec{\nabla}\right)_t|\phi_j\Big\rangle\\ &+2\sum_\alpha\frac{1}{ic}u_{\alpha i}^{(1)}\Big\langle\phi_i\Big|\left(\frac{\vec{r}_N}{r_N^3}\times\vec{\nabla}\right)_t|\phi_j\Big\rangle\end{aligned} \tag{2.82}$$

2.3.3. Gauge-including atomic orbitals - GIAO

Magnetic properties will be calculated by adding the magnetic vector potential $A(r)$, which depends on the gauge origin, to the kinetic operator (see section 2.3.2, equation 2.69). The results of magnetic property calculations are origin-independent if a complete basis is used, but in a truncated basis the independency of the origin is not longer ensured.[28] Especially for heavy elements, the large number of electrons does not allow for a very large let alone a complete basis set. Following Ditchfield[29] so-called London orbitals[26] or GIAO have been used to minimize the gauge error in calculations of magnetic shielding and other magnetic properties at the CPHF-level. Because London orbitals have their own origin, the gauge error in a finite base is minimized. The same is true for the calculated derivatives such as magnetic properties.

By using London orbitals in case of NMR shieldings, the atomic orbitals χ_μ are multiplied with a field-dependent, complex phase factor as seen in 2.81. The atomic orbital (AO) χ_μ is centered on the nucleus M at the position of $\vec{R}_\mu$.

Thereby $\vec{R}_{\mu O}$ denotes the dependency of the orbital position $\vec{R}_\mu$ to the origin $\vec{O}$ (2.83).

$$\vec{R}_{\mu O} = \vec{R}_\mu - \vec{O} \tag{2.83}$$

It is shown that the London orbitals depend paramterically on the field strength B, the gauge origin O and the orbital position R_μ.[28]

2.4. Relativistic effects

Relativistic quantum chemistry of electron systems deals with finding accurate solutions of the Dirac equation. This central equation merges the quantum mechanics with special relativity.[30] The Dirac equation in a inertial system to separate space and time can be written as in 2.84.

$$\begin{aligned} \mathcal{H}_D \Psi(\vec{r}) &= E' \Psi(\vec{r}) \\ \Big(c\vec{\alpha}(\vec{p} + e\vec{A}) + \beta mc^2 - e\phi\Big)\Psi(\vec{r}) &= E' \Psi(\vec{r}) \end{aligned} \tag{2.84}$$

c denotes the speed of light, m the mass of an electron, $\vec{A}$ is a vector potential and ϕ and scalar potential which is multiplied by the charge of an electron e. Note that $\vec{\alpha}$ and β are 4-dimensional square matrices. $\vec{\alpha}$ contains the Pauli spin matrices (2.86) in a vector according to

$$\vec{\alpha} = \begin{pmatrix} \alpha_1 \\ \alpha_2 \\ \alpha_3 \end{pmatrix} \quad \alpha_i = \begin{pmatrix} \mathbf{0}_2 & \sigma_i \\ \sigma_i & \mathbf{0}_2 \end{pmatrix} \quad i = 1, 2, 3 \tag{2.85}$$

$$\text{with} \quad \sigma_1 = \begin{pmatrix} 0 & 1 \\ 1 & 0 \end{pmatrix} \quad \sigma_2 = \begin{pmatrix} 0 & -i \\ i & 0 \end{pmatrix} \quad \sigma_3 = \begin{pmatrix} 1 & 0 \\ 0 & -1 \end{pmatrix} \tag{2.86}$$

and β is given by

$$\beta = \begin{pmatrix} \mathbf{1}_2 & 0 \\ 0 & -\mathbf{1}_2 \end{pmatrix} \tag{2.87}$$

The wave function Ψ is a four dimensional vector, called a 4-spinor.[31] Ψ can be split into a large ψ^L and a small ψ^S component.

$$\Psi = \begin{pmatrix} \psi_1 \\ \psi_2 \\ \psi_3 \\ \psi_4 \end{pmatrix} = \begin{pmatrix} \psi^L \\ \psi^S \end{pmatrix} \tag{2.88}$$

The solutions of the Dirac equation for a free particle include two possible values: $E = \pm mc^2$. Solutions for a bound particle lie between these two values. There is a continuum above $E = +mc^2$ and below $E = -mc^2$. The positive continuum is already known from the non-relativistic solutions of the Schrödinger equation. For the negative continuum there are many possible interpretations e.g. Dirac's hole theory[32]. In the following the zero point of the energy is shifted by $+mc^2$ in order that the positive continuum starts there to make the formalism comparable to the non-relativistic case. Using $\vec{A} = 0$, $V = -e\phi$ and $E = E' + mc^2$ it is possible to formulate the two component Dirac equation (2.89).

$$V \cdot \psi^L + c\vec{\sigma}\vec{p} \cdot \psi^S = E\psi^L \tag{2.89a}$$

$$c\vec{\sigma}\vec{p} \cdot \psi^L + (V - 2mc^2) \cdot \psi^S = E\psi^S \tag{2.89b}$$

Based on 2.89, approximations can be introduced to obtain expressions

for the relativistic corrections. Therefore, 2.89b is rearranged to ψ^S and the relation 2.90 is resulting.

$$\psi^S = \frac{c\vec{\sigma}\vec{p}}{2mc^2 + E - V}\psi^L \tag{2.90}$$

Using of the relation of the small and the large component in 2.89a and Dirac's relation[33]

$$(\vec{\sigma}\vec{u})(\vec{\sigma}\vec{v}) = \vec{u}\vec{v}\mathbf{1}_2 + i\vec{\sigma}\cdot(\vec{u}\times\vec{v}) \tag{2.91a}$$

$$\text{if } \vec{u} = \vec{v} \text{ then } (\vec{\sigma}\vec{u})(\vec{\sigma}\vec{u}) = \vec{u}^2\mathbf{1}_2 \tag{2.91b}$$

it is possible to set up a eigenvalue equation of the large component, which contains the non-relativistic limit and relativistic corrections.

$$\begin{aligned}\Bigg(&\underbrace{\frac{\vec{p}^2}{2m} + V - E}_{\text{non relativistic}} \underbrace{\underbrace{+\frac{V-E}{2mc^2+E-V}}_{\text{velocity correction}}\cdot\frac{\vec{p}^2}{2m} - \frac{c^2}{(2mc^2+E-V)}\vec{p}V\vec{p}}_{\text{scalar relativstic}} \\ &\underbrace{-\frac{c^2}{(2mc^2+E-V)}i\big(\vec{\sigma}\vec{p}V\times\vec{p}\big)}_{\text{spin-orbit coupling}}\Bigg)\psi^L = 0\end{aligned} \tag{2.92}$$

The relativistic corrections are the velocity correction of the kinetic energy and a scalar correction due to the third part. The velocity and scalar corrections are the scalar relativistic corrections. The last Term contains the SOC. Which term of the relativistic corrections dominates the correction in calculations depends on the atom types.

2.4.1. Relativistic Hamiltonians

In 2.84 the Dirac equation for one electron is shown. This contains no two-electron interactions. In 2.93 and second electron and the Coulomb

interaction is added. For an overview the indices 1 and 2 are used to identify the electron, even if electrons are not distinguishable.

$$\begin{aligned}&\Big\{\Big[c\vec{\alpha}_1\Big(\vec{p}_1-\frac{1}{2c}\frac{q_1q_2}{r_{12}}\Big)+\beta_1mc^2+\frac{1}{2}\frac{q_1q_2}{r_{12}}+V_{Ke}(r_1)\Big]\\&+\Big[c\vec{\alpha}_2\Big(\vec{p}_2-\frac{1}{2c}\frac{q_2q_1}{r_{12}}\Big)+\beta_2mc^2+\frac{1}{2}\frac{q_2q_1}{r_{12}}+V_{Ke}(r_2)\Big]\Big\}\xi=E\xi\end{aligned} \tag{2.93}$$

$$\begin{aligned}&\Big\{c\vec{\alpha}_1\vec{p}_1+c\vec{\alpha}_2\vec{p}_2+\beta_1mc^2+\beta_2mc^2+V_{Ke}(r_1)+V_{Ke}(r_2)\\&\quad+\frac{1}{2}\frac{q_1q_2}{r_{12}}-\frac{1}{2}q_1q_2\frac{\vec{\alpha}_1\vec{\alpha}_2}{r_{12}}\Big\}\xi=E\xi\end{aligned} \tag{2.94}$$

In comparison to the non relativistic case, the two electron interaction (second line of 2.94) contains the Coulomb interaction and an additional term, called the Gaunt interaction. The Coulomb interaction describes the spin-same interaction and the Gaunt term the spin-other-interaction by an instantaneous spin-spin-coupling.[31, 34] In nature the magnetic interaction between electrons is not instantaneous, but retarded. Derived by the quantum electrodynamics or relativistic interaction of charged particles with quantization, the two-electron relativistic Breit operator (2.95) results.

$$g^{Breit}(\vec{r}_1,\vec{r}_2)=-\frac{q_1q_2}{2r_{12}}\left(\vec{\alpha}_1\vec{\alpha}_2+\frac{(\vec{\alpha}_1\vec{r}_1)(\vec{\alpha}_2\vec{r}_2)}{r_{12}^2}\right) \tag{2.95}$$

In the many-particle case, a four-component Hamiltonian can be written as

$$\mathcal{H}=\sum_i^N\mathcal{H}^D(i)+\sum_{i<j}^N g(i,j)+V_{KK} \tag{2.96a}$$

$$\text{with } \mathcal{H}^D(i)=c\vec{\alpha}_i\vec{p}_i+\beta_imc^2+V_{Ke} \tag{2.96b}$$

Using the Coulomb potential for $g(i,j)$, the Dirac-Coulomb Hamiltonian

results. If the Breit interaction (2.95) is introduced, the Dirac-Coulomb-Breit Hamiltonian is obtained.[31] Both Hamiltonians give electronic solutions of both positive and negative energy. For technical reasons, four-component Hamiltonians can only be employed for small molecules. Approximations are made in order to calculate relativistic corrections of large systems and to reduce the computational costs. One possible procedure is the elimination technique[31], e.g. the Pauli elimination yields the Pauli Hamiltonian (2.97)[35].

$$\Big(\underbrace{\frac{\vec{p}^2}{2m}+V}_{\text{non-rel.}}\underbrace{-\frac{\vec{p}^4}{8m^3c^2}}_{\text{mass-velocity}}\underbrace{+\frac{\hbar^2}{8m^2c^2}(\Delta V)}_{\text{Darwin}}\underbrace{+\frac{\hbar}{4m^2c^2}\sigma(\nabla V\times\vec{p})}_{\text{spin-orbit coupling}}\Big)\psi^L=E\psi^L \quad (2.97)$$

The derivation is shown in the appendix (A.10.3).

Note that the Pauli Hamiltonian contains the non-relativistic Hamiltonian, a mass-velocity operator, a Darwin term and a spin-orbit coupling term. Because of the mass-velocity term and the singularity of the Darwin term this Hamiltonian is not bounded from below and ill-defined.[31] A better approach is a decoupling strategy of the small and large component. In this thesis, the exact-2-component (X2C) and the BSS Hamiltonians, obtained after the Barysz-Sadlej-Snijders transformation, where used.

X2C approach The starting point of the exact-2-component decoupling method is the Dirac-Roothaan equation

$$f\Psi=(\sum_i^N\mathcal{H}^D(i)+V)\Psi=E\Psi \quad (2.98)$$

The 2-component spinor funtions $\Psi=\begin{pmatrix}\psi^L\\ \psi^S\end{pmatrix}$ are expanded into one-dimensional scalar basis functions λ_μ multiplied by spin functions $\{\lambda_m u\}\otimes\{\alpha,\beta\}$ (2.99).

$$\psi_i^L(r) = \sum_\mu c_{i\mu,+}^L \lambda_\mu(r) \tag{2.99a}$$

$$\psi_i^S(r) = \sum_\mu c_{i\mu,+}^S \lambda_\mu(r) \tag{2.99b}$$

c_+^L and c_+^S denote the coefficient of the basis set expansion of the large and small components, respectively. As shown in 2.90, also a relation between the coefficients of the small and large components can be made.

$$c_+^S = X c_+^L \tag{2.100}$$

The operator X can be determined (2.101) by multiplying 2.100 from the right by $(c_+^L)^{-1}$.

$$X = c_+^S (c_+^L)^{-1} \tag{2.101}$$

This operator is used to generate the decoupling unitary transformation matrix U_{X2C}.[31]

$$U_{X2C} = \begin{pmatrix} \frac{1}{\sqrt{1+X^\dagger X}} & -X^\dagger \frac{1}{\sqrt{1+X^\dagger X}} \\ X \frac{1}{\sqrt{1+X^\dagger X}} & \frac{1}{\sqrt{1+X^\dagger X}} \end{pmatrix} \tag{2.102}$$

To generate the X operator, the Dirac-Roothaan equation (2.98) is diagonalized. This step requires an approximation of the potential V_{ee}, which does not contain the full electron-electron interaction. Using of U_{X2C} in an unitary transformation, such as the Foldy-Wouthuysen transformation, the exact decoupling of the Dirac equation is possible. The advantage of this approach is, that only one decoupling-step is required. The two-electron part of this approach is treated in the non-relativistic limit. It is possible to change that part through e.g. an atomic mean field two-electron spin-orbit correction.[31]

Note that there is a kinetic-balance condition between the small and large component: $\psi_\mu^S \in \{\psi_\nu^L\}$. A decoupling is possible by kinetic balance unitary transformations. Using the relation $\psi_\mu^S \in \{\psi_\nu^L\}$ a 1:1 ratio between the the large and small component basis sets, so the restricted kinetic balance (RKB) is chosen.[36] This holds the magnetic balance in the absence of a magnetic field.

There are problems using RKB to calculate magnetic properties as shown by Olejniczak *et. al*[37]. In this case, the magnetic balance is no longer fulfilled. A better approach is then to span the generated RKB basis functions to obtain unrestricted kinetic balance (UKB). In the UKB, only the generated basis functions by RKB of the small component are required. In general, UKB leads to larger basis sets for the small component and gives a more flexible basis.[36]

BSS Hamiltonian Instead of the one-step transformation such as the X2C approach, the BSS Hamiltonian is a two-step transformation. This approach uses the Barysz-Sadlej-Snijders transformation. Therefore the free-particle Foldy-Wouthuysen transformation with $\mathbf{U}$ in addition to the orthonormal transformation with $\mathbf{K}$ is made. The transformed four-component Hamiltonian matrix $\tilde{\mathbf{H}}$ can be written as[31]

$$\tilde{\mathbf{H}} = \mathbf{U}_0^\dagger \mathbf{K}^\dagger \mathbf{H} \mathbf{K} \mathbf{U}_0 \tag{2.103}$$

Using this approach, it is possible to generate a Hamiltonian which only acts on the large component.

ZORA Hamiltonian The ZORA Hamiltonian is determined by the known relation of the small and large components shown in 2.90. For this purpose,

the relation X between the large and small components is rewritten as

$$X_{ZORA} = X = \frac{c}{2c^2 - V}[1 + \frac{E}{2c^2 - V}]^{-1}\vec{\sigma}\vec{p} \tag{2.104}$$

The derivation is shown in the appendix (A.10.4).
A drastic assumption is made to get ZORA. X_{ZORA} is to be simplified using $E << 2c^2 - V$. This results in the removal of the fraction in the square brackets of 2.104. The resulting Hamiltonian can be written as

$$\mathcal{H} = V + c\vec{\sigma}\vec{p}\frac{c}{2c^2 - V}\vec{\sigma}\vec{p} = V + \vec{\sigma}\vec{p}\frac{c^2}{2c^2 - V}\vec{\sigma}\vec{p} \tag{2.105}$$

The current Hamiltonian is expanded in powers of $\frac{E}{2c^2-V}$ (2.106).[38]

$$\mathcal{H} \approx V + \vec{\sigma}\vec{p}\frac{c}{2c^2 - V}\vec{\sigma}\vec{p} - \vec{\sigma}\vec{p}\left(\frac{c}{2c^2 - V}\right)\left(\frac{E}{2c^2 - V}\right)\vec{\sigma}\vec{p} + \dots \tag{2.106}$$

The zeroth order contains the effective relativistic correction and is the ZORA Hamiltonian. Proceeding to the first order, the first-order regular approximation (FORA) is obtained. The IORA Hamiltonian can be developed in order to improve the ZORA, but the added higher orders do not yield the exact Dirac eigenvalues. [31, 39] The ZORA Hamiltonian is given by

$$\begin{aligned} \mathcal{H}^{ZORA} &= V + \vec{\sigma}\vec{p}\frac{K}{2}\vec{\sigma}\vec{p} \\ with\ K &= \left(\frac{1 - V}{2c^2}\right)^{-1} \end{aligned} \tag{2.107}$$

Using the ZORA Hamiltonian, the total ZORA energy is obtained. However, problems arise from the first approximation of $E << 2c^2 - V$ in 2.105. This approximation violates the description close to the core region. The problem does not only emerge in ZORA. Remember the Pauli Hamiltonian, which is also simply expanded in powers of c^{-2} (Appendix A.10.3),

and all other Hamiltonians based on this similar expansion are generally singular and ill-defined. In these cases, the variational procedures are no options.[31] Note that the ZORA method uses numeric integration for the calculation of the Hamiltonian matrix elements,[38, 40] therefore the calculations using ZORA are grid depended.

SOC Hamiltonian in *ORCA* In *ORCA* SOC approaches are implemented including the spin-orbit mean-field (SOMF) Hamiltonian, Atomic Mean-Field Integral (AMFI) approximation, AMFI-A approximation and the Veff-SOC Hamiltonian. After the reduction of the full four component relativistic theory by using the Breit-Pauli procedure[41, 42] the SOC Hamiltonian can be written as a sum of one- $\mathcal{H}_{SOC}^{(1)}$ and two electron contribution $\mathcal{H}_{SOC}^{(2)}$ as

$$\mathcal{H}_{SOC} = \mathcal{H}_{SOC}^{(1)} + \mathcal{H}_{SOC}^{(2)} \tag{2.108}$$

where the two electron contribution contains spin-same-orbit (SSO) and spin-other-orbit (SOO) terms. The use of the full two-electron Breit-Pauli-SOC operator is possible, but requires a high computational effort. The *ORCA* package is more likely used for larger molecules, therefore accurate approximations were made.[43] In case of the SOMF Hamiltonian, the Breit-Pauli-SOC Operator is approximated by an effective one-electron operator with the form

$$\mathcal{H}_{SOMF} = \sum_i \hat{z}_i \hat{s}_i \tag{2.109}$$

where $\hat{s}_i$ is the spin operator and $\hat{z}_i$ is an appropriate effective spatial operator which includes the most of two-electron effects. The one-electron part from the Breit-Pauli operator is taken and the two-electron contribution has to be transformed. The SOO and SSO parts contribute to the SOMF

Hamiltonian by spin-averaging which is an approximation.

In case of the AMFI approximation all multi-center terms are neglected and replaced by mean-field terms. In the AMFI-A approach atomic HF or KS densities generates the mean-field.[44]

In the effective potential SOC (VEFF-SOC) approach (2.110) the two-electron contribution to the SOC is considered by effectively screening the core-potential.

$$\mathcal{H}_{eff} = \sum_{A} \sum_{i} \frac{Z^{eff}_{A,l}}{\hat{r}^3_{Ai_A}} \vec{\hat{l}}_{Ai_A} \vec{\hat{s}}_{i_A} \tag{2.110}$$

A denotes an atom, i_A an electron occupying an orbital at center A and $\hat{l}$ the orbital angular momentum operator. In the *ORCA* code the effective nuclear charges of Koseki *et al.*[45] are implemented. The VEFF-SOC approach has the same one-electron integrals as the SOMF approach. The difference is that in VEFF-SOC the SSO part is modeled and does not contain the SOO contribution. This is justified by *Schreckenbach* and *Ziegler*[46], who argued that the SOO interaction vanishes, if in a model system an unpaired electron interacts with a closed-shell system. Probably the SOO interaction is still small, if there is a second unpaired electron. The VEFF-SOC approximation usually has an error smaller than 10 %, but in some cases the error can be above than 20 %.[44]

2.4.2. Relativistic effects in NMR shieldings

NMR parameters e.g. isotropic shielding, depend strongly on the electronic structure near the considered nucleus, therefore these parameters are affected by relativistic effects much earlier in the periodic table in comparison to other properties.[47] There are three main effects which arise in the relativistic theory. There is relativistic contraction of the s- and p-shells,

relativistic expansion of the d- and f-shell, and the spin-orbit splitting.[48] From the first mentioned effect, e.g. electrons move closer to the nucleus and thus faster, it is easy to concluded, that relativistic effects play a role in calculations of NMR observables of mainly heavy elements and cannot be neglected. However, heavy elements close to light elements influence e.g. NMR shifts of the light elements. This is called HALA describes that the SOC interaction of the heavy neighboring atom exerts a dominant effect on the chemical shift of the light atom.[49] Kaupp, Malkina and Malkin[50] have shown that the dramatic decrease of the ^{13}C shift from CCl_3^+ to CI_3^+, for example, is caused by a SOC effect. The HALA effect is also a possible explanation of the normal halogen dependence (NHD)[51], which is a decrease of the chemical shift of the atom next to a halogen with increasing nuclear charge.[50] The reverse case is also found and called IHD.

Relativistic shielding tensor In the presence of the spin-orbit interaction the shielding tensor σ_{st} is extended by a spin-dipole (SD) σ^{SD} and Fermi-contact (FC) term σ^{FC}. [52] Thus the relativistic shielding tensor can be written as

$$\sigma_{st}^{Rel} = \sigma^{dia} + \sigma^{para} + \sigma^{SD} + \sigma^{FC} \tag{2.111}$$

Where the two additional tensors come from is shown below.

The total relativistic Hamiltonian in atomic units in the presence of the external magnetic field and the nuclear-magnetic moment can be written as[52]

$$\begin{aligned}\mathcal{H} =& \frac{1}{2}\sum_i \left(\vec{p}_i + \frac{1}{c}A(\vec{r}_i)\right)^2 + \sum_{i>j}\frac{1}{r_{ij}} - \sum_A\sum_i \frac{Z_A}{r_{Ai}} \\ &+ \mathcal{H}_{SOC} + \mathcal{H}_{ZM}\end{aligned} \tag{2.112}$$

The first line of 2.112 contains the non-relativistic terms and the second the complementary relativistic terms consisting of the SOC operator $\mathcal{H}_{SOC}$ and the Zeeman operator $\mathcal{H}_{ZM}$. These can be formulated as

$$\mathcal{H}_{SOC} = \frac{1}{2c^2}\sum_A\sum_i Z_A \frac{\vec{l}_{Ai}\cdot\vec{s}_i}{\vec{r}_{Ai}^3} - \frac{1}{2c^2}\sum_i\sum_{j\neq i}\frac{\vec{l}_{ij}\cdot\vec{s}_i + 2\vec{l}_{ij}\cdot\vec{s}_i}{\vec{r}_{ij}^3} \tag{2.113}$$

$$\mathcal{H}_{ZM} = \frac{1}{c}\sum_i \vec{s}_i\cdot[\vec{\nabla}_i\times A(\vec{r}_i)] \tag{2.114}$$

$\vec{s}_i$ denotes the spin and $\vec{l}_i$ the orbital angular momentum operator of the electron i. The first term of $\mathcal{H}_{SO}$ denotes the one-electron and the second term the two-electron spin-orbit (SO) contribution. The two-electron SO contribution consists of spin-same-orbit and spin-other-orbit parts.

To obtain a concrete expression of the relativistic shielding tensor, the total Hamiltonian (2.112) is expanded in powers of the external magnetic field $\vec{B}$ and the nuclear magnetic moment $\vec{m}_K$.

$$\mathcal{H} = \mathcal{H}^{0,0} + \sum_s B_s\mathcal{H}_s^{1,0} + \sum_N\sum_t m_{K_t}\mathcal{H}_t^{0,1} + \sum_N\sum_t\sum_s m_{K_t}\mathcal{H}^{1,1}B_s + ... \tag{2.115}$$

The superscript indices denote the derivative with respect to B_s, m_{K_t} or

both. $\mathcal{H}^{0,0}$ is already shown in 2.112. $\mathcal{H}^{1,0}$, $\mathcal{H}^{0,1}$ and $\mathcal{H}^{1,1}$ are given by

$$\mathcal{H}^{1,0} = \frac{\partial \mathcal{H}(\vec{B}, \vec{m}_k)}{\partial B_s} = \frac{1}{2c} \sum_i (\vec{r}_i \times \vec{p}_i)_s + \frac{1}{c} \sum_i \vec{s}_{is} \tag{2.116}$$

$$\mathcal{H}^{0,1} = \frac{\partial \mathcal{H}(\vec{B}, \vec{m}_k)}{\partial m_{K_t}} = \mathcal{H}^{para} + \mathcal{H}^{SP} + \mathcal{H}^{FC} \tag{2.117}$$

$$= \underbrace{\frac{1}{c} \sum_i \frac{(\vec{r}_{Ai} \times \vec{p}_i)t}{\vec{r}_{Ai}^3}}_{\text{para}} \tag{2.118}$$

$$+ \frac{1}{c} \left(\underbrace{\frac{3\vec{r}_{Ait}(\vec{s}_i \cdot \vec{r}_{Ai}) - \vec{s}_{it}\vec{r}_{Ai}^2}{\vec{r}_{Ai}^5}}_{\text{SP}} + \underbrace{\frac{8}{3}\pi\delta(\vec{r}_{Ai}\vec{s}_{it})}_{\text{FC}} \right) \tag{2.119}$$

$$\mathcal{H}^{1,1} = \frac{\partial^2 \mathcal{H}(\vec{B}, \vec{m}_k)}{\partial B_s \partial m_{K_t}} = \mathcal{H}^{dia} = \frac{1}{2c^2} \sum_i \frac{\vec{r}_i \cdot \vec{r}_{Ai}\delta_{st} - \vec{r}_{it}\vec{r}_{Ais}}{\vec{r}_{Ai}^3} \tag{2.120}$$

The diamagnetic $\mathcal{H}^{dia}$ and paramagnetic Hamiltonian $\mathcal{H}^{para}$ are the same as in the non relativistic case. Due to the SOC interaction, two additional terms result from the derivative of the nuclear magnetic moment, the SD and FC term. Therefore the relativistic shielding tensor can be written as

$$\sigma_{st}^{Rel} = \langle \xi | \mathcal{H}^{dia} | \xi \rangle + \frac{\partial}{\partial B_s} \langle \xi(\vec{B}) | \mathcal{H}^{para} | \xi(\vec{B}) \rangle \tag{2.121a}$$

$$+ \frac{\partial}{\partial B_s} \langle \xi(\vec{B}) | \mathcal{H}^{SD} | \xi(\vec{B}) \rangle \tag{2.121b}$$

$$+ \frac{\partial}{\partial B_s} \langle \xi(\vec{B}) | \mathcal{H}^{FC} | \xi(\vec{B}) \rangle \tag{2.121c}$$

HALA effect Shielding and deshielding effects in NMR spectroscopy can be explained by larger or smaller electron densities. The effect can also be observed for light elements close to heavy elements, especially when comparing elements of the same group in the periodic table e.g. IHD. Many spectroscopics also talk about shielding or deshielding. However, this effect can be explained by the interaction between the nuclear spin and an unpaired electron spin by a FC mechanism. The FC contribution

is considered due to the SOC. This contribution is a central part in the explanation of the HALA effect in the SO-FC mechanism[53]. Note that scalar relativistic effects are negligible.[54, 55]

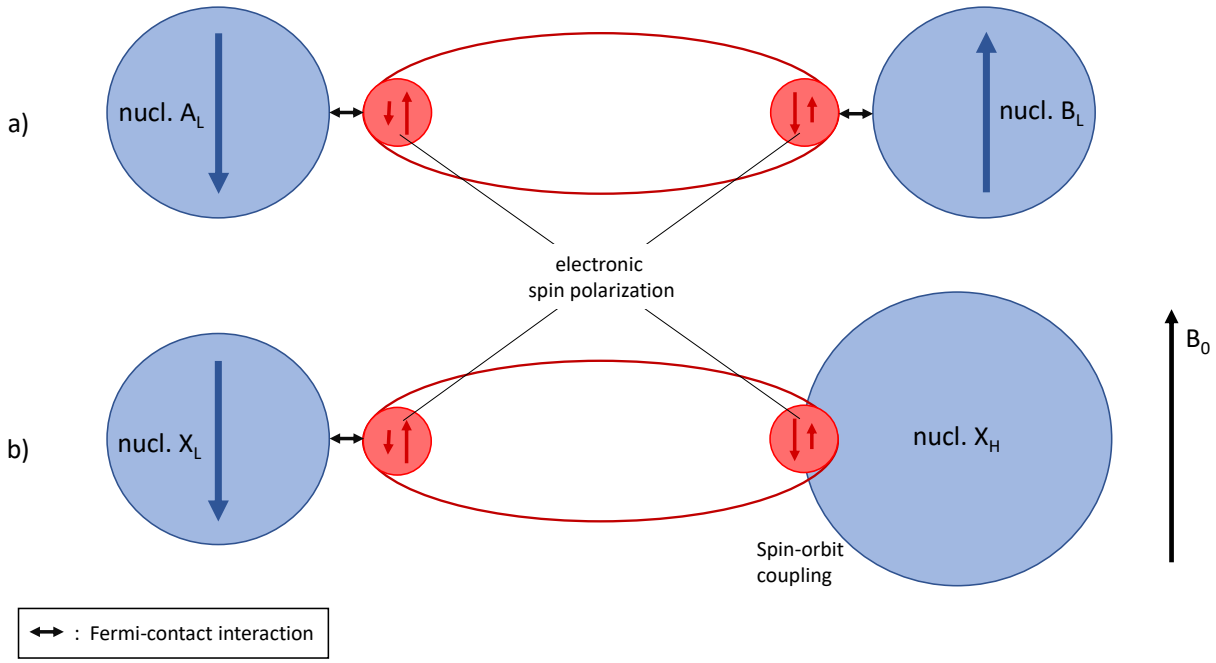

Figure 2.1: Schematic illustration of a) FC spin-spin coupling and b) SO-FC mechanism.

Due to the presence of the nuclear-magnetic moment close to the spin of the electrons in the inner shell, spin-polarization results (left side of fig. 2.1). If there is two nuclei A_L and B_L next to each other, the spins of the electrons interact and further spin polarization occurs. The polarized spin density interacts via FC with the nuclear-magnetic moment (left side of Fig. 2.1a).

In case of the neighborhood of a light X_L and a heavy atom X_H (HALA), further spin-polarization is generated by SOC of the heavy atom, by mixing singlet and triplet states (right side of Fig. 2.1). The polarized spin density by SOC interacts via FC with the nuclear-magnetic moment (left side of Fig. 2.1b)[56] and the influence of the nuclear spin induces shielding or deshielding[57]. Note that there are many other HALA effects, but in this thesis the focus is on the SO-HALA effect.

2.5. New Implementations in *ORCA*

The following new approaches in *ORCA* are not implemented by me. There will be a short explanation of what was done.

2.5.1. NMR shielding Tensor with the inclusion of spin-orbit-coupling

In the new implementation a simple approach was used to calculate the SO corrections of the isotropic NMR shieldings. For this purpose the non-relativistic density is perturbed by a SOC Hamiltonian. This mixes the singlet and triplet states, thus a polarized density is obtained. The response to the magnetic field is calculated for the new density. The individual steps are explained in more detail below.

When a non-relativistic KS determinant is perturbed by a SOC Hamiltonian, the obtained complex determinant is diagonalized by

$$\psi_i^\sigma = \sum_{k\alpha} d_{k_\alpha i} \left|\phi_k^\alpha\right\rangle + \sum_{k\beta} d_{k_\beta i} \left|\phi_k^\beta\right\rangle \tag{2.122}$$

ϕ_k^σ are the restricted KS-MOs. The MOs are expanded as usual in basis functions χ with molecular orbital (MO)-coefficients, but are blocked by the spin 2.123.

$$\phi_k^\sigma = \sum_\mu c_{\mu k}^\sigma \underbrace{\left|\chi_\mu\right\rangle \otimes \left|\sigma\right\rangle}_{\chi_\mu^\sigma} \tag{2.123}$$

Note that σ denotes the spin.

Since the SOC Hamiltonian mixes singlet and triplet states and the non relativistic α and β MOs are still identical, the polarized SOC-MO coefficients $\tilde{c}_{\mu i}^\sigma$ must be transformed with the polarized coefficients $d_{k_\sigma i}$ as

$$\tilde{c}_{\mu i}^\sigma = \sum_{k_\sigma} d_{k_\sigma i} c_{\mu k}^\sigma \tag{2.124}$$

therefore the polarized KS determinant can be written in AO basis functions as

$$|\psi_i^\sigma\rangle = \sum_\mu \left(\tilde{c}_{\mu i}^\alpha \, |\chi_\mu^\alpha\rangle + \tilde{c}_{\mu i}^\beta \, |\chi_\mu^\beta\rangle \right) \tag{2.125}$$

Note that GIAOs are used as basis functions.

The polarized complex density $\tilde{P}_{mu\nu}^{\sigma\sigma'}$ is formulated in real and imaginary parts. The real part can be used to determine the diamagnetic contribution σ^{dia} to the NMR shielding by

$$\begin{aligned} \sigma_{st}^{dia} &= \langle \Psi | \mathcal{H}_{B_s, m_{K_t}}^{1,1} | \Psi \rangle \\ &= \sum_{\mu\nu} \tilde{P}_{\mu\nu} \, \langle \chi_\mu^\sigma | \mathcal{H}_{B_s, m_{K_t}}^{1,1} | \chi_\nu^{\sigma'} \rangle \end{aligned} \tag{2.126}$$

$$\text{with } \mathcal{H}_{B, m_K}^{1,1} = \frac{1}{2c^2} \frac{(r_k \cdot r_{Nk})\mathbf{1} - r_k \tilde{r}_N + i\mathbf{Q}_{MN} r \tilde{L}_K}{r_k^3} \tag{2.127}$$

where $\frac{1}{c^2}$ results from the fine-structure constant in atomic units. $\mathbf{Q}_{MN}$ denotes an anitsymmetric matrix containing the positions of the nuclei. $\tilde{r}_N$ and $\tilde{\mathbf{L}}_K$ are the transposed forms (for more details see [28]). Note that L_K is complex; $L_K = ir_k \times \nabla$.[28]

For the calculation of the derivative of the polarized SOC density $\tilde{P}_{\mu\nu}$ with respect to the magnetic field B, the polarized SOC coefficients $\tilde{c}_{\mu i}^\sigma$ are expanded in the basis of the perturbed CPHF coefficients u_{qp} (2.61, 2.62). Therefore, the paramagnetic contribution can be formulated as in 2.128 by using the derivative of the Hamiltonian with respect to the nuclear-magnetic moment (2.129).

$$\begin{aligned} \sigma_{st}^{para} &= \frac{\partial}{\partial B_{k_s}} \langle \Psi | \mathcal{H}_{B_s m_{K_t}}^{0,1} | \Psi \rangle \\ &= \sum_{\mu\nu} \mathbf{u}_{\mu\nu}^{\sigma\sigma'} \, \langle \chi_m u | \mathcal{H}_{B_s m_{K_t}}^{0,1} | \chi_n u \rangle \end{aligned} \tag{2.128}$$

$$\text{with } \mathcal{H}_{B_s m_{K_t}}^{0,1} = \frac{1}{c^2} \frac{L_K}{r_k^3} \tag{2.129}$$

$\frac{1}{c^2}$ results again from the fine structure constant in atomic units. Note that the diamagnetic part is purely imaginary.

In addition to the dia- and paramagnetic contributions, the response of the magnetic field only includes the FC contribution in this approach. This can be calculated by

$$\begin{aligned}
\sigma^{FC} &= \frac{\partial}{\partial B_{k_s}} \langle \Psi | \mathcal{H}^{FC} | \Psi \rangle \\
&= \frac{\alpha^2 8\pi}{3} \sum_{\mu\nu} \mathbf{u}_{\mu\nu}^{\sigma\sigma'} \langle \chi_\mu^\sigma | \delta(r_K) \mathbf{S} | \chi_\nu^\sigma \rangle \\
&= \frac{\alpha^2 8\pi}{3} \sum_{\mu\nu} \mathbf{u}_{\mu\nu}^{\sigma\sigma'} \langle \sigma | \mathbf{S} | \sigma' \rangle \langle \chi_\mu | \delta(r_K) | \chi_\nu \rangle \\
&= \frac{\alpha^2 8\pi}{3} \sum_{\mu\nu} \mathbf{u}_{\mu\nu}^{\sigma\sigma'} \mathbf{S}^{\sigma\sigma'} \langle \chi_\mu | \delta(r_K) | \chi_\nu \rangle
\end{aligned} \tag{2.130}$$

$$\text{with } \mathcal{H}^{0,1}_{B_s m_{K_t}} = \frac{\alpha^2 8\pi}{3} \delta(r_K) s \tag{2.131}$$

2.5.2. Pilot implementation RIZORA

Calculations based on the ZORA method are grid dependent, through the numeric integration for obtaining Hamiltonian matrix elements.[38, 40] The approach of Cremer and Filatov[58] allows the fully analytic calculation of Hamiltonian matrix elements using e.g. ZORA. Based on their idea, there now is a pilot implementation in *ORCA* to calculate the paramagnetic contributions to the shielding tensor via RIZORA.

The integral of the paramagnetic contribution is transformed to

$$\begin{aligned}
\sigma^{para} = 2 \langle \frac{\partial}{\partial B_s} \Psi | i \mathcal{H}^{para} & \\
&+ \mathbf{W}\mathbf{T}^{-1} \mathcal{H}^{para} \mathbf{T}^{-1} \mathbf{W} \\
&+ \mathbf{W}\mathbf{T}^{-1} \mathcal{H}^{para} \mathbf{W}_0^{-1} \mathbf{W} \\
&+ \frac{i}{2m} \mathbf{W}\mathbf{W}_0^{-1} \mathcal{H}^{para} \mathbf{T}^{-1} \mathbf{W} \, | \Psi \rangle
\end{aligned} \tag{2.132}$$

As seen in 2.132, further matrices are used to determine the RIZORA integrals. In the ZORA case (2.107), minimal substitution (2.69) results in an operator with terms containing r^{-3} and r^{-6}. These are unpleasant for the numerical integration. Using of $\mathbf{T}^{-1}$, which is the inverse kinetic integral matrix, the integral is determined analytically. Since $\frac{1}{V(r)}$ integrals appear in the ZORA method, the matrix $\mathbf{W}_0$ is necessary to make them analytically integrable. $\mathbf{W}_0$ is given by

$$(\mathbf{W}_0)_{\mu\nu} = \frac{1}{4m^2c^2} \langle \chi_\mu | (\sigma \cdot p) V_{eK} (\sigma \cdot p) | \chi_{nu} \rangle \tag{2.133}$$

and the $\mathbf{W}$ matrix is given by

$$\mathbf{W} = \mathbf{W}_0 + \mathbf{W}_0 \mathbf{T}^{-1} \mathbf{W} \tag{2.134}$$

Using this approach $\mathbf{W}_0$, $\mathbf{W}$, $\mathbf{W}_0^{-1}$, $\mathbf{T}$ and $\mathbf{T}^{-1}$ are calculated beforehand and then the paramagnetic contribution via RIZORA can be calculated (2.132).

Note that in the paper [58] spin-spin couplings constants are discussed and the final expression contains only the first two terms.

3. Computational Details

The calculations were performed with three quantum chemical programs. Among them are *ORCA*[1], *NWChem*[59] and *Dirac*[60]. The 4.2.1 version of *ORCA*, the 7.0.0 version of *NWChem* and *Dirac*19 were employed. The *Avogadro*[61] program was used for the construction of the molecular structures.

The geometry optimization was pre-calculated in *ORCA* using DFT with B3LYP[14–16]. Furthermore the def2-TZVP[62] basis set, tightscf and grid 7 were used. Note that from krypton on there is no all-electron basis set, but the *Stuttgart-Dresden* effective core potentials (ECPs) are selected as default. However, these geometries were not used for further calculations except for the bismuth compounds. *NWChem* performs a symmetrization step of the geometries, which does not result an absolutely identical structure and it was not possible to turn this off. This resulted different nuclear repulsion energies compared to the *ORCA* geometry. For this reason, a single point or property calculation was first performed with the obtained structures from *ORCA* in *NWChem*, and the transformed geometry were used for further calculations.

Property calculations were performed using DFT with BP86. The def2-TZVP[62] basis set was chosen for the light atoms and the Sapporo-TZP-2012[63] for the heavier atoms. The Sapporo-TZP-2012 basis set is only available up to xenon, therefore for heavy elements (6th period) Sapporo-DKH3-TZP-2012[64, 65] was used. Note that the default setting for heavier nuclei than krypton in *ORCA* contains ECPs in the basis set. These default setting have been disabled. The basis sets used in *NWChem* were loaded from the *Basis Set Exchange*[66], but the exponents of the con-

tracted basis functions in the def2-TZVP basis set differ from the *ORCA* exponents. For that reason the exponents from *ORCA* were transferred to the *NWChem* input file. In addition, each comparison calculation must take into account that *NWChem* by default uses Cartesian Gaussian functions, whereas *ORCA* employs spherical harmonics. Therefore *NWChem* was also switched to spherical harmonics Gaussian functions. The latter point is absolutely important to achieve the same results with *ORCA* and *NWChem*.

The *Dirac* calculations were performed both with a four-component Hamiltonian and two different two-component Hamiltonians. The four-component Hamiltonian was the default Hamiltonian, which is the Dirac-Coulomb Hamiltonian in which the two-electron integrals over the small-component are neglected.[67] The calculation using the four-component approach is split into two calculations: first the SCF and then the property calculation. The SCF calculation used RKB and in the property calculation the UKB is switched on. For atoms lighter than Ar the aug-cc-pVQZ basis set was used and from argon on the dyall.ae4z basis set. The non-relativistic four-component limit is calculated with the Levy-Leblond Hamiltonian. This procedure is suggested by the *DIRAC* manual. The X2C and BSS two-component Hamiltonians were used. Their non-relativistic limits were reached by setting the speed of light to 2000. Using X2C, the scalar-relativistic case is calculated by the keyword "spinfree". In case of the BSS Hamiltonian, the keyword "099" activated scalar-relativistic+SOC. In the scalar-relativistic case, the keywords "109" and "spinfree" were used instead of "099". London orbitals were switched on in case of property calculations. By using the keyword "spinfree", the scalar-relativistic case was calculated. In all *Dirac* calculations, the dyall.ae2z, dyall.ae2z and aug-cc-pVQZ basis

sets are used in their uncontracted forms.

4. Results

4.1. Benchmark Set

In a first approach, examples were selected from the literature to create a good benchmark set. The examples should contain DFT and ZORA computations with and without SOC and all parameters and values should be given in detail in the literature. To match the literature values with *ORCA* in the first step, non relativistic calculations were performed in those settings that fit the results from the literature. When this was fulfilled, scalar relativity was switched on by using ZORA Hamiltonian. However, some difficulties arose in the first step which did not allow for an absolute agreement with the results reported in the literature. One problem was to find suitable examples. Most of the published values from literature were calculated by using the *Amsterdam Density Functional (ADF)* package from *Baerends et al.* [68][69][70]. As *ADF* employs Slater-type orbitals instead of Gaussian basis sets, a one-to-one comparison of results proved to be difficult. As particularly suitable proved the papers by *Hayashi* et. al [71], by *Franzke* and *Weigend*[18] and by *Antušek* et. al [72].

A series of selenium and tellurium compounds was selected from the *Hayashi* [71] paper. The authors also specify the individual ZORA results for the selenium, but not for the tellurium compounds. They used the *ADF* 2013 package[73–75] in conjunction with the BLYP[14, 15] functional. For this reason, the same functional was chosen it the *ORCA* calculations. Various basis sets in the *ORCA* calculations were tested to obtain the non-relativistic values matching to the published values of *Hayashi* [71] (see table 4.1). The only limitation for the choice of the basis set was to avoid ECPs, thus an all-electron basis set was chosen. The results of

the comparison of the non relativistic (NR) and scalar relativistic (scR) ZORA-values are shown in 4.1 and the used basis set is listed.

Xenon fluoride compounds were selected from the publication of *Franzke* and *Weigend*[18]. They used the *TURBOMOLE*[76–78] program with BP86[14, 17] and different basis sets for the xenon and the fluorine atom. For xenon the TZVPaals2 and for fluorine the def2-TZVP basis set was chosen. Since the xenon basis set was not available, different basis sets were tried for these compounds. The Sapporo-DZP-2012 in combination with the simple keyword "autoaux" proved to be a good solution for an agreement. The basis sets for fluorine were different and listed with the results.

Lastly, iron hexacarbonyl was selected from the *Antušek*[72] paper. *Antušek et al.* calculated with the *NWChem*[59] program, the B3LYP[14–16] functional, the uncontracted ANO-RCC basis set for iron and the uANO.ucc-pVDZ basis set for the other lighter atoms. In the *ORCA* calculation, the def2-QZVPPD for iron and the cc-pVDZ basis set proved to be a good choice.

All calculations were carried out with the RI-approximation activated with the simple keyword 'autoaux', which activates the automatic generation of a near-complete auxiliary basis set.[79] Additionally, grid 6 and the keyword 'verytightscf' were chosen. Note that in any calculation with an atom heavier than krypton, the keyword 'DelECP' was also used to ensure an all-electron base set for this atom.

Table 4.1: Calculated NR- and scR-NMR shieldings of some molecules by using the *ORCA* program. As scalar relativistic Hamiltonian was used the ZORA-Hamiltonian. The deviations to the literature are shown in percent.

Molecule	**Orca** Shielding NR (scR)[ppm]	**Literature**[71][18][72] Shielding NR (scR) [ppm]	**Deviation NR (scR) [%]**
SeH_2	2093.16 (2057.49)[1)]	2093.00 (1978.20)	0.01 (4.01)
$SeMe_2$	1580.27 (1614.17)[2)]	2093.00 (1978.20)	2.34 (8.28)
SeF_4	367.89 (475.14)[3)]	375.20 (323.10)	1.95 (47.06)
$SeCl_4$	154.75 (251.56)[4)]	144.50 (-66.00)	7.09 (481.15)
XeF_2	2503.85 (2807.77)[5)]	2492.00 (2213.00)	0.48 (26.88)
XeF_4	91.01 (664.32)[6)]	109.00 (-513.00)	16.50 (299.50)
XeF_6	-64.21 (274.86)[7)]	-71.00 (-485.00)	9.56 (156.67)
$Fe(CO)_5$	-2654.14 (-2640.41)[8)]	-2627.00 (-2490.00)	1.03 (6.04)

Each caclulation was done with the simple keyword autoaux, verytightscf and grid 6;
1) def-QZVPP 2) def-QZVPPD 3) F: SV; Se TZV 4) Cl: SVP; Se: TZV(P) 5) F: def2-TZVP; Xe: Sapporo-DZP-2012 6) F: TZV; Xe: Sapporo-DZP-2012 7) F: def2-TZVP; Xe: Sapporo-DZP-2012 8) C/O: cc-pVDZ; Fe: def2-QZVPPD

It can be clearly seen from the values that by adjusting the basis sets, the non relativistic calculations agree well with the values from the literature in the most cases. In some cases, despite enlargement and reduction of the basis set size, no deviation as small as for the others could be found.

A very good match, that means deviation below 0.5 %, of the tested basis sets in a non relativistic calculation is found with hydrogen selenide (H_2Se), followed by xenon difluoride (XeF_2). Also in good agreement is dimethyl selenide ($SeMe_2$), selenium tetrafluoride (SeF_4) and iron hexacarbonyl ($Fe(CO)_6$). Not such a good match was obtained for selenium tetrachloride ($SeCl_4$) and xenon hexafluoride (XeF_6) because their deviations are in the range between about 7-10 %. A really poor match is found with xenon tetrafluoride (XeF_4), the deviation is larger than 16 %. It was not possible to find out where the large deviations come from.

By switching on the ZORA-Hamiltonian, however, much larger deviations were obtained in all cases. Even the initially very small deviation for H_2Se increases from 0.01 % to 4 %. SeF_4 and XeF_4 are particularly

affected by this increasing deviation. Possible reasons for the deviations of the selenium compounds are due to the non-identical implementations of the ZORA Hamiltonian in *ADF* and *ORCA*. For the xenon compounds, a completely different and much more accurate theory was used, since Franzke and Weigend *et al.*[18] calculated the scalar-relativistic corrections using a two-component theory. In the case of $Fe(CO)_5$, solvent effects were also taken into account. Furthermore there is no information in the published data about used the accuracy of the numerical integrations. Some *ORCA* calculations resulted in problems of achieving convergence. It can be said, that the large number of possible error sources leads to very large differences from published values.

If the deviation for the non relativistic calculations was in the same range as the scalar relativistic ones, the values might have been used for comparison and the approach via published values might have been successful. However, this is not the case. For these reasons this approach to generate a suitable benchmark set by comparing it with known literature was dropped.

Note that there were some more molecules that have been calculated with *ORCA* and compared to the literature (see the appendix A.1). The large deviations between *ORCA* using ZORA and literature values do not only occur from the shown compounds (4.1), the deviations are also found for the other compounds.

In a new approach, a benchmark set was compiled for the p-block elements. The *ORCA* values were compared with values of an independent implementation at the same level. *NWChem* was used as a comparison quantum chemistry package because it fulfills this requirement and was

available. Among the benchmark molecules are the trifluorides of the 13th group, tetrahydrogens of the the 14th group, trimethylenes and trifluorides of the pnictogens, dihydrogens of the chalcogens, hydrogen compounds of the halogens and di-, tetra- and hexafluorides of the nobel gases. The structures were computed as described in the computational details (sec. 3).

To verify the optimized geometries, calculations were first performed at the lowest theory level, HF. It was also used to determine the correct settings for both *ORCA* and *NWChem*. For example, the default setting of *NWChem* of the spherical harmonics basis functions was found out and changed accordingly. For HF-calculations by *ORCA*, verytightscf and the SCF mode direct was chosen. The RI-approximation was switched off by the "eprnmr"-block through the argument of the analytical integration of the one- and two-electron terms. The settings in the *NWChem* program were also the SCF mode direct, the symmetrization of the wave function coefficients was switched off and the integral screening threshold was set to 10^{-9}. Note, that no ZORA-calculation was performed by this theory-level, because *NWChem* 7.0.0 did not make this possible. There was a communication error in the program.

The calculations with *ORCA* and *NWChem* were compared to the nuclear-repulsion energy and the converged SCF energy. The first one was chosen to prove that both use the same geometry. As a result, it was found that *NWChem* performs a non-disabled geometry symmetrization. Therefore the path of obtaining the structures was chosen as described in the computations details (sec. 3). The values of the nuclear repulsion energy for the chalcogen compounds are shown in table 4.2.

Table 4.2: Calculated nuclear repulsion energies at HF-level (values in hartree) with *ORCA* and *NWChem*. The deviation between the programs are given in percent.

Molecule	**nuclear repulsion energy**		**Deviation**
	ORCA [E_h]	*NWChem* [E_h]	[%]
H_2O	9.1382847	9.138285401878	$7.68 \cdot 10^{-6}$
H_2S	12.88104165	12.881042594728	$7.33 \cdot 10^{-6}$
H_2Se	24.71573959	24.715741491088	$7.69 \cdot 10^{-6}$
H_2Te	33.34233604	33.342338603648	$7.69 \cdot 10^{-6}$
H_2Po	51.01184488	51.011848833325	$7.75 \cdot 10^{-6}$

For nuclear repulsion energies, the values are expected to be identical up to the last decimal place. Despite using the same geometries in *ORCA* and *NWChem*, the values do not match to the 6th decimal place. This is because *NWChem* does not work with the same unit of the given geometry. The geometries were given in Ångström. However, *NWChem* calculated with atomic units and the transformation factor is not quite identical to that of *ORCA*. It was tested how much the SCF energies differ when *NWChem* gets the geometry in a.u., calculated with the *ORCA* transformation factor. Nevertheless the same SCF energies are obtained. The values of the other molecules are given in the appendix (tab. A.2 and A.3).

The comparison of the last SCF energy was made to verify the other settings. The values for the final used set up of the last SCF energy are shown in Table 4.3.

Table 4.3: Calculated last SCF energies at HF-level (values in hartree) with *ORCA* and *NWChem*. The deviation between the programs are given in percent.

Molecule	**last SCF energy**		**Deviation**
	ORCA [E_h]	*NWChem* [E_h]	[%]
H_2O	-76.04806822	-76.048068229300	$1.22 \cdot 10^{-8}$
H_2S	-398.67618702	-398.676187024500	$1.13 \cdot 10^{-9}$
H_2Se	-2401.00010831	-2401.0001083141	$1.71 \cdot 10^{-10}$
H_2Te	-6612.82429920	-6612.8242992028	$4.23 \cdot 10^{-11}$
H_2Po	-17557.35466	-17557.3546577044	$7.75 \cdot 10^{-11}$

The calculated SCF energy values fit well. The deviations of the SCF

energies are even smaller than the deviations of the nuclear repulsion energy (Tab. 4.2). This suggests a comparable set up for further calculations. Therefore the isotropic shieldings were compared. The values are given in Table 4.4. A deviation of 0.5 % was selected as good agreement value.

Table 4.4: Calculated isotropic shieldings of the heavier element at HF-level (values in ppm) with *ORCA* and *NWChem*. The deviation between the programs are given in percent.

Molecule	**isotropic shielding**		**Deviation**
	ORCA [ppm]	*NWChem* [ppm]	[%]
H_2O	334.223	334.0442	0.05
H_2S	700.108	700 0762	$4.54 \cdot 10^{-3}$
H_2Se	2148.434	2148.7222	0.01
H_2Te	3694.095	3695.20448	0.03
H_2Po	217.248	217.8863	0.29

The values of the isotropic shieldings of the chalcogens show a very good agreement. The deviation between the results of the two programs are below 0.5 %. The same results are found for the other molecules (see the appendix tab. A.2 and A.3) except RnF_6 and PbH_4, for which large deviations were found.

Since the majority of molecules turned out to be suitable, non-relativistic DFT calculations were performed to reproduce the results with this method.

The settings in the DFT-calculations in the *ORCA*-program were grid 6 with nofinalgrid, again the SCF-mode direct, the RI-approximation was turned off by the above arguments as with the HF-calculation and the additional simple keyword 'conv'. In addition, the tolerance of the energy between two cycles was set to 10^{-9} E_h, the maximum of the change of the density was set to 10^{-8} and the orbital gradient convergence to 10^{-6} were chosen as tight convergence criteria. In the *NWChem* program the settings were chosen very close to *ORCA*, including the grid setting fine and the convergence settings of the energy, density and of the gradient to 10^{-9} E_h, 10^{-8} and 10^{-6}. Furthermore, the radial- und angular grids were specified

by *Gausschebychev* and *Lebedev* 14.

The calculated isotropic shieldings for the chalcogens are listed in Table 4.5.

Table 4.5: Calculated isotropic shieldings of the heavier element at DFT-level (values in ppm) with *ORCA* and *NWChem*. The deviation between the programs are given in percent.

Molecule	**isotropic shielding**		**Deviation**
	ORCA [ppm]	*NWChem* [ppm]	[%]
H_2O	333.238	333.2605	0.01
H_2S	692.054	692.4586	0.06
H_2Se	2064.058	2065.0663	0.05
H_2Te	3528.554	3530.4475	0.05
H_2Po	2340.202	2349.8693	0.41

The deviations between the two programs using DFT in the non relativistic case are still below 0.5 %. For this reason the values are considered to be fitting. With the same input files and the additional activation of ZORA the scalar relativistic calculations were performed and listed in Table 4.6 for the chalcogen dihydrides.

Table 4.6: Calculated scalar-relativistic isotropic shieldings of the heavier element at DFT-level (values in ppm) with *ORCA* and *NWChem*. The deviation between the programs are given in percent.

Molecule	**isotropic shielding**		**Deviation**
	ORCA [ppm]	*NWChem* [ppm]	[%]
H_2O	332.793	332.6463	0.04
H_2S	689.279	687.8733	0.20
H_2Se	2035.598	2018.5956	0.84
H_2Te	3562.821	3504.6881	1.66
H_2Po	5057.567	5043.6337	0.28

As can be seen from the results in Table 4.6, most deviations are below 0.5 %. However, a greater difference between the two programs can be found for the 5th period (TeH_2). In the other groups (13-18, see the appendix A.6 and A.7) the same can be observed. There, larger deviations already occur from the 5th period onward and remain in the 6th period.

The differences in the isotropic shieldings can originate from different sources. The deviation of the last SCF energies are larger for the ZORA

case than the NR values. The deviations of the NR values are in the range of 10^{-3}-10^{-5} E_h, for the ZORA calculations they are already larger than 1-10^{-2} E_h (tab. A.6 and A.7). The deviation can be observed for the heavier atoms such as Te, Bi etc. where the ZORA correction is than for the light nuclei. It is possible that the different implementations of ZORA in *ORCA* and *NWChem* result in slightly different values. The numerical integration is characterized by the grid, so DFT calculations are grid dependent. However, there is another grid-dependent part in the calculations. The Hamiltonian matrix is also formed via numerical integration, because of using the ZORA Hamiltonian. Thus there is a higher grid dependence than in the NR DFT calculations. This can be the reason for the deviations of the SCF energies and the isotropic shielding constants. The sum of several small errors can lead to a deviation of 1-2 %.

4.1.1. Grid dependency of ZORA calculations

How much the calculated isotropic shieldings depend on the grid is shown below. To this end a sample calculation for TeH_2 was performed. As Table 4.6 shows, there is a bigger difference in the isotropic shielding between *ORCA* and *NWChem*. Therefore the same level of theory as used for the calculation of the values in Table 4.6, was chosen and the grid was varied between 4 and 7. The grid dependencies of the diamagnetic (a) and paramagnetic (b) contributions and the total isotropic shielding (c) are shown in Figure 4.1.

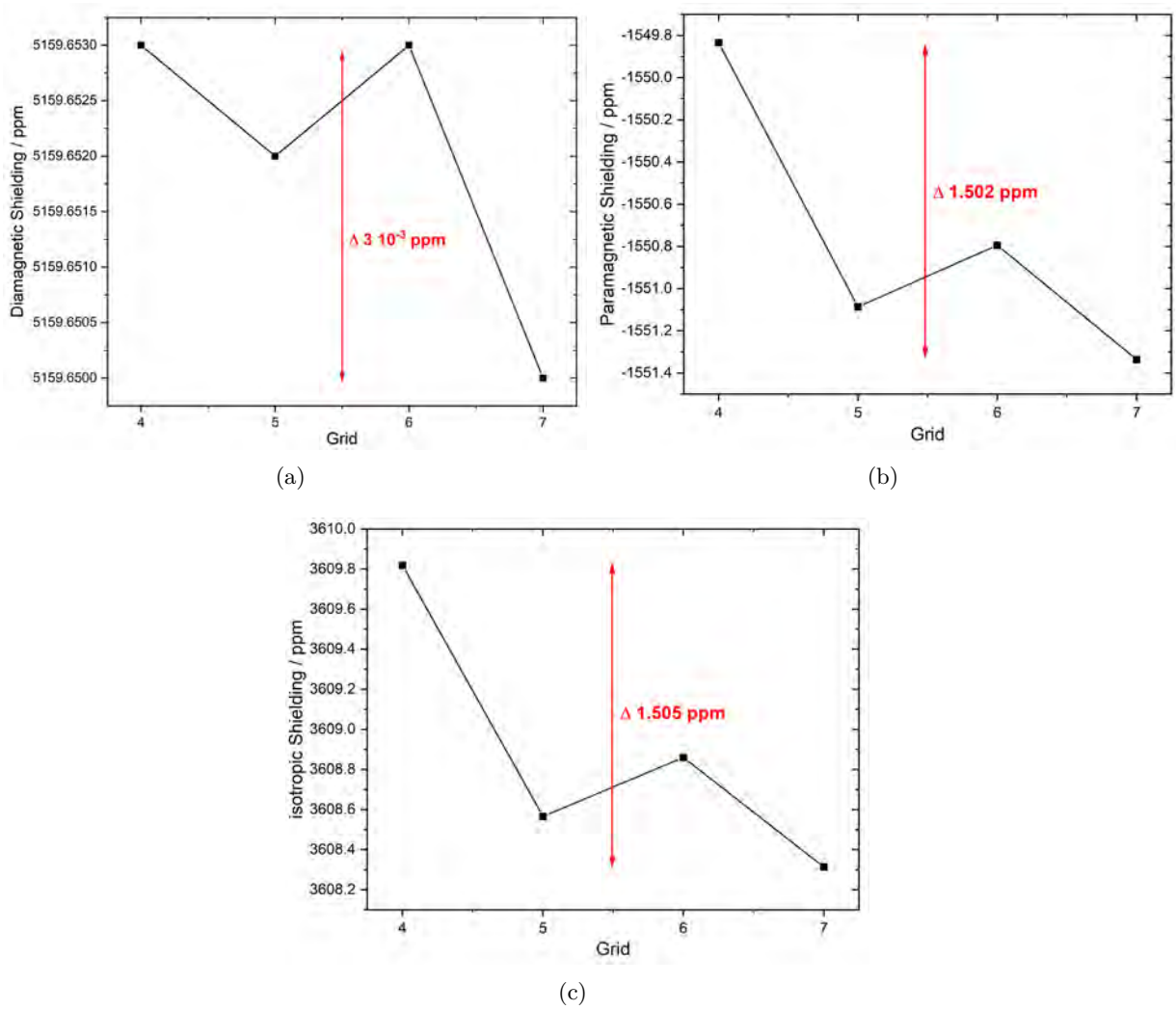

Figure 4.1: Using BP86 to show the grid dependence of the NMR ZORA calculation of TeH_2. Shown are the isotropic shieldings of the Te-atom: in a) the diamagnetic b) the paramagnetic contribution and in c) the total isotropic shielding.

Obviously, the diamagnetic and paramagnetic contributions and thus the total isotropic shieldings are grid dependent. However, the axes scales of subfigures a-c in Figure 4.1 must be considered. The diamagnetic contribution has a significantly lower grid dependence of just $3 \cdot 10^{-3}$ ppm. The paramagnetic contribution varies by about 1.5 ppm. Therefore the total isotropic shielding varies by the same value. Assuming that *NWChem* also has this order of magnitude of grid dependency, the grid dependency cannot be the reason for the increasing deviation between *ORCA* and *NWChem* in Table 4.6 by switching on the ZORA Hamiltonian.

The grid dependence of the isotropic shielding of the H-atom in TeH_2 is significantly lower. The corresponding figure is shown in the appendix (Fig. A.1). Between grid 4-7 there is no grid dependence of the diamagnetic contribution and a small grid dependence of $1 \cdot 10^{-3}$ ppm for the paramagnetic and thus also for the total isotropic shielding. A good grid setting is the choice of grid 6, where only a small grid error can be assumed.

4.2. RIZORA

The pilot implementation of RIZORA (sec. 2.5.2) should eliminate the grid dependency of the paramagnetic part. Thus the only grid dependency is given by DFT integration. For the dioxo compounds of the chalocogens, the paramagnetic part was calculated with ZORA and RIZORA at different grids between 4-7. The same calculations were performed for the trifluoride compounds of the 15th group, shown in the appendix. The level of theory is described in the computations section (sec. 3) for property calculations. Additionally, the RI-approximation by using "autoaux" and decontracted basis sets by activating the keyword "decontract true" were used. For the 6th period "kdiis", another SCF algorithm was used and "nososcf" was activated. These keywords helped to converge the calculations.

The calculated values of the grid dependency of ZORA compared to RIZORA were normalized to grid 7 RIZORA. This point was chosen because a visible faster grid convergence is achieved with RIZORA. The results for the 16th group are shown in Figure 4.2 (and for the 15th group in the Appendix A.3). Note that filled circles denote the ZORA values and the rings the RIZORA values.

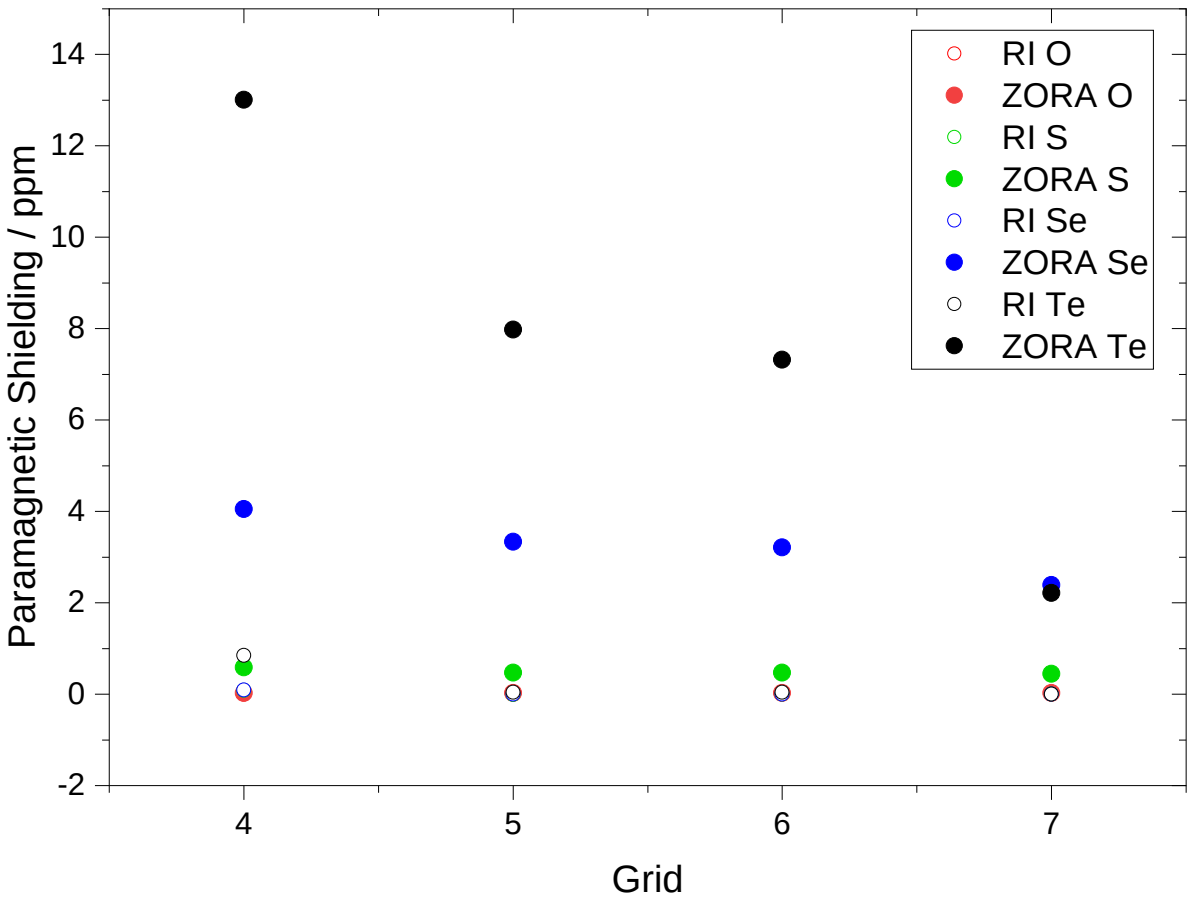

Figure 4.2: Grid dependece of the paramagnetic contribution of the dioxo compounds of the 16th group. Shown for the heavy atom. Comparison of RIZORA (filled circles) and ZORA (open circles). All values were normalized to Grid 7 from RIZORA for the individual compound.

Figure 4.2 shows that there is a larger grid dependence for the paramagnetic contribution of the ZORA calculation. The size of the grid dependence increases significantly from O to Te. The small grid dependence of O is hidden by the other spots. The individual figures of the grid dependencies of ZORA and RIZORA for each heavy atom are shown in the Appendix (Fig. A.2).

The goal to reduce the grid dependence of the paramagnetic contribution by RIZORA is fulfilled. The open circles in Figure 4.2 representing the RIZORA values reach the zero line very early. Therefore it can be assumed that a small grid (e.g. grid 5) and the use of RIZORA provides very good paramagnetic contributions. The computation times of the NMR

calculation using ZORA and RIZORA are listed in Table 4.7.

Table 4.7: Comparison between ZORA and RIZORA of the calculated isotropic paramagnetic shieldings and the compution time of the NMR calculation. Using of grid 7 and "nofinalgrid".

Molecule	**paramagnetic isotropic shielding**			**Time** [s]	
	RIZORA [ppm]	ZORA [ppm]	Deviation [%]	RIZORA	ZORA
H_2O	-55.335	-55.311	0.04	121.005	16.367
H_2S	-361.345	-360.900	0.12	268.117	32.088
H_2Se	-975.089	-972.698	0.25	814.789	99.331
H_2Te	-1987.447	-1985.233	0.11	1110.57	130.15
H_2Po	-4097.247	-4485.596	8.66	1381.427	189.222

From the columns of the isotropic paramagnetic shielding (Tab. 4.7) it can be seen that the error of RIZORA to ZORA is not very large until the 5th period. This error is below 0.25 % (H_2Se). For the 6th period, the results of ZORA and RIZORA start to differ significantly. This result is consistent with the other groups (13-18) in the p-block of the periodic table. The values are listed in the Appendix in table A.8. Looking at the times it is clear that RIZORA takes ten times more time to calculate the shieldings than using ZORA. It can be concluded that the grid dependency has been successfully eliminated by the test implementation of RIZORA and could be used up to the 5th period. However, if RIZORA is to be used in production level version, the efficiency of the implementation has to be improved significantly.

4.3. SOC Implemenation

Before the benchmark molecules are calculated with the new SOC implementation in *ORCA*, the convergence with the basis set size, the dependence of the results on the functionals and the variation of the results by using using other SOC Hamiltonians was assessed first. The SOC correction from the a-posteriori approach for the NMR shieldings is the FC contribution (eq. 2.130). Therefore this is discussed below.

4.3.1. Basis Set convergence

The basis set convergence is shown for the examples H_2S and HBr. The level of theory is BP86 and additionally the def2/J auxiliary basis set were used in the RI approximation. Since the FC term is very sensitive and depends mainly on the s-functions[49, 56, 57], decontracted basis sets were used by the keyword "decontract true". The isotropic shieldings of H_2S are shown for the S-atom in Figure 4.3a and for the H-atom in Figure 4.3b. The sto-3g basis set is not included, because this minimal basis deviates significantly.

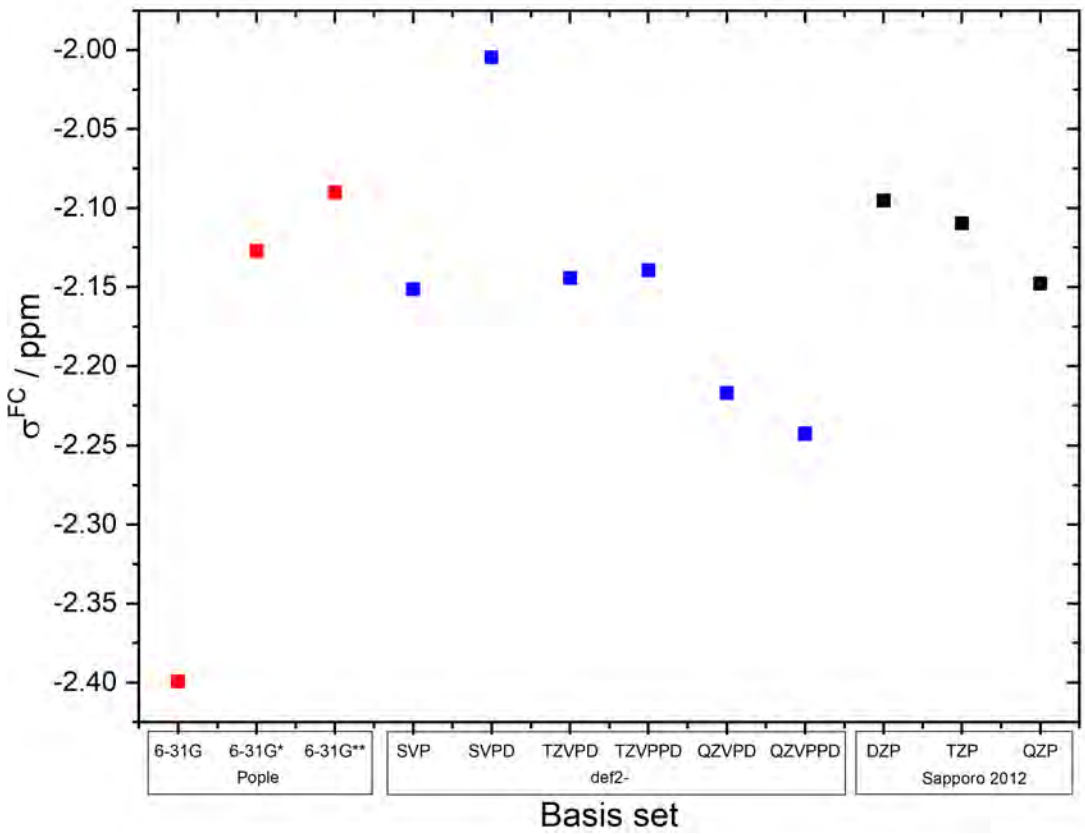

(a)

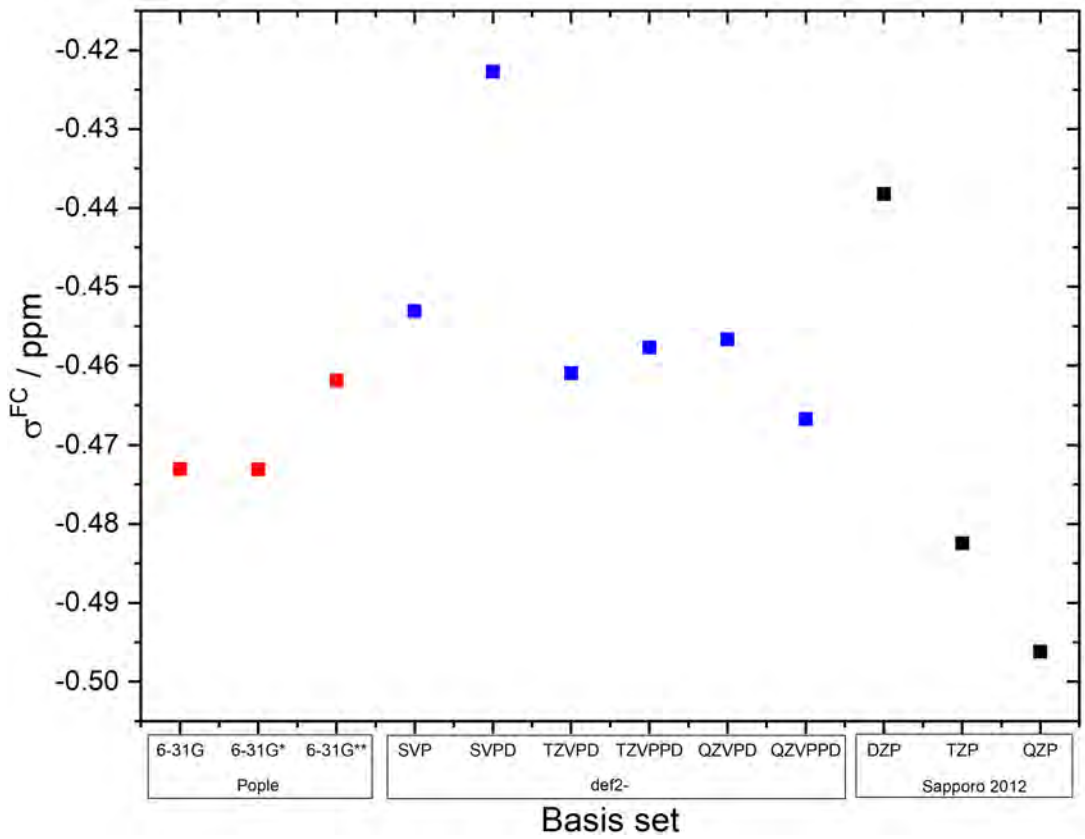

(b)

Figure 4.3: Basis set convergence of the SOC implementation of *ORCA*. The Pople, def2 of the Karlsruhe group and Sapporo-2012 basis sets were used and the SOC contribution to the isotropic shielding is shown in a) for the S-atom in b) for the H-atom of H_2S.

As shown in Figure 4.3, there is a difference in the isotropic shielding for the used basis sets. The basis set results by a maximum of about 0.4 ppm for S and 0.07 ppm for H. The convergence is not achieved with increasing basis set size. In the range of def2-TZVPPD, a small plateau is initially observed, but with a larger basis set a further deviation is reached. As a good compromise between accuracy and efficiency def2-TZVPPD is selected for the light elements in further calculations. The found deviation between def2-TZVPPD and def2-QZVPD is similar to the difference between the results using Sapporo-TZP and Sapporo-QZP. Sapporo-TZP-2012 is chosen for the heavy atoms in further calculations, because of accuracy and efficiency. The same results are obtained for HBr. The figures for HBr and values for both HBr and H_2S are shown in the Appendix (Sec. A.4.1).

4.3.2. Functional dependence

The functional dependence is shown for H_2S, H_2Se, HCl and HBr. The level of theory for the light atoms is def2-TZVPPD with def2/J and for the heavy atoms Sapporo-TZP-2012 basis set with "autoaux". Also the decontract keyword was switched on. The functional dependence for H_2Se and HBr is shown for the heavy-atom in A.5a and for the light atoms in A.5b.

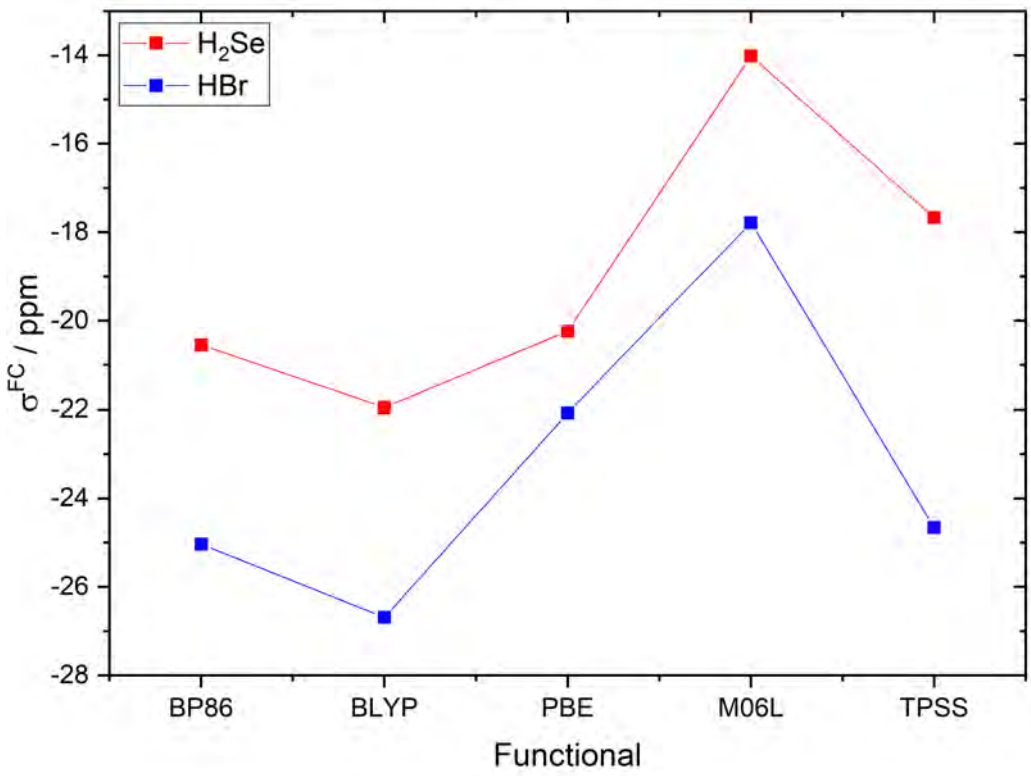

(a)

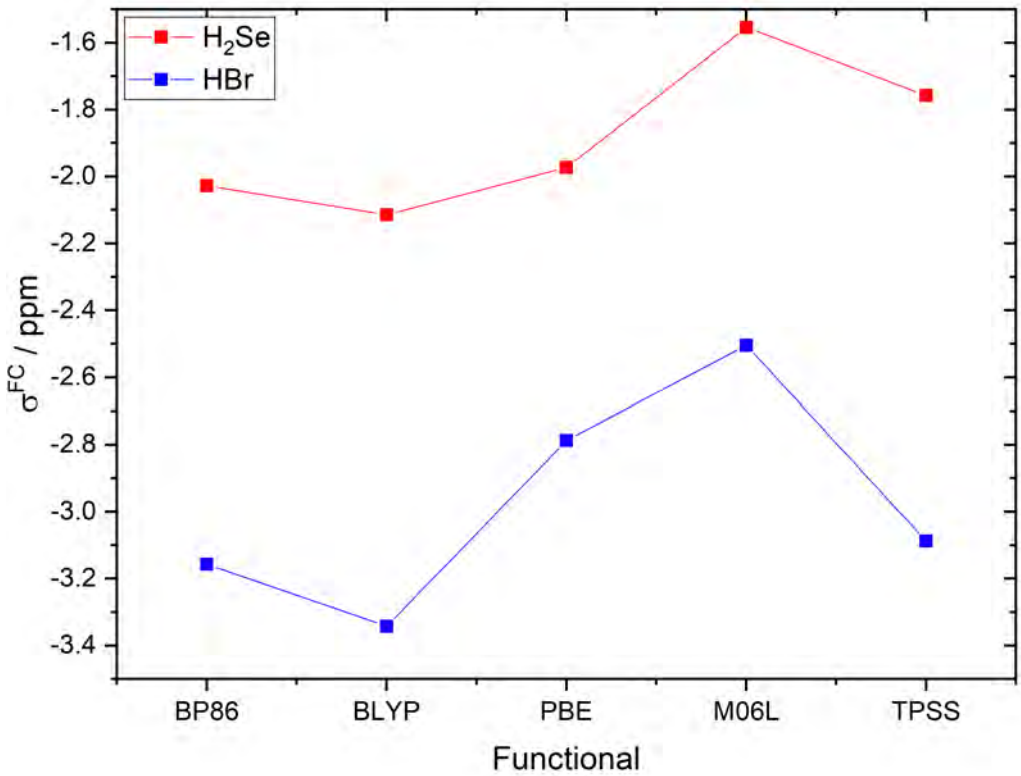

(b)

Figure 4.4: Functional dependence of the SOC implementation of *ORCA*. BP86, BLYP, PBE, M06L and TPSS functionals were used and the SOC contribution to the isotropic shielding are shown in a) for the heavy atoms and in b) for the H-atoms of H_2Se and HBr.

Figure A.5 shows that the SOC varies with the functionals for both H_2S and HBr. A maximum difference of about 8 ppm for Se-atom in H_2Se and of 7 ppm for the Br-atom in HBr, of 0.5 ppm for H in H_2Se and of 0.9 ppm for H in HBr between BLYP and M06L can be determined. For the further calculations BP86 is chosen. Similar results can be found for the other molecules. The values are shown in the Appendix (Tab. A.13 and A.14).

4.3.3. SOC Hamiltonian

The results using different SOC Hamiltonians are shown for H_2S in figure 4.5 and for HBr in table A.15. The level of theory is BP86, def2-TZVPPD with def2/J for the light atoms, Sapporo-TZP-2012 basis set with "autoaux" for the heavy atoms and using of the SOC Hamiltonian: SOMF, AMFI, AMFI-A and VEFF-SOC. The SOC Hamiltonians are used in the a posteriori approach in the diagonalization step of $\langle\Psi|\mathcal{H}_{SOC}|\Psi\rangle$. The result using different SOC approaches are shown in Figure 4.5a for the S-atom and in 4.5b for the H-atom of H_2S.

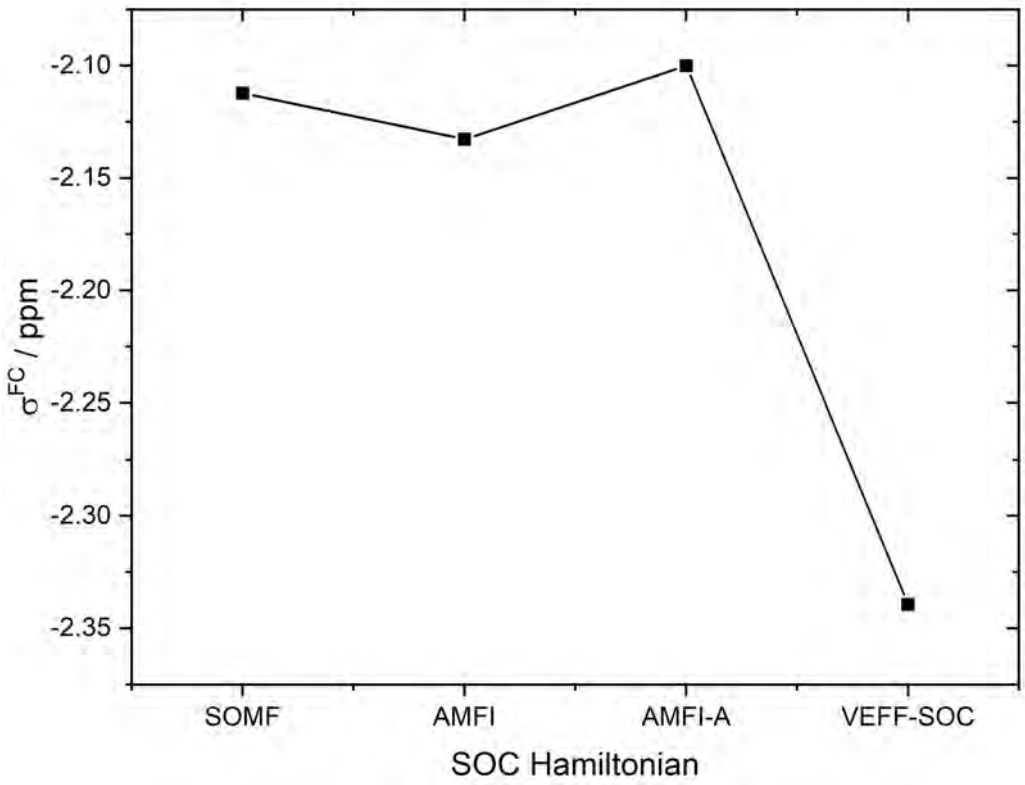

(a)

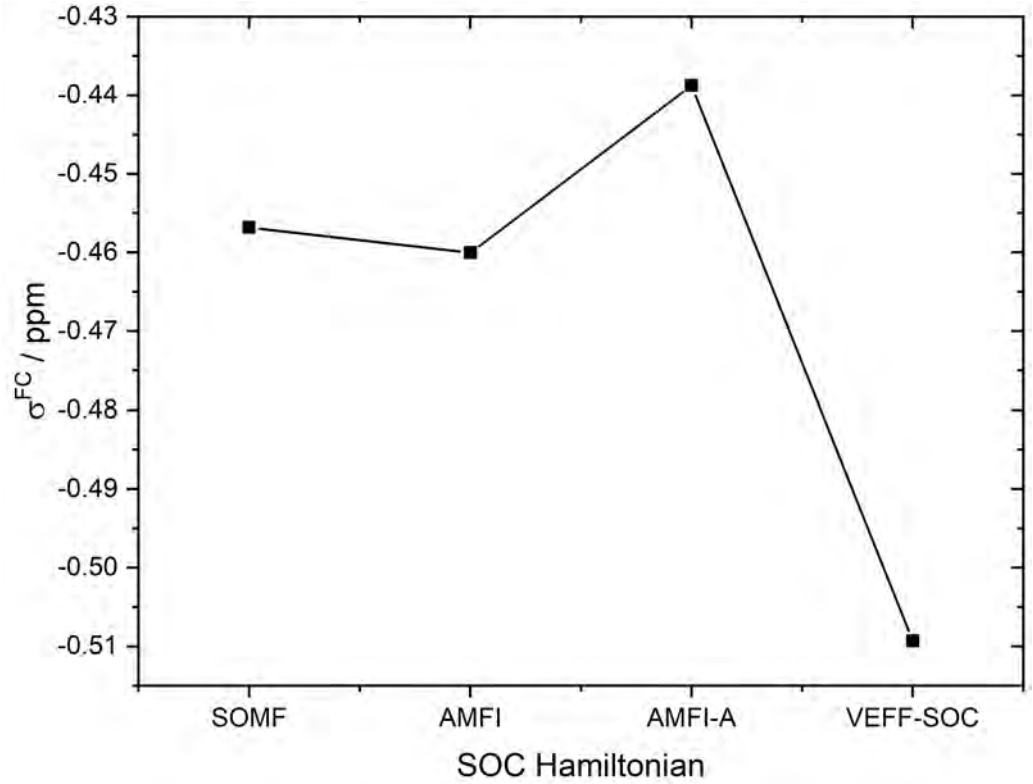

(b)

Figure 4.5: Using of different SOC Hamiltonian in the SOC implementation of *ORCA*. SOMF, AMFI, AMFI-A and VEFF-SOC were selected and the SOC are shown in a) for the S-atom and in b) for the H-atom of H_2S.

Figure 4.5 shows that different isotropic shieldings can be determined if other SOC approaches are used. It is noticeable that the mean-field approximations SOMF, AMFI and AMIF-A give very similar results. The effective SOC Hamiltonian VEFF-SOC differs from the other approaches by about 0.25 ppm for the S-atom and 0.06 ppm for the H-atom. In case of HBr, the difference for the Br-atom between the mean-field and VEFF-SOC Hamiltonians increases to about 1 ppm. The values are shown in the Appendix (Tab. A.15). Nevertheless, any SOC Hamiltonian can be used, as the variations are very small. In the following the default Hamiltonian SOMF is used.

4.4. Two- and four-Component Calculations

In this section the *ORCA* calculations are compared with two-component and four-component calculations of *DIRAC*. In the following it is shown how the results using ZORA in *ORCA* for ScR corrections are assessed. The following shows how to evaluate the ScR corrections with ZORA in *ORCA*. Likewise, the calculated SOC contributions with the new a-posteriori approach in *ORCA* are compared with *DIRAC* calculations, to see if the calculated SOC contribution with *ORCA* is in the right order of magnitude. As examples calculations the hydrogen halides are chosen.

For the SOC calculations using *ORCA* the level of theory is BP86, basis set of the light atom: def2-TZVPPD with RI-approximation by the auxiliary basis set def2/J; for the heavy atom: Sapporo-TZP-2012 with "autoaux". Since the FC term is very sensitive and depends mainly on the s-functions[49, 56, 57], decontracted basis sets were used by the keyword "decontract true". Note that the default SOC Hamiltonian is chosen. The *DIRAC* calculations were performed as described in the computational de-

tails (sec. 3). There are already published values for these compounds, which are also used for comparisons. The publication of Visscher *et al.*[80] was selected, using the *Dalton* program[81]. The non-relativistic values were obtained by a non-relativistic linear response formalism with London orbitals, the scalar relativistic MVEF-FC corrections by linear response theory and the spin-orbit corrections by quadratic response theory.[80] The calculated and literature values are listed in the Tables 4.8 for the heavy atom and in 4.9 for the light atoms. Additionally, the relativistic contributions are shown. The full relativistic effect is given by $Rel - NR$, the scalar relativistic contribution by $ScR - NR$ and SOC by $Rel - ScR$.

4.4.1. Results for heavy atoms

The results using the a posteriori approach in *ORCA*, BSS, X2C and a four-component approach in *DIRAC* are shown for the heavy nuclei of the hydrogen halides in Table 4.8. Literature values[80] are added for further classification of the values.

Table 4.8: Comparison of *ORCA* and *DIRAC* results of non-relativistic (NR) scalar-relativistic (ScR) and relativistic (Rel) calculations. In the *DIRAC* calculation was used the BSS and X2C Hamiltonian. The four-component *DIRAC* calculations used the Dirac-Coulomb Hamiltonian and a UKB basis. Literature values were taken from Visscher *et al.*[80]. Visscher *et al.* used a non-relativistic linear response formalism with London orbitals, for the scalar relativistic MVEF-FC corrections a linear response theory and the spin-orbit corrections was calculated with a quadratic response theory. All calculations were carried out in Dalton.[80] Rel means ScR+SOC. The full relativistic contribution is obtained by $Rel - NR$. The ScR contribution by $ScR - NR$. The SOC contribution is obtained by $Rel - ScR$. Shown for the heavy atom of the 17th group, hydrogen halides.

	Mole-	**isotropic shielding [ppm]**			**relativistic contributions [ppm]**		
	cule	NR	ScR	Rel	full rel.	ScR	SOC
ORCA	HF	412.608	412.047	404.564079	-8.043921	-0.561	-7.482921
a posteriori	HCl	928.161	925.041	928.012812	-0.418188	-3.12	2.971812
	HBr	2550.804	2501.362	2478.12362	-72.680376	-49.442	-23.238376
	HI	4401.406	4318.03	4219.13499	-182.262012	-83.376	-98.886012
DIRAC	HF*	407.9006	416.4254	417.1288	9.2282	8.5248	0.7034
BSS	HCl*	938.588	998.1839	1001.966	63.378	59.5959	3.7821
	HBr*	2557.508	3103.593	3150.0791	592.5711	546.085	46.4861
	HI***	4419.2303	6398.7214	6598.6969	2179.4666	1979.4911	199.9755
DIRAC	HF	903.3107	909.2732	818.6825	-84.6282	5.9625	-90.5907
X2C**	HCl	1871.3165	1913.8307	1909.5189	38.2024	42.5142	-4.3118
	HBr	4607.4004	5020.6621	4979.0782	371.6778	413.2617	-41.5839
	HI	7386.1651	8916.6308	8768.2265	1382.0614	1530.4657	-148.4043
DIRAC	HF	407.8568		410.8857	3.03		
4-comp.	HCl	938.265		968.3777	30.11		
	HBr	3085.0332		3399.3599	314.33		
	HI	5395.8280		6695.1859	1299.36		
Visscher	HF	414.3	422.9	423.2	8.9	8.6	0.3
et al.[80]	HCl	957	1017.5	1020.1	63.1	60.5	2.6
	HBr	2634.2	3177.4	3210.5	576.3	543.2	33.1
	HI	4541.4	6460.5	6602.2	2060.8	1919.1	141.7

*aug-cc-pVDZ; **dyall.ae2z; ***dyall.ae4z

Comparing *ORCA*, *DIRAC* and the literature in 4.8 it is clear that the values of the X2C Hamiltonian in *DIRAC* fall out. These values are about twice as high as the other listed values. A possible explanation is the kinetic balance. *DIRAC* has RKB as default setting, but as shown in section 2.4.1, UKB should be used for property calculations when using X2C.

The comparison of the full relativistic contribution between four-component and BSS shows that BSS represents the correct size of range of the relativistic effect. However, from the 4th period on, larger deviations can be

seen, which are caused by the fact that the BSS calculation is only two-component and ScR and SOC are considered separately. The relativistic corrections for the 4th or 5th period can only be completely determined by a four-component approach. The comparison shows that BSS can still be used as a good two-component calculation. The comparison of BSS and literature data shows that the values of BSS fit very well to published values and reflect the correct trend of ScR and SOC effects. Therefore it can be assumed that the remaining calculated *ORCA* values can be compared well with BSS, but not with X2C.

Comparing the relativistic contributions between the a-posteriori approach and BSS it is clearly visible that the calculated *ORCA* values have the wrong sign for the ScR and SOC contributions. This means that the ScR and SOC correction by ZORA and a-posteriori become smaller down the group, but the BSS and literature results predict that they increase down the group. The comparison of the ZORA results using ORCA and NWChem in Section 4.1 showed that the ZORA implementation in ORCA is correct. Therefore it can be assumed that this approach is not suitable to calculate the scalar relativistic corrections for the isotropic shieldings at this point. However, the calculated SOC contributions in *ORCA* do not have a clear trend as expected from the comparison to BSS. Also the SOC contributions for HF and HCl by using a-posteriori are clearly larger than the ScR corrections. However, the BSS and literature values show the opposite. Therefore both the ScR and SOC corrections followed the wrong trend. It can be said that the ScR and SOC contributions in *ORCA* do not reflect the correct relativistic effects.

4.4.2. Results for light atoms

The theory developed in *ORCA* was not intended to calculate the heavy atoms in compounds. It was developed to calculate the correct influence of heavy atoms on the isotropic shielding of light atoms, to calculate the HALA effect correctly. The results of the light atoms are shown in table 4.9

Table 4.9: Comparison of *ORCA* and *DIRAC* results of non-relativistic (NR) scalar-relativistic (ScR) and relativistic (Rel) calculations. In the *DIRAC* calculation was used the BSS and X2C Hamiltonian. The four-component *DIRAC* calculations used the Dirac-Coulomb Hamiltonian and a UKB basis. Literature values were taken from Visscher *et al.*[80]. Visscher *et al.* used a non-relativistic linear response formalism with London orbitals, for the scalar relativistic MVEF-FC corrections a linear response theory and the spin-orbit corrections was calculated with a quadratic response theory. All calculations were carried out in Dalton.[80] Rel means ScR+SOC. The full relativistic contribution is obtained by $Rel - NR$. The ScR contribution by $ScR - NR$. The SOC contribution is obtained by $Rel - ScR$. Shown for the hydrogen-atoms of the 17th group, hydrogen halides.

	Mole-	**isotropic shielding [ppm]**			**relativistic contributions [ppm]**		
	cule	NR	ScR	Rel	full rel.	ScR	SOC
ORCA	HF	30.316	30.333	30.058815	-0.257185	0.017	-0.274185
a posteriori	HCl	31.555	31.573	30.898428	-0.656572	0.018	-0.674572
	HBr	31.605	31.586	28.391235	-3.213765	-0.019	-3.194765
	HI	31.869	31.761	21.980857	-9.888143	-0.108	-9.780143
DIRAC	HF*	29.6007	29.5783	29.778	0.1773	-0.0224	0.1997
BSS	HCl*	31.2762	31.313	32.248	0.9718	0.0368	0.935
	HBr*	31.4423	31.4775	36.5937	5.1514	0.0352	5.1162
	HI***	31.8027	31.7578	46.2884	14.4857	-0.0449	14.5306
DIRAC	HF	18.8062	18.7896	29.7936	10.9874	-0.0166	11.004
X2C**	HCl	17.3234	17.298	17.0462	-0.2772	-0.0254	-0.2518
	HBr	18.2922	18.1747	17.4132	-0.879	-0.1175	-0.7615
	HI	20.091	19.8608	19.2629	-0.8281	-0.2302	-0.5979
DIRAC	HF	29.6001		29.4855	-0.11		
4-comp.	HCl	31.2717		31.9126	0.64		
	HBr	71.2230		70.6295	-0.59		
	HI	67.3819		68.8383	1.46		
Visscher	HF	27.73	27.71	27.84	0.11	-0.02	0.13
et al.[80]	HCl	30.12	30.11	30.95	0.83	-0.01	0.84
	HBr	30.55	30.53	36.12	5.57	-0.02	5.59
	HI	31.05	31.03	49.41	18.36	-0.02	18.38

*aug-cc-pVDZ; **dyall.ae2z; ***dyall.ae4z

The comparison between *ORCA*, *DIRAC* and the literature shows that the calculated X2C values and the relativistic contributions do not have the same size range as the remaining values, already shown for the heavy

atoms in the hydrogen halides.

An illustration of the values of the a posteriori approach, BSS and the four-component Hamiltonian is shown in Fogure 4.6, additionally the values of Visscher *et al.*[80] are displayed for a further classification. Note that the X2C values are not shown, since they considerably differ from the other values, whereby their significance would be reduced in the illustration

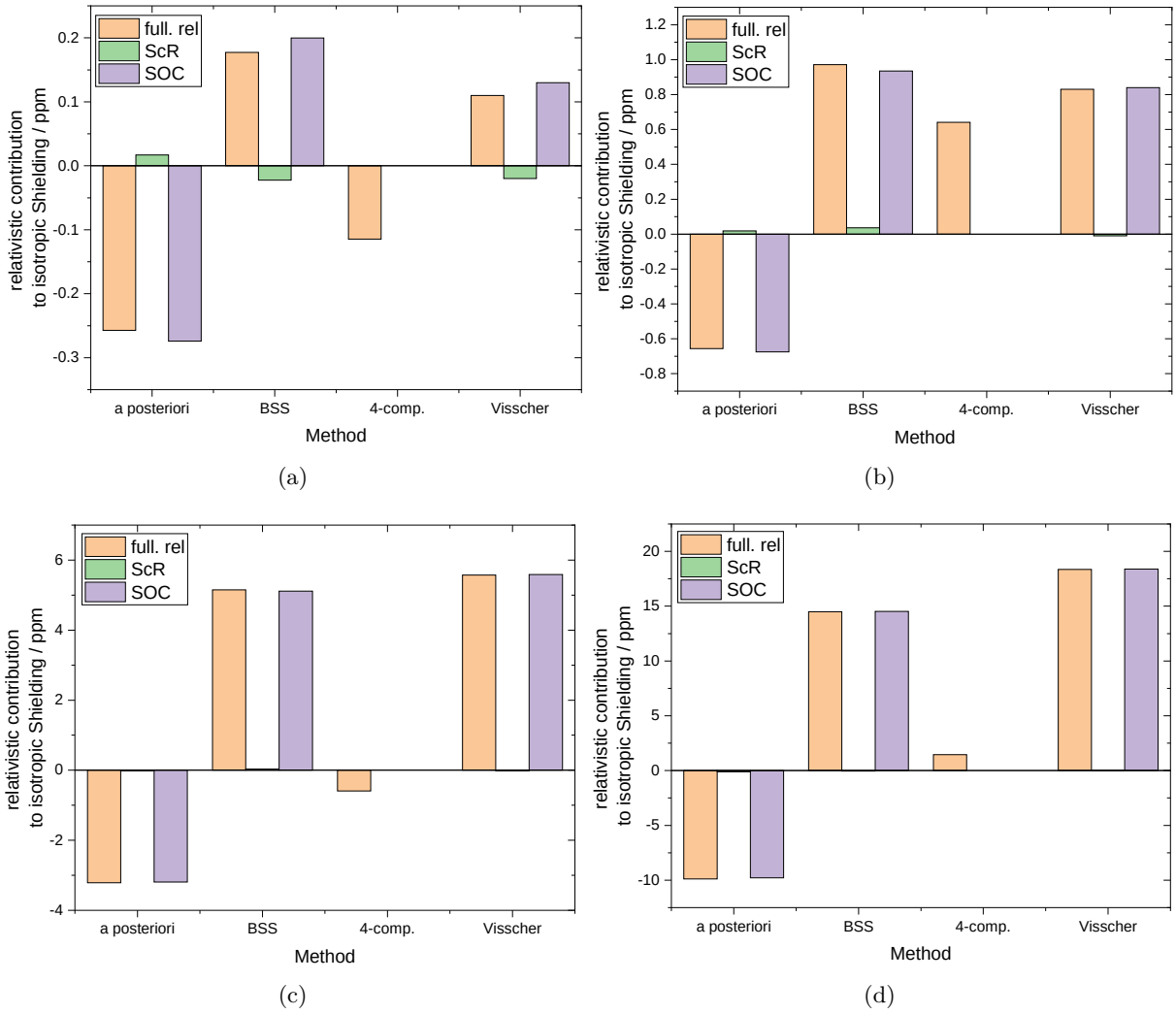

Figure 4.6: Illustrated comparison of the full relativistic correction, the ScR and SOC contributions. Shown for the a posteriori approach, BSS and the values of Visscher *et al.*[80]. The results are shown in a) for HF, in b) for HCl, in c) for HBr and in d) for HI.

The rough comparison in Figure 4.6 shows that the resulting relativistic contributions from the BSS calculations correspond to the contributions calculated in the literature. The relativistic trend of the isotropic shield-

ings of the light nuclei shows that the ScR contributions are almost zero and therefore negligible[54, 55]. The largest relativistic correction comes from the SOC. This has already been described as a characteristic of the HALA effect in section 2.4.2. The comparison of the full relativistic effect between BSS and four-component shows that BSS does not correctly reflect the trend. However, it is noticeable that something went wrong with the four-component calculation from Br on. The calculations were performed according to the instruction of the *DIRAC* authors, thus the problems cannot be explained further. Therefore, the comparison to the four-component calculations will not be pursued further at this point.

The comparison of the ScR contribution between a-posteriori and BSS shows that *ORCA* correctly reflects this correction, which is about zero. As there is no uniformity of the sign e.g. between the BSS and literature results, no trend of the scalar relativistic effect of the light atoms can be found. The comparison of the SOC contributions show that the correct size range is reproduced by *ORCA*, but has the wrong sign. Based on these values it was checked whether the wrong sign was existing in the SOC implementation. However, the check showed this is not the case.

The a-posteriori scheme implemented in *ORCA* fails to reproduce the right SOC effect om the NMR shieldings for the HALA effect. A possible source of error for the determination of the SOC contribution is given by the theory in *ORCA*. It does not seem sufficient to introduce the SOC perturbation a-posteriori. Furthermore only the FC term is calculated and the SD contribution is neglected. Although the FC terms is larger in most cases, this can contribute to the error.

4.4.3. HALA Effect

Although, as shown above, the relativistic corrections or the isotropic shielding by X2C and *ORCA* are not reproduced correctly, in the following the HALA effect is studied also with these methods to see whether this effect can be reproduced correctly. H-compounds were selected for groups 13-17 to compare the HALA effect down the group and between the groups of the ^{1}H shielding. Again, the geometries were created as described in the computational details (Sec. 3). The trihydrogen triels, tetrahydrogens tetrels, trihydrogen pentels, dihydrogen chalcogens and the hydrogen halides were selected. Note that for the 16th and 17th group no additional calculations had to be done. The further procedure of the property calculations is the same as described at the beginning of this section.

To get an overview of the HALA effect, the calculated isotropic shieldings were plotted along the period for each group in Figure 4.7 (values are shown in the Appendix Tab. A.26, A.27 and A.28). This was done with the results of BSS, X2C and the SOC results of *ORCA*. Note that for BSS and X2C relativistic values have been applied, which includes ScR+SOC, while for the a-posteriori approach NR+SOC has been applied. This makes no difference for the observation, as the ScR values for the light nuclei are close to zero.

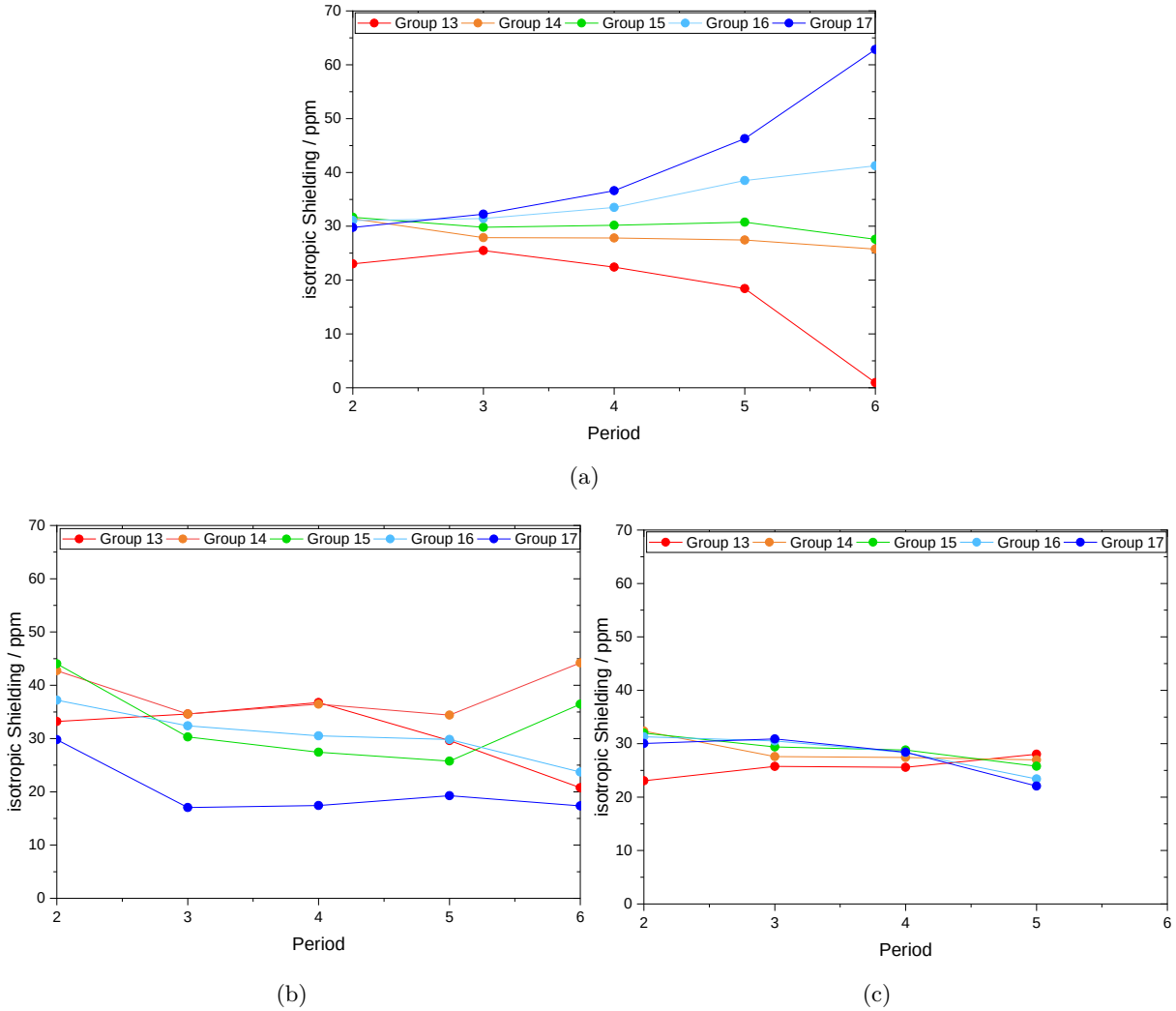

Figure 4.7: Illustration of the absolute HALA effect of the isotropic shielding for the hydrogen compounds of the 13th-17th group. Comparison between a) using BSS in *DIRAC* b) using X2C in *DIRAC* and c) using the new SOC implementation in *ORCA*.

A comparison between all three subfigures a-c in Figure 4.7 shows no similarity. In the literature[53, 82] the same trend as shown in Figure 4.7a is described. Note that chemical shifts are usually discussed in the literature, in this case the trend is reversed. If the ^{1}H shifts of Figure 4.7a would be calculated, the same reversed order of the groups would result. The trend is described in the literature by deshielding and shielding effects. In the NMR language, deshielding describes the range of increasing shifts and shielding describes the range of the decreasing shifts. Using the absolute values, the isotropic shieldings, it is the other way around. This means, a

deshielding effect shows decreasing and a shielding effect increasing values. *Vicha*[53] and *Rusakov*[82] formulate the HALA trend for the p-block as:

1. In the 13th group an increasing deshielding SO-HALA effect down the group is observed. This is called the triel dependence[82].
2. For the 14th group a compensation of shielding and deshielding effects can be observed.
3. The maximum SO-HALA shielding is expected for the 17th group.

If the result of BSS is checked for 1.-3., it can be clearly stated that BSS describes the HALA effect correctly.

The ordinates between b)-d) are the same to make the comparison between BSS to X2C and a-posteriori easier. When comparing BSS to X2C (b and c) it can be clearly seen that X2C describes a HALA effect down the group, but not the expected trend. This could be due to a missing magnetic balance by RKB as described above. The comparison between BSS and the a-posteriori approach in *ORCA* also shows that the a-posteriori approach does not correctly describe the HALA effect. In fact, *ORCA* hardly describes any visible effect.

For a clearer comparison, the SOC contributions of BSS and a-posteriori are compared again in another illustration in Figure 4.8. A positive SOC contribution is shown in shades of red and a negative SOC contribution in shades of blue for the 13th-17th group. Note that the 6th period could not be calculated using *ORCA* and therefore blacked out.

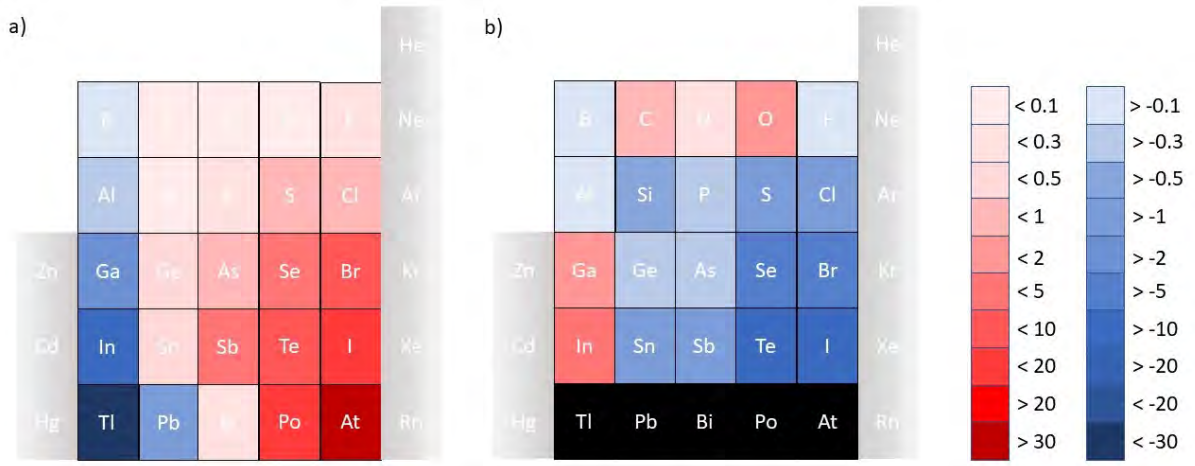

Figure 4.8: Color illustration of the absolute HALA effect of the isotropic shielding for the hydrogen compounds of the 13th-17th group. Calculated a) with the BSS Hamiltonian in *DIRAC* and b) with the a-posteriori approach in *ORCA*.

The description of the SOC contributions to isotropic shielding for BSS (Fig. 4.8a) reflects again the the above mentioned points 1-3 by *Vicha*[53] and *Rusakov*[82]. The triel dependency of the 13th group can be shown by the color of the SOC sign, because this is the only group marked in blue. The light colors of the 14th group also show the compensation effect of this group. In addition, the increase of the SOC down the groups of the 15th-17th group and especially for the 17th group is very pronounced. However, the calculation of trihydrogen bismuth has to be seen as an exception.

The illustration of the a-posteriori calculated values (4.8b) shows again clearly that safe for small exceptions (e.g. BH3, AlH3, CH4, NH3, H2O) the SOC contributions have the wrong sign and are too small from the 4th period on. Since the relativistic effects increase with the nuclear charge, i.e. down the group, it was assumed that this simple SOC approach could be sufficient until the 4th period. However, as shown in the Figures 4.7 and 4.8, already from the 3th period the wrong result is obtained.

Both illustrations 4.7 and 4.8 of the HALA effect show strong arguments that the a-posteriori approach in *ORCA* is not sufficient for calculated the

SOC contribution correctly. As shown in Section 4.4.1, also the magnitude of the SOC contributions for the heavy elements is smaller than expected. Therefore it can be assumed that the SOC perturbation is too small. This may be due to the fact that the SOC effect is not obtained iteratively, but a-posteriori. Thus only small perturbations are represented instead of a real SOC.

4.5. Computational results for an application with experimental background

As already shown in the previous sections, the description of the HALA effect should be based on using *DIRAC* with the BSS Hamiltonian and the dyall.ae2z basis set. For some organic bismuth compounds, an interesting effect was found in the literature[2] for the ^{1}H NMR spectra. It shall be studied, whether this effect could be of SO-HALA nature.

The bismuth compounds consist of one (Fig. 4.10a) or two (Fig. 4.9a) bonds to an organic residue which is a conjugated π-system. One (Fig. 4.9a) or two (Fig. 4.10a) halides are also bound to the bismuth-atom. It was found that there is a weak hydrogen bond between the H-6 proton placed in the *ortho* position to the bismuth atom. An increasing shift of the H-6 proton was observed in the following order Cl $<$ Br $<$ I (Fig. 4.9b and 4.10b).[2] It is believed that the finding of the increasing shift down the group is due to the IHD. The corresponding NMR spectra from the literature are shown for (2-Ph-C_6H_5)$_2$BiX in Figure 4.10 and for (2-Ph-C_6H_5)BiX$_2$ in Figure 4.10.

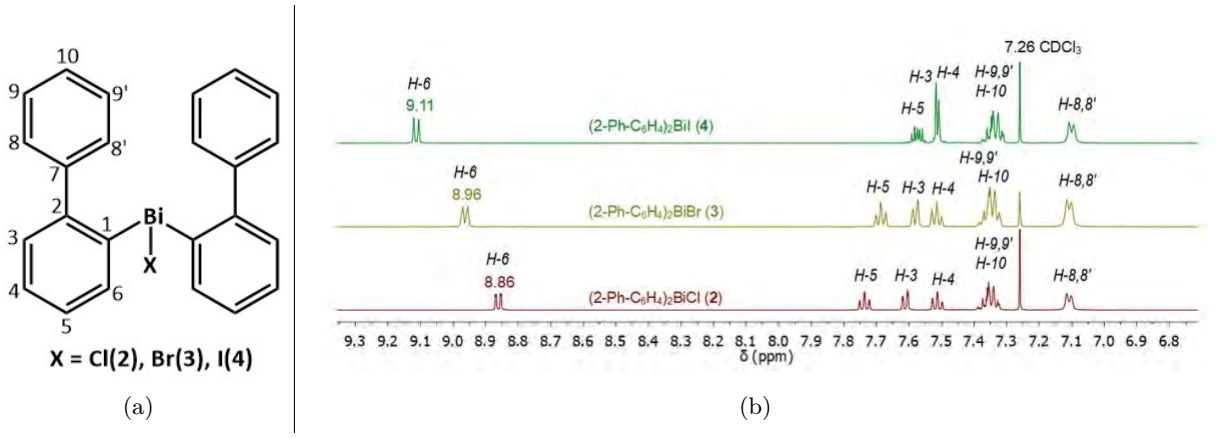

Figure 4.9: Representation of a) the chemical structure of (2-Ph-C_6H_4)$_2$BiX. X can be chloride, bromide oder iodide. b) The corresponding ^{1}H NMR spectra taken from Fritsche *et al.*[2].

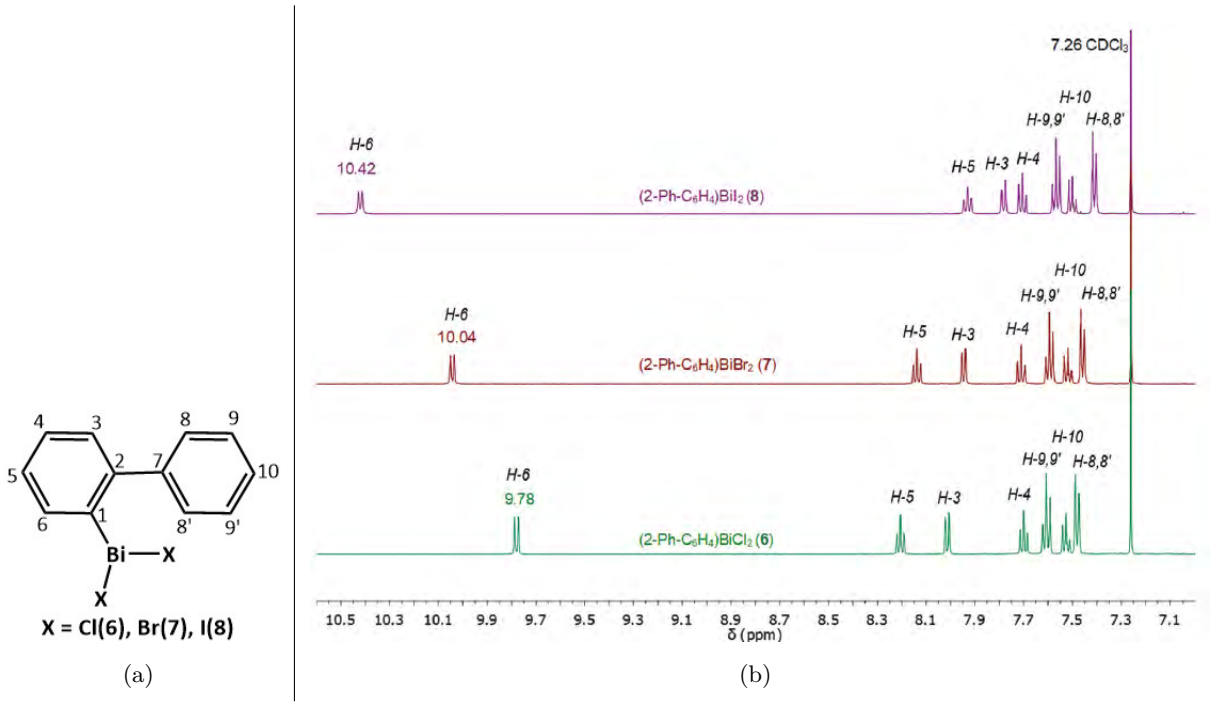

Figure 4.10: Representation of a) the chemical structure of (2-Ph-C_6H_4)BiX_2. X can be chloride, bromide oder iodide. b) The corresponding ^{1}H NMR spectra taken from Fritsche *et al.*[2].

From both NMR spectra it can be clearly seen that the ^{1}H shift is further shifted in the heavier halides, corresponding to the IHD effect. While NHD is clearly attributed to the SO-HALA effect, contradictory reasons for the presence of IHDs are found in the literature. *Moncho* and *Autschbach's* publication states that the "IHD typically is attributed to changes in the paramagnetic shielding component[83, 84] in situations where the effective

transfer of the SO coupling shielding terms is suppressed [...]."[85] *Araru* and *Saielli* state that "if the light atom contributes little valence s orbital character to the HA-LA bond, an inverse halogen dependence (IHD) occurs [...]. It originates primarily from paramagnetic shielding components, rather than SO coupling itself, and is attributed to magnetic coupling of bonding and antibonding orbitals."[86] In contrast, *Auer* and *Mehring* state: "the so-called Inverse Halogen Dependence (IHD) which is caused by spin-orbit coupling on the heavy halogen atom [...]"[2]. Auer *et al.*[2] report, that the increasing chemical shift cannot be observed using non-relativistic or scalar relativistic (ZORA) calculations. Whether it is a HALA effect, can only be shown by considering the SOC. To identify the underlying reasons, a comparable molecule was calculated with *DIRAC*. The trial molecule has the structure shown in Figure 4.12a. However, *DIRAC* has a memory limit, so these larger systems cannot be calculated. Therefore, a model was calculated which is shown in Figure 4.12b.

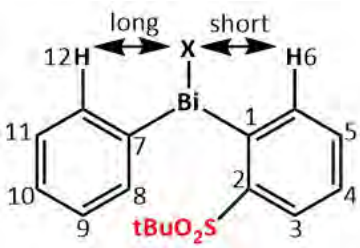

(a)

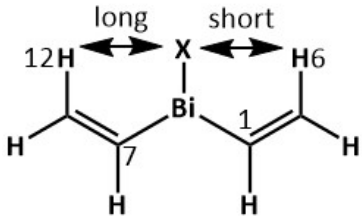

(b)

Figure 4.11: a) Bismuth trial molecule for investigation of the possible HALA effect of the H6 proton and b) the calculated model.

The trial molecule (4.12a) is not planar due to the *tert*-butyl sulfinate at position 2, so there is a short distance between X and H6 and a longer distance between X and H12. The short distance varied between 2.399 Å for fluoride to 3.018 Å for iodide. The long distance varied between 3.596 Å for fluoride to 4.422 Å for iodide. The model was calculated with the same

distances using the BSS Hamiltonian in *DIRAC* (see sec. 3 for computational details). The dyall.ae2z basis set was used. The results of the NR, ScR and Rel isotropic shieldings for X = F, Cl, Br are shown in Table 4.10. For X = I the calculations were not possible, because of convergence problems.

Table 4.10: Calculated isotropic shielding values of NR, ScR and Rel level. The BSS Hamiltonian in *DIRAC* was used.

X	**Proton**	**distance X-H [Å]**	**isotropic shielding [ppm]** NR	ScR	Rel
F	H6	2.399	24.6174	24.602	23.8857
	H12	3.596	25.8846	25.9106	24.3385
Cl	H6	2.727	25.059	25.0761	23.2416
	H12	4.027	25.573	25.5863	23.4482
Br	H6	2.848	24.8432	24.8696	23.1988
	H12	4.197	26.001	26.0112	24.5782

As can be seen from Table 4.10, there is no difference of the isotropic shielding of H6 and H12 using a non-relativistic or relativistic approach. Thus it can be excluded that this is a SO-HALA effect. The only difference of the isotropic shielding, which can be observed, is for H6 und H12 for F and Cl. These results lead to a new assumption, according to which a strong distance dependence in the shift might cause the observed effect. Therefore a very simple model was used to check this hypothesis.

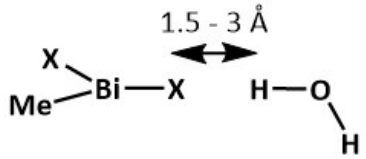

Figure 4.12: Distance model Dihalid(methly)bismuthane in relation to water in distances between 1.5-3 Å.

With this distance model, relaxed scans using *ORCA* were performed to determine the geometries. In further steps, NR *ORCA* calculations were carried out to determine the isotropic shielding. The level of theory is BP86, def2-TZVPPD def2/J for the light atoms and Sapporo-TZP-2012

or Sapporo-DKH3-TZP-2012 for the heavy atoms. Decontracted basis sets were used. For accelerating SCF convergence in some property calculations, the alternative kdiis algorithm with nososoc was used. The isotropic shieldings for all protons depend on the distance between X and H as shown in the Table 4.11. An illustration of the calculated isotropic shieldings is shown in Figure 4.13.

Table 4.11: Calculated isotropic shieldings of the distance model for the X-atom of the bismuth molecule and the H-atom of water. Shown are the isotropic shieldings of the protons of the methyl group bound to bismuth and for the water protons. The proton that is directed to the halide is shaded grey. NR-calculations with *ORCA* were carried out.

		Distance [Å]					
Halide	**Atom**	1.5	1.636	2.045	2.318	2.591	3
F	H (Me)	30.712	30.742*	30.749*	30.768	30.788	30.771
	H (Me)	30.217	30.301*	30.417*	30.473	30.518	30.532
	H (Me)	30.254	30.287*	30.362*	30.386	30.394	30.410
	H (H_2O)	29.532	29.599*	29.666*	29.758	29.897	29.973
	H (H_2O)	23.012	25.202*	28.568*	29.386	29.727	29.888
Cl*	H (Me)	30.153	30.291	30.370	30.370	30.366	30.367
	H (Me)	30.120	30.139	30.249	30.322	30.366	30.401
	H (Me)	29.729	29.777	29.875	29.898	29.922	29.940
	H (H_2O)	28.267	28.791	29.547	29.731	29.853	29.992
	H (H_2O)	14.917	18.498	25.762	27.913	29.019	29.697
Br	H (Me)	30.225	30.221	30.249	30.230	30.228	30.226
	H (Me)	30.052	29.998	30.096	30.200	30.254	30.312
	H (Me)	29.723	29.728	29.738	29.767	29.786	29.808
	H (H_2O)	28.206	29.470	29.331	29.625	29.799	29.980
	H (H_2O)	21.283	22.198	24.417	27.083	28.530	29.519
I	H (Me)	30.195*	30.196*	30.164	30.190*	30.213*	30.216
	H (Me)	29.983*	30.014*	30.065	30.069*	30.099*	30.124
	H (Me)	29.618*	29.621*	28.164	28.263*	28.235*	28.406
	H (H_2O)	25.983*	27.541*	29.828	30.197*	30.368*	30.540
	H (H_2O)	20.536*	22.203*	24.373	27.286*	28.901*	30.018

*using kdiis and nososcf

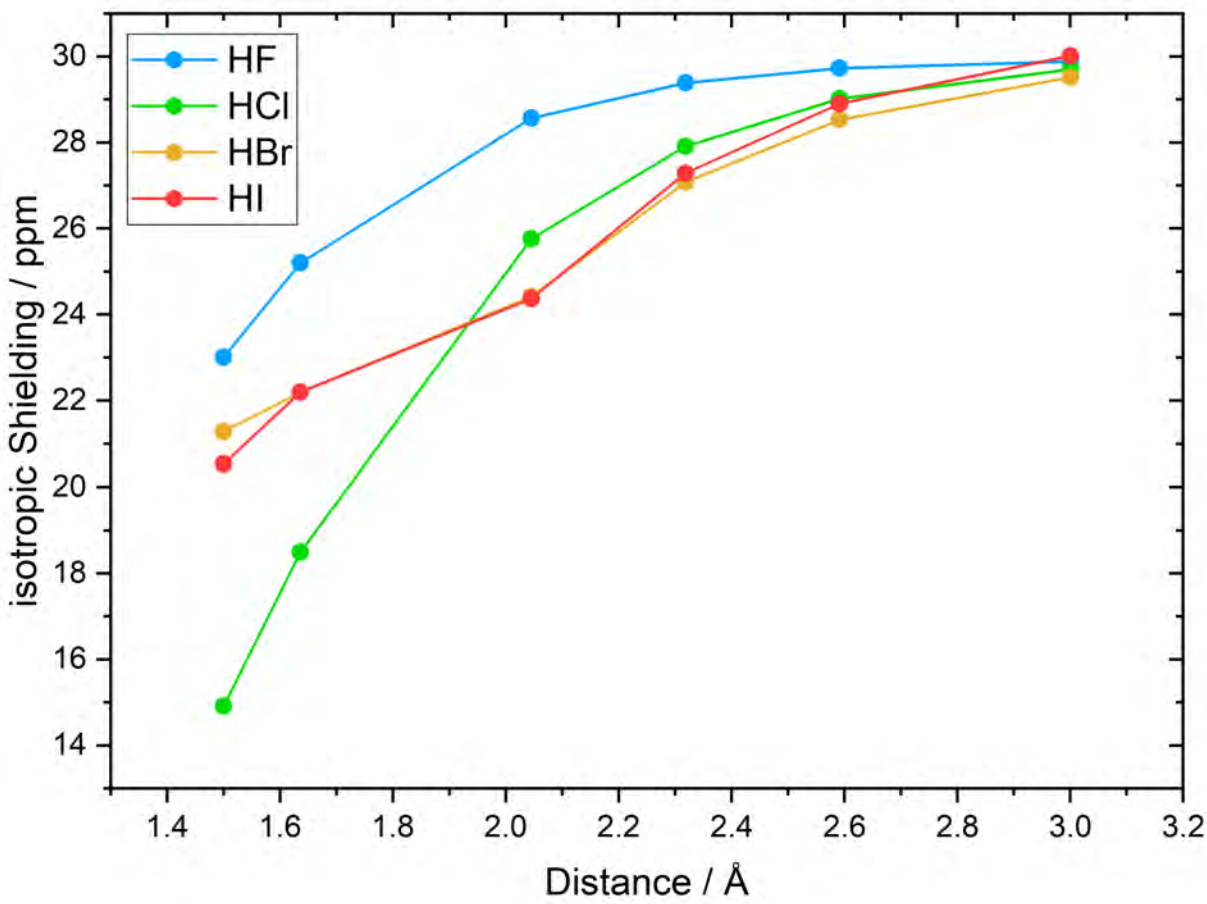

Figure 4.13: Distance dependence of the isotropic shielding for different halides F (blue), Cl (green), Br (orange) and I (red). Shown is the isotropic shielding of the water proton directed to the halide.

As can be seen from the values in Table 4.11 and Figure 4.13, the isotropic shielding of the proton directed towards the halide increases with increasing distance between X and H for all halides. Furthermore the isotropic shielding decrease from F to I for the same distance. Below 2 Å, the chlorine model breaks out of the trend. However, it can be assumed that this area is no longer representative, because in this range, the halide and proton are clearly too close to each other.

It can be shown from Table 4.11 that there is a strong distance dependence of the observed chemical shift of the proton directed towards the halide. Note, that the other values of the protons do not change as much as the proton marked in grey.

The SCF energies of the systems with different halides for varying distances are illustrated in the Appendix A.6. Figure 4.14 shows the isotropic shielding as a function of the distance and the normalized SCF energy as a function of the distance for the hydrogen halides. The SCF energies are shifted to zero.

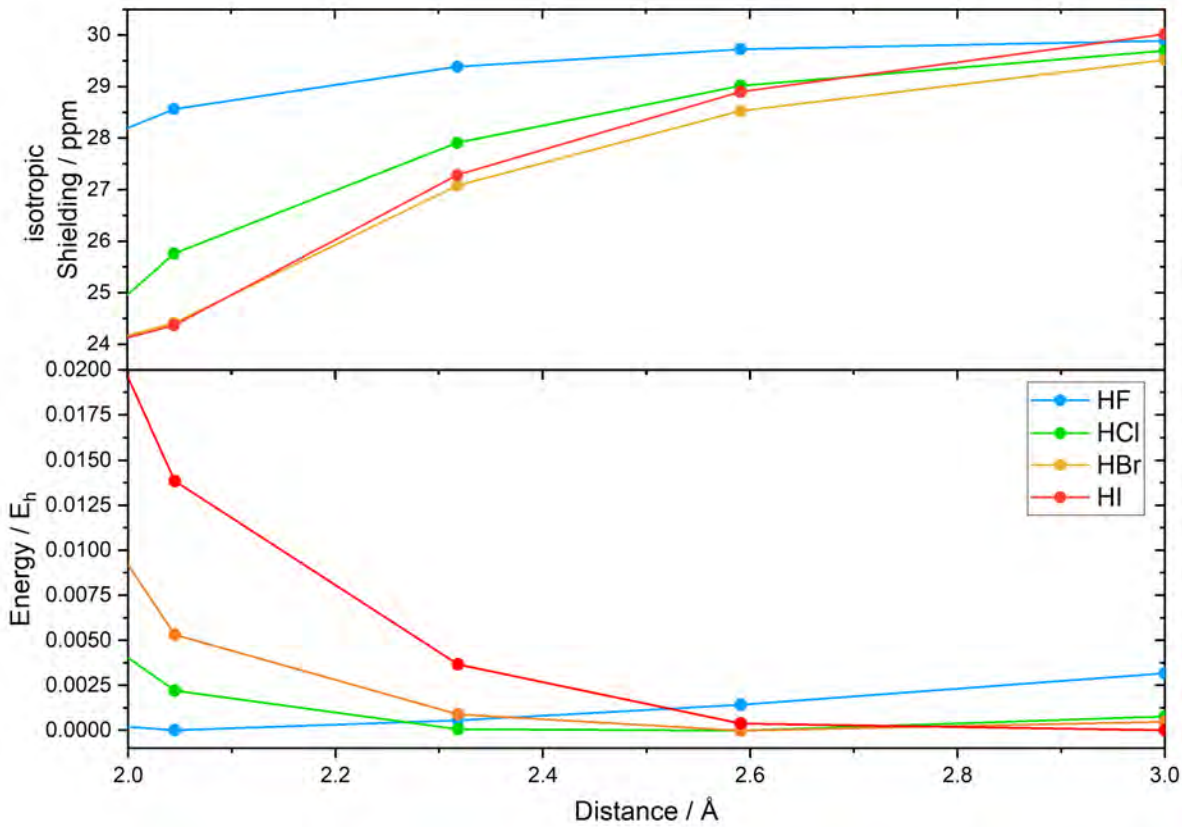

Figure 4.14: Distance dependence of the isotropic shielding and the normalized SCF energy for the hydrogen haliedes. The energie are shifted to zero.

From the energy profile along the X...H distance in Figure 4.14 it can be seen that these are flat potentials, especially at a distance larger than 2.4 Å. The joint consideration of both the distance dependence of the isotropic shieldings and the potential surfaces shows that small changes of the distance already allow large changes of the isotropic shielding. From this result the assumption that the isotropic shieldings varies more strongly by zero point oscillation. Also possible would be the anharmonic in the oscillation. In a harmonic system, the probability of the lowest states is in

the middle, but in a anharmonic potential, the probability shifts, thus a stretched or compressed bond is present.

Further calculations should be made using vibrational effects and anharmonic analysis to find out whether this effects could in fact be the solution for the found IHD.

5. Summary and Outlook

The aim of this work was to obtain a suitable benchmark set with which the ZORA results can be checked and further calculations for testing the new a-posteriori SOC approach in *ORCA* can be performed. Furthermore, it should be investigated whether the IHD arising in the NMR experiment could be a SO-HALA effect.

The benchmark set created by comparing calculations with literature results proved to be unsuitable. The comparison to the literature (especially ADF values) proved to be difficult. It was possible to partially reproduce the non-relativistic values for selenium, tellurium, xenon and iron compounds. However, the ZORA values in *ORCA* showed a disappointing disagreement with the published scalar relativistic values.

A better alternative was to create an own benchmark set from the p-block elements of the periodic table and to compare the results to *NWChem* values. Good agreement was found between the different implementations in *ORCA* and *NWChem* given the right settings were used. ZORA calculations showed a slight grid dependence of up to 1.5 ppm for the heavy atom shown for TeH_2, mainly due to the paramagnetic contribution. The pilot implementation RIZORA could successfully eliminate the grid dependence of the paramagnetic part until the 5th period. For RIZORA, a grid of 4 is sufficient to get good results, whereas the choice with ZORA would be 6 or 7. However, the efficiency of the pilot implementation is not yet competitive.

The selected benchmark molecules were also used to evaluate the new SOC approach for NMR calculations in *ORCA*. In order to compare different approaches, four-component, BSS and X2C calculations were carried

out using *DIRAC*. The BSS Hamiltonian proved to be particularly suitable for the comparisons. The ZORA results in *ORCA* did not show the correct magnitude and trend of the ScR correction for the heavy atoms of the benchmark molecules. This is due to the fact that the heavy atoms exhibit the largest relativistic correction caused by the mass velocity term, shown for the 17th group by Vicha *et al.*[54]. Since the ScR correction of the light atoms like hydrogen and carbon are very small (< 0.02 ppm), they can be disregarded, even if there is a heavy atom in vicinity. The value for e.g. HI shows only a small correction of about -0.05 ppm (tab. 4.9). However, the ZORA approach in *ORCA* shows a larger ScR correction of about -0.1 ppm which is also be negligible.

Basis set convergence of the a-posteriori approach in *ORCA* was not confirmed. It was shown that def2-TZVPPD for the light and Sapporo-TZP basis set were the best compromise for accuracy and efficiency. Furthermore GGA and meta-GGA functionals were tested. A rather larger scattering for the isotropic shielding of the heavy atom was found. It would be useful to test further functionals, especially hybrid functionals. The use of different already implemented SOC approximations in *ORCA*, including SOMF, AMFI, AMFI-A and VEFF-SOC, showed hardly any different results for elements of the 3rd period. For the sulfur atom in H_2S it was shown, that there is a difference of about 0.25 ppm between the result using VEFF-SOC in comparison to the results of the other SOC Hamiltonians. For bromine, in HBr the difference of the results between the SOC-Hamiltonian increase to 1 ppm. It makes sense to look at the scattering in the 5th period in further calculations in order to see whether the choice of the SOC Hamiltonian is in fact not important.

The values of a-posteriori approach compared to BSS and the literature

showed disappointing results. This comparison should show whether the simple SOC approach in *ORCA* for preferably organic molecules with heavy atoms is sufficient to calculate the SO-HALA effect in isotropic shielding. The a-posteriori approach in *ORCA* does not result in the correct sign of the SOC correction and the correct HALA effect trend down the group. Molecules with elements of the 6th period could not be calculated with the SOC implementation, yet. Currently the choice of the BSS Hamiltonian in *DIRAC* is probably still the best compromise to get good SOC values.

One aim of this work is to investigate organic compounds containing bismuth and halides atoms being known from the literature[2]. The bismuth atom is bound to one or two halides (see Fig. 4.9 and Fig. 4.10). In the NMR experiments, an IHD was found for the *ortho*-proton to the bismuth atom. The calculations of Auer *et al.*[2] showed no indication that the origin of the effect can be described by NR and ScR approaches. The consideration of SOC in this work could not reproduce the IHD either. A possible distance dependence was suspected. Therefore the isotropic shielding of $MeBiX_2$ in different distances to H_2O was calculated with *ORCA* and non-relativistic options. Here strong distance dependence would be shown. However, the calculations of the distance model should repeated, because not the same conditions were chosen for all calculations. The results indicate that zero-point oscillation were a possible cause for the ihd. Another assumption was that the anharmonics were the possible explanation of the Distance dependence of the isotropic shieldings. Further calculations considering vibration effects and an anharmonics analysis should be carry out to find out if this effects could be the solution for the found IHD.

Looking ahead, it can be said that the SOC implementation should be

proofed, thought over and revised in *ORCA*. It is obviously not sufficient to perturb a non-relativistic density with a SOC Hamiltonian and calculate the response to the magnetic field. A possibility to calculate the relativistic density should be looked for, but not with ZORA. One could try to use scaled-ZORA, because this Hamiltonian corrects the error of the one-electron energy. Therefore the deep-core region is better described.[39] A perturbation by a SOC Hamiltonian on the calculated density by scaled-ZORA could show a fast improvement.

From the calculations for the bismuth compounds it can be concluded that it is very unlikely that the occurring IHD has its origin in relativistic effects. The large influence of the chemical shift due to the distance dependence rather indicates that the position of the proton seems to have been decisive. Therefore, oscillation and geometry effects should be investigated more closely.

References

[1] F. Neese. The ORCA program system. *Wiley Interdisciplinary Reviews: Computational Molecular Science*, 2(1):73–78, 2012.

[2] A.-M. Fritzsche, S. Scholz, M. Krasowska, K. Bhattacharyya, A. M. Toma, C. Silvestru, M. Korb, T. Rüffer, H. Lang, A. A. Auer, and M. Mehring. Evaluation of bismuth-based dispersion energy donors-synthesis, structure and theoretical study of 2-biphenylbismuth (iii) derivatives. *Physical Chemistry Chemical Physics*, 22(18):10189–10211, 2020.

[3] A. Szabo and N. S. Ostlund. *Modern quantum chemistry: Introduction to Advanced Electronic Structure Theory*. DOVER, 2017.

[4] P. W. Atkins and J. De Paula. *Physikalische Chemie*. John Wiley & Sons, 2013.

[5] W. Pauli. Pauli exclusion principle. *Naturwiss*, 12:741, 1924.

[6] D. Cremer. Density functional theory: coverage of dynamic and non-dynamic electron correlation effects. *Molecular Physics*, 99(23):1899–1940, 2001.

[7] W. Kohn and L. J. Sham. Self-consistent equations including exchange and correlation effects. *Physical review*, 140(4A):A1133, 1965.

[8] L. H. Thomas. The calculation of atomic fields. In *Mathematical Proceedings of the Cambridge Philosophical Society*, volume 23 of number 5, pages 542–548. Cambridge University Press, 1927.

[9] E. Fermi. Statistical method to determine some properties of atoms. *Rend. Accad. Naz. Lincei*, 6(602-607):5, 1927.

[10] D. Pines. Elementary excitations in solids, WA benjamin inc. *New York*, 1963.

[11] P. Hohenberg and W. Kohn. Inhomogeneous electron gas. *Physical review*, 136(3B):B864, 1964.

[12] W. Kohn, A. D. Becke, and R. G. Parr. Density functional theory of electronic structure. *The Journal of Physical Chemistry*, 100(31):12974–12980, 1996.

[13] L. Goerigk, A. Hansen, C. Bauer, S. Ehrlich, A. Najibi, and S. Grimme. A look at the density functional theory zoo with the advanced GMTKN55 database for general main group thermochemistry, kinetics and noncovalent interactions. *Physical Chemistry Chemical Physics*, 19(48):32184–32215, 2017.

[14] A. D. Becke. Density-functional exchange-energy approximation with correct asymptotic behavior. *Physical review A*, 38(6):3098, 1988.

[15] C. Lee, W. Yang, and R. G. Parr. Development of the colle-salvetti correlation-energy formula into a functional of the electron density. *Physical review B*, 37(2):785, 1988.

[16] S. H. Vosko, L. Wilk, and M. Nusair. Accurate spin-dependent electron liquid correlation energies for local spin density calculations: a critical analysis. *Canadian Journal of physics*, 58(8):1200–1211, 1980.

[17] J. P. Perdew. Density-functional approximation for the correlation energy of the inhomogeneous electron gas. *Physical Review B*, 33(12):8822, 1986.

[18] Y. J. Franzke and F. Weigend. NMR shielding tensors and chemical shifts in scalar-relativistic local exact two-component theory. *Journal of chemical theory and computation*, 15(2):1028–1043, 2019.

[19] H. Hellman. Einführung in die quantenchemie. *Franz Deuticke, Leipzig*, 285, 1937.

[20] R. P. Feynman. Forces in molecules. *Physical review*, 56(4):340, 1939.

[21] J. Pople, R. Krishnan, H. Schlegel, and J. S. Binkley. Derivative studies in hartree-fock and møller-plesset theories. *International Journal of Quantum Chemistry*, 16(S13):225–241, 1979.

[22] J. Grotendorst. *Modern methods and algorithms of quantum chemistry*, volume 1. NIC, 2000.

[23] G. Schreckenbach and T. Ziegler. Calculation of NMR shielding tensors based on density functional theory and a scalar relativistic pauli-type hamiltonian. the application to transition metal complexes. *International Journal of Quantum Chemistry*, 61(6):899–918, 1997.

[24] A. D. Buckingham and S. M. Malm. Asymmetry in the nuclear magnetic shielding tensor. *Molecular Physics*, 22(6):1127–1130, 1971.

[25] T. Helgaker, M. Jaszunski, and K. Ruud. Ab initio methods for the calculation of NMR shielding and indirect spin- spin coupling constants. *Chemical Reviews*, 99(1):293–352, 1999.

[26] F. London. Théorie quantique des courants interatomiques dans les combinaisons aromatiques, 1937.

[27] G. Schreckenbach and T. Ziegler. Calculation of NMR shielding tensors using gauge-including atomic orbitals and modern density functional theory. *The Journal of Physical Chemistry*, 99(2):606–611, 1995.

[28] T. Helgaker and P. Jørgensen. An electronic hamiltonian for origin independent calculations of magnetic properties. *The Journal of chemical physics*, 95(4):2595–2601, 1991.

[29] R. Ditchfield. Molecular orbital theory of magnetic shielding and magnetic susceptibility. *The Journal of Chemical Physics*, 56(11):5688–5691, 1972.

[30] R. Gerritsma, G. Kirchmair, F. Zähringer, E. Solano, R. Blatt, and C. Roos. Quantum simulation of the dirac equation. *Nature*, 463(7277):68–71, 2010.

[31] M. Reiher and A. Wolf. *Relative Quantum Chemistry second Edition*. WILEY-VCH, 2015.

[32] P. A. M. Dirac. A theory of electrons and protons. *Proceedings of the Royal Society of London. Series A, Containing papers of a mathematical and physical character*, 126(801):360–365, 1930.

[33] P. A. M. Dirac. The quantum theory of the electron. *Proceedings of the Royal Society of London. Series A, Containing Papers of a Mathematical and Physical Character*, 117(778):610–624, 1928.

[34] T. Saue. Relativistic hamiltonians for chemistry: a primer. *ChemPhysChem*, 12(17):3077–3094, 2011.

[35] S. K. Wolff, T. Ziegler, E. V. Lenthe, and E. J. Baerends. Density functional calculations of nuclear magnetic shieldings using the zeroth-order regular approximation (ZORA) for relativistic effects: ZORA nuclear magnetic resonance. *The Journal of chemical physics*, 110(16):7689–7698, 1999.

[36] M. Iliaš and T. Saue. An infinite-order two-component relativistic hamiltonian by a simple one-step transformation. *The Journal of chemical physics*, 126(6):064102, 2007.

[37] M. Olejniczak, R. Bast, T. Saue, and M. Pecul. A simple scheme for magnetic balance in four-component relativistic kohn–sham calculations of nuclear magnetic resonance shielding constants in a gaussian basis. *The Journal of Chemical Physics*, 136(1):014108, 2012.

[38] E. van Lenthe, E. J. Baerends, and J. G. Snijders. Relativistic regular two-component hamiltonians. *The Journal of chemical physics*, 99(6):4597–4610, 1993.

[39] E. van Lenthe, E.-J. Baerends, and J. G. Snijders. Relativistic total energy using regular approximations. *The Journal of chemical physics*, 101(11):9783–9792, 1994.

[40] J. Autschbach and T. Ziegler. Nuclear spin–spin coupling constants from regular approximate relativistic density functional calculations. i. formalism and scalar relativistic results for heavy metal compounds. *The Journal of Chemical Physics*, 113(3):936–947, 2000.

[41] P. Jensen and P. R. Bunker. *Computational molecular spectroscopy*. Wiley Chichester, 2000.

[42] B. Hess, C. Marian, and S. Peyerimhoff. Modern electronic structure theory. *World Scientific, Singapore*, 1995.

[43] F. Neese. Efficient and accurate approximations to the molecular spin-orbit coupling operator and their use in molecular g-tensor calculations. *The Journal of chemical physics*, 122(3):034107, 2005.

[44] F. Neese. *ORCA - An ab initio, DFT and semiempirical SCF-MO package - Version 4.0.1 - RELEASE-*. Max-Planck-Institute for Chemical Energy Conversion Stiftstr. 34-36, 45470 Mülheim a. d. Ruhr, Germany.

[45] S. Koseki, M. W. Schmidt, and M. S. Gordon. Effective nuclear charges for the first- through third-row transition metal elements in spin-orbit calculations. *The Journal of Physical Chemistry A*, 102(50):10430–10435, 1998.

[46] G. Schreckenbach and T. Ziegler. Calculation of the g-tensor of electron paramagnetic resonance spectroscopy using gauge-including atomic orbitals and density functional theory. *The Journal of Physical Chemistry A*, 101(18):3388–3399, 1997.

[47] V. G. Malkin, O. L. Malkina, and D. R. Salahub. Spin-orbit correction to NMR shielding constants from density functional theory. *Chemical physics letters*, 261(3):335–345, 1996.

[48] P. Pyykko and J. P. Desclaux. Relativity and the periodic system of elements. *Accounts of Chemical Research*, 12(8):276–281, 1979.

[49] M. Kaupp. Relativistic effects on NMR chemical shifts. In *Theoretical and Computational Chemistry*. Volume 14, pages 552–597. Elsevier, 2004.

[50] M. Kaupp, O. L. Malkin, and V. G. Malkin. Interpretation of 13c NMR chemical shifts in halomethyl cations. on the importance of spin-orbit coupling and electron correlation. *Chemical physics letters*, 265(1-2):55–59, 1997.

[51] R. G. Kidd. The oxidation-state dependence of transition-metal shieldings. In *Annual Reports on NMR Spectroscopy*. Volume 23, pages 85–139. Elsevier, 1991.

[52] H. Nakatsuji, H. Takashima, and M. Hada. Spin-orbit effect on the magnetic shielding constant using the ab initio UHF method. *Chemical physics letters*, 233(1-2):95–101, 1995.

[53] J. Vicha, J. Novotny, S. Komorovsky, M. Straka, M. Kaupp, and R. Marek. Relativistic heavy-neighbor-atom effects on NMR shifts: concepts and trends across the periodic table. *Chemical Reviews*, 120(15):7065–7103, 2020.

[54] J. Vaara, K. Ruud, O. Vahtras, H. Ågren, and J. Jokisaari. Quadratic response calculations of the electronic spin-orbit contribution to nuclear shielding tensors. *The Journal of chemical physics*, 109(4):1212–1222, 1998.

[55] C. C. Ballard, M. Hada, H. Kaneko, and H. Nakatsuji. Relativistic study of nuclear magnetic shielding constants: hydrogen halides. *Chemical physics letters*, 254(3-4):170–178, 1996.

[56] M. Kaupp, O. L. Malkina, V. G. Malkin, and P. Pyykkö. How do spin–orbit-induced heavy-atom effects on NMR chemical shifts function? validation of a simple analogy to spin–spin coupling by density functional theory (DFT) calculations on some iodo compounds. *Chemistry–A European Journal*, 4(1):118–126, 1998.

[57] J. Vicha, M. Straka, M. L. Munzarova, and R. Marek. Mechanism of spin–orbit effects on the ligand NMR chemical shift in transition-metal complexes: linking NMR to EPR. *Journal of chemical theory and computation*, 10(4):1489–1499, 2014.

[58] M. Filatov and D. Cremer. Calculation of indirect nuclear spin–spin coupling constants within the regular approximation for relativistic effects. *The Journal of chemical physics*, 120(24):11407–11422, 2004.

[59] M. Valiev, E. J. Bylaska, N. Govind, K. Kowalski, T. P. Straatsma, H. J. Van Dam, D. Wang, J. Nieplocha, E. Apra, T. L. Windus, et al. NWChem: a comprehensive and scalable open-source solution for large scale molecular simulations. *Computer Physics Communications*, 181(9):1477–1489, 2010.

[60] T. Saue, R. Bast, A. S. P. Gomes, H. J. A. Jensen, L. Visscher, I. A. Aucar, R. Di Remigio, K. G. Dyall, E. Eliav, E. Fasshauer, et al. The DIRAC code for relativistic molecular calculations. *The Journal of Chemical Physics*, 152(20):204104, 2020.

[61] M. D. Hanwell, D. E. Curtis, D. C. Lonie, T. Vandermeersch, E. Zurek, and G. R. Hutchison. Avogadro: an advanced semantic chemical editor, visualization, and analysis platform. *Journal of cheminformatics*, 4(1):17, 2012.

[62] F. Weigend and R. Ahlrichs. Balanced basis sets of split valence, triple zeta valence and quadruple zeta valence quality for h to rn: design and assessment of accuracy. *Physical Chemistry Chemical Physics*, 7(18):3297–3305, 2005.

[63] R. Weber, B. Hovda, G. Schoendorff, and A. K. Wilson. Behavior of the sapporo-nZP-2012 basis set family. *Chemical Physics Letters*, 637:120–126, 2015.

[64] T. Noro, M. Sekiya, and T. Koga. Segmented contracted basis sets for atoms h through xe: sapporo-(DK)-nZP sets (n= d, t, q). *Theoretical Chemistry Accounts*, 131(2):1124, 2012.

[65] T. Noro, M. Sekiya, and T. Koga. Sapporo-(DKH3)-nZP (n= d, t, q) sets for the sixth period s-, d-, and p-block atoms. *Theoretical Chemistry Accounts*, 132(5):1363, 2013.

[66] B. P. Pritchard, D. Altarawy, B. Didier, T. D. Gibson, and T. L. Windus. New basis set exchange: an open, up-to-date resource for the molecular sciences community. *Journal of chemical information and modeling*, 59(11):4814–4820, 2019.

[67] L. Visscher. Approximate molecular relativistic dirac-coulomb calculations using a simple coulombic correction. *Theoretical Chemistry Accounts*, 98(2-3):68–70, 1997.

[68] E. Baerends, T. Ziegler, J. Autschbach, D. Bashford, A. Bérces, F. Bickelhaupt, C. Bo, P. Boerrigter, L. Cavallo, D. Chong, et al. ADF. *SCM, Theoretical Chemistry, Vrije Universiteit, Amsterdam, See http://www. scm. com*, 2013.

[69] G. t. Te Velde, F. M. Bickelhaupt, E. J. Baerends, C. Fonseca Guerra, S. J. van Gisbergen, J. G. Snijders, and T. Ziegler. Chemistry with ADF. *Journal of Computational Chemistry*, 22(9):931–967, 2001.

[70] C. F. Guerra, J. Snijders, G. t. te Velde, and E. J. Baerends. Towards an order-n DFT method. *Theoretical Chemistry Accounts*, 99(6):391–403, 1998.

[71] S. Hayashi, K. Matsuiwa, and W. Nakanishi. Relativistic effects on the 125 te and 33 s NMR chemical shifts of various tellurium and sulfur species, together with 77 se of selenium congeners, in the framework of a zeroth-order regular approximation: applicability to tellurium compounds. *RSC Advances*, 4(84):44795–44810, 2014.

[72] A. Antušek and M. Repisky. NMR absolute shielding scales and nuclear magnetic dipole moments of transition metal nuclei. *Physical Chemistry Chemical Physics*, 22(13):7065–7076, 2020.

[73] G. Te Velde, F. Bickelhaupt, E. Baerends, C. Fonseca Guerra, and S. Van Gisbergen. A.; snijders, JG; ziegler, t. *Chemistry with ADF. J. Comput. Chem*, 22(9):931–967, 2001.

[74] C. F. Guerra, J. Snijders, G. t. te Velde, and E. J. Baerends. Towards an order-n DFT method. *Theoretical Chemistry Accounts*, 99(6):391–403, 1998.

[75] E. J. Baerends, T. Ziegler, J. Autschbach, D. Bashford, A. Bérces, F. Bickelhaupt, C. Bo, P. Boerrigter, L. Cavallo, D. Chong, et al. ADF2013, SCM, theoretical chemistry, vrije universiteit, amsterdam, the netherlands. *URL: http://www. scm. com*, 2014.

[76] T. v7.3 2017. A development of university of karlsruhe and forschungszentrum karlsruhe gmbh, 1989-2007. URL: `https://www.turbomole.com`.

[77] R. Ahlrichs, M. Bär, M. Häser, H. Horn, and C. Kölmel. Electronic structure calculations on workstation computers: the program system turbomole. *Chemical Physics Letters*, 162(3):165–169, 1989.

[78] F. Furche, R. Ahlrichs, C. Hättig, W. Klopper, M. Sierka, and F. T. Weigend. WIREs comput. *Mol. Sci*, 4(2):91–100, 2014.

[79] G. L. Stoychev, A. A. Auer, and F. Neese. Automatic generation of auxiliary basis sets. *Journal of chemical theory and computation*, 13(2):554–562, 2017.

[80] L. Visscher, T. Enevoldsen, T. Saue, H. J. A. Jensen, and J. Oddershede. Full four-component relativistic calculations of NMR shielding and indirect spin–spin coupling tensors in hydrogen halides. *Journal of computational chemistry*, 20(12):1262–1273, 1999.

[81] K. Aidas, C. Angeli, K. L. Bak, V. Bakken, R. Bast, L. Boman, O. Christiansen, R. Cimiraglia, S. Coriani, P. Dahle, et al. The dalton quantum chemistry program system. *Wiley Interdisciplinary Reviews: Computational Molecular Science*, 4(3):269–284, 2014.

[82] Y. Y. Rusakov, I. L. Rusakova, and L. B. Krivdin. On the HALA effect in the NMR carbon shielding constants of the compounds containing heavy p-elements. *International Journal of Quantum Chemistry*, 116(19):1404–1412, 2016.

[83] H. Nakatsuji. Electronic mechanisms of metal chemical shifts from ab initio theory. In *Nuclear Magnetic Shieldings and Molecular Structure*, pages 263–278. Springer, 1993.

[84] H. Nakatsuji, Z.-M. Hu, and T. Nakajima. Spin-orbit effect on the magnetic shielding constant: niobium hexahalides and titanium tetrahalides. *Chemical physics letters*, 275(3-4):429–436, 1997.

[85] S. Moncho and J. Autschbach. Molecular orbital analysis of the inverse halogen dependence of nuclear magnetic shielding in lax3, x= f, cl, br, i. *Magnetic Resonance in Chemistry*, 48(S1):S76–S85, 2010.

[86] J. Ariai and G. Saielli. “through-space” relativistic effects on NMR chemical shifts of pyridinium halide ionic liquids. *ChemPhysChem*, 20(1):108–115, 2019.

A. Appendix

A.1. Comparison of *ORCA* to literature values

Table A.1: Calculated NR- and scR-NMR shiledings from some molecules by using the *ORCA* program and their deviations to the literature. As scalar relativistic hamiltonian was used the ZORA-hamiltonian.

Molecule	**Orca** Shielding NR (scR) [ppm]	**Literature**[71][46] Shielding NR (scR) [ppm]	**Deviation NR (scR) [%]**
$Mo(CO)_6$	1388.39 (1393.53)[1)]	1431.00 (1704.00)	2.98 (18.22)
SeMeH	1789.16(1772.78)[1)]	1837.00 (1711.30)	2.60 (3.59)
SeEtH	1712.59 (1731.05)[2)]	1673.10 (1633.00)	2.36 (6.00)
$SeEt_2$	1424.92 (1456.72)[3)]	1375.70 (1320.80)	3.58 (10.29)
TeH_2	3508.13[3)]	3503.60	0.13
TeMeH	3064.50[3)]	3049.00	0.51
$TeMe_2$	2667.18[2)]	2643.40	0.90
TeEtH	2983.16[3)]	2968.00	0.51
$TeEt_2$	2477.19[2)]	2450.90	1.07
TeF_4	1695.33[4)]	1674.40	1.25
TeF_6	2305.80[5)]	2293.00	0.56
$TeCl_4$	1234.37[6)]	1191.70	3.58

Each caclulation was done with the simple keyword Autoaux, Verytightscf and grid 6;
1) Mo: Sapporo-TZP-2012; Other: def2-TZVPP 2) Se/Te: Sappooro-QZP-2012; Other: def2-QZVPPD 3) Se/Te: Sapporo-QZP-2012; Other: def2-QZVPP 4) Te: Sapporo-TZP-2012; Other: def2-TZVPP 5) Te: Sapporo-TZP-2012; Other: def2-TZVPPD 6) Te: Sapporo-TZP-2012; Other: def2-TZVPP

A.2. Comparison of *ORCA* and *NWChem*

Table A.2: Comparison of *ORCA* and *NWChem* in a HF-calculation regarding nuclear repulsion energy, converged SCF energy and isotropic shielding. For the latter, the values for the heavy nuclei are listed. Note the decimal places of *NWChem* were partly shortened.

Molecule	Nuclear Repulsion Energy [E_h]		Deviation [%]	last SCF Energy [E_h]		Deviation [%]	isotropic Shielding [ppm]		Deviation [%]
	ORCA	***NWChem***		***ORCA***	***NWChem***		***ORCA***	***NWChem***	
BF_3	110.70661290	110.70662148	$7.75 \cdot 10^{-06}$	-323.34214144	-323.34214139	$1.38 \cdot 10^{-08}$	105.579	105.5603	0.02
AlF_3	159.05015060	159.05016268	$7.60 \cdot 10^{-06}$	-540.59817905	-540.35981790	$1.11 \cdot 10^{-10}$	544.335	544.2112	0.02
GaF_3	298.18740727	298.18743030	$7.73 \cdot 10^{-06}$	-2221.82742123	-2221.82742123	$1.89 \cdot 10^{-10}$	1865.467	1865.0785	0.02
InF_3	400.67060231	400.67063309	$7.68 \cdot 10^{-06}$	-6038.626700338	-6038.62670038	$6.96 \cdot 10^{-11}$	3830.216	3829.7854	0.01
TlF_3	611.98649870	611.98654659	$7.83 \cdot 10^{-06}$	-16603.16712338	-16603.16707241	$3.07 \cdot 10^{-7}$	5667.828	5666.3341	0.03
CH_4	13.44098602	13.44098705	$7.67 \cdot 10^{-06}$	-40.20835223	-40.20835223	$1.02 \cdot 10^{-08}$	194.675	194.7115	0.02
SiH_4	21.32305139	21.32305303	$7.70 \cdot 10^{-06}$	-291.23472314	-291.23472313	$3.44 \cdot 10^{-11}$	472.038	472.0525	$3.07 \cdot 10^{-03}$
GeH_4	45.34839206	45.34839555	$7.70 \cdot 10^{-06}$	-2077.67484608	-2077.67484607	$1.44 \cdot 10^{-10}$	1780.228	1779.2603	0.05
SnH_4	63.05010623	63.05011108	$7.70 \cdot 10^{-06}$	-6025.14335241	-6025.14335240	$1.24 \cdot 10^{-10}$	3316.582	3315.3618	0.04
PbH_4	99.66173165	99.66173931	$7.69 \cdot 10^{-06}$	-16709.50555758	-16715.32258099	$3.48 \cdot 10^{-02}$	1139.050	1501.3449	24.13
NF_3	132.57741613	132.57742613	$7.54 \cdot 10^{-06}$	-352.68807828	-352.68807828	$1.47 \cdot 10^{-09}$	-107.985	-107.9250	0.06
PF_3	189.54594789	189.54596190	$7.40 \cdot 10^{-06}$	-639.29139840	-639.29139839	$3.18 \cdot 10^{-10}$	246.81	246.5418	0.11
AsF_3	322.53019003	322.53021425	$7.51 \cdot 10^{-06}$	-2532.73083958	-2532.73083960	$9.40 \cdot 10^{-10}$	1342.555	1342.5449	$7.52 \cdot 10^{-04}$
SbF_3	428.75707817	428.75711183	$7.85 \cdot 10^{-06}$	-6611.92155874	-6611.92155875	$2.60 \cdot 10^{-10}$	2995.06	2995.0772	$5.74 \cdot 10^{-04}$
BiF_3	634.49628090	634.49633183	$8.03 \cdot 10^{-06}$	-17430.56490906	-17430.56489991	$5.24 \cdot 10^{-08}$	-65748.188	-65753.919	0.01
NMe_3	138.53206635	138.53207714	$7.79 \cdot 10^{-06}$	-173.3289492	-173.32894920	$4.62 \cdot 10^{-10}$	250.197	249.9140	0.11
PMe_3	176.83535827	176.83537193	$7.73 \cdot 10^{-06}$	-459.61707345	-459.61707339	$1.19 \cdot 10^{-08}$	405.676	405.5709	0.03
$AsMe_3$	288.08491285	288.08491279	$1.83 \cdot 10^{-08}$	-2353.08491285	-2353.08491279	$2.24 \cdot 10^{-09}$	1601.365	1601.2211	0.01
$SbMe_3$	377.09375087	377.09378001	$7.73 \cdot 10^{-06}$	-6432.24336518	-6432.24336516	$2.86 \cdot 10^{-10}$	2913.417	2913.2284	0.01
$BiMe_3$	550.49866301	550.49870567	$7.75 \cdot 10^{-06}$	-17250.91207197	-17250.91194085	$7.60 \cdot 10^{-07}$	-2964.807	-3228.4783	8.17
H_2O	9.1382847	9.13828540	$7.68 \cdot 10^{-06}$	-76.04806822	-76.0480682293	$1.22 \cdot 10^{-08}$	334.223	334.0442	0.05
H_2S	12.88104165	12.88104259	$7.33 \cdot 10^{-06}$	-398.67618702	-398.6761870245	$1.13 \cdot 10^{-09}$	700.108	700.0762	$4.54 \cdot 10^{-3}$
H_2Se	24.71573959	24.71574149	$7.69 \cdot 10^{-06}$	-2401.00010831	-2401.0001083141	$1.71 \cdot 10^{-10}$	2148.434	2148.7222	0.01
H_2Te	33.34233604	33.34233860	$7.69 \cdot 10^{-06}$	-6612.82429920	-6612.8242992028	$4.23 \cdot 10^{-11}$	3694.095	3695.2044	0.03
H_2Po	51.01184488	51.01184883	$7.75 \cdot 10^{-06}$	-17557.35465771	-17557.3546577044	$3.19 \cdot 10^{-11}$	217.248	217.8863	0.29

Table A.3: Comparison of *ORCA* and *NWChem* in a HF-calculation regarding nuclear repulsion energy, converged SCF energy and isotropic shielding. For the latter, the values for the heavy nuclei are listed. Note the decimal places of *NWChem* were partly shortened.

Molecule	**Nuclear Repulsion Energy [E_h]**		**Deviation [%]**	**last SCF Energy [E_h]**		**Deviation [%]**	**isotropic Shielding [ppm]**		**Deviation [%]**
	ORCA	***NWChem***		***ORCA***	***NWChem***		***ORCA***	***NWChem***	
HF	5.15029909	5.15029948	$7.68 \cdot 10^{-06}$	-100.04783032	-100.0478303225	$2.57 \cdot 10^{-09}$	417.005	417.0486	0.01
HCl	7.01523335	7.01523388	$7.62 \cdot 10^{-06}$	-460.06347410	-460.0634741038	$8.26 \cdot 10^{-10}$	943.839	942.8446	0.11
HBr	12.99525570	12.99525669	$7.69 \cdot 10^{-06}$	-2572.98333016	-2572.9833301686	$3.34 \cdot 10^{-10}$	2625.175	2624.8562	0.01
HI	17.35597762	17.35597895	$7.71 \cdot 10^{-06}$	-6918.44941647	-6918.4494164710	$1.45 \cdot 10^{-11}$	4535.361	4535.9710	0.01
HAt	26.33767612	26.33767814	$7.69 \cdot 10^{-06}$	-17989.66640883	-17989.6664088769	$2.61 \cdot 10^{-10}$	8165.835	8165.3435	0.01
NeF_2	63.11447203	63.11447688	$7.70 \cdot 10^{-06}$	-326.9698111	-326.96958108	$7.03 \cdot 10^{-5}$	-5972.269	-5971.9254	0.01
ArF_2	106.57588824	106.57589643	$7.69 \cdot 10^{-06}$	-725.397762480	-725.39776250	$3.52 \cdot 10^{-09}$	659.027	659.3294	0.05
KrF_2	192.08101868	192.08103345	$7.69 \cdot 10^{-06}$	-2950.69557942	-2950.69557941	$3.39 \cdot 10^{-11}$	1460.448	1461.0316	0.04
XeF_2	267.11877961	267.11880015	$7.69 \cdot 10^{-06}$	-7430.78823736	-7430.78823738	$3.04 \cdot 10^{-10}$	2078.937	2079.7409	0.04
RnF_2	403.02726428	403.02729527	$7.69 \cdot 10^{-06}$	-18633.00013553	-18633.00005042	$4.57 \cdot 10^{-07}$	12652.494	12647.8507	0.04
ArF_4	281.52701066	281.52703336	$8.06 \cdot 10^{-06}$	-923.97129442	-923.97129449	$7.73 \cdot 10^{-09}$	510.712	511.5250	0.16
KrF_4	454.66524368	454.66527948	$7.88 \cdot 10^{-06}$	-3149.35024616	-3149.35246111	$7.03 \cdot 10^{-05}$	722.856	723.6470	0.11
XeF_4	607.36944531	607.36949173	$7.64 \cdot 10^{-06}$	-7629.55187581	-7629.55187580	$2.62 \cdot 10^{-12}$	744.651	745.3437	0.09
RnF_4	885.50642844	885.50649431	$7.44 \cdot 10^{-06}$	-18831.99163475	-18831.98674549	$2.60 \cdot 10^{-05}$	23078.603	23128.3932	0.22
ArF_6	521.03295495	521.03299454	$7.60 \cdot 10^{-06}$	-1122.49346337	-1122.49346347	$9.55 \cdot 10^{-09}$	164.332	164.8480	0.31
KrF_6	782.25670687	782.25676667	$7.64 \cdot 10^{-06}$	-3347.95332234	-3347.95332226	$2.26 \cdot 10^{-09}$	134.552	134.5382	0.01
XeF_6	1013.29896820	1013.29904724	$7.80 \cdot 10^{-06}$	-7828.26549883	-7828.26549872	$1.30 \cdot 10^{-09}$	1259.629	1259.5712	$4.59 \cdot 10^{-3}$
RnF_6	1443.09301705	1443.09312923	$7.77 \cdot 10^{-06}$	-19031.0467647346	-19031.05892329	$6.39 \cdot 10^{-05}$	-6791.761	1149.0066	691.10

Table A.4: Comparison of *ORCA* and *NWChem* in a DFT-calculation regarding the converged SCF energy and isotropic shielding. For the latter, the values for the heavy nuclei are listed.

Molecule	**last SCF Energy [E_h]**		**Deviation [%]**	**isotropic Shielding [ppm]**		**Deviation [%]**
	ORCA	***NWChem***		***ORCA***	***NWChem***	
BF_3	-324.70168403	-324.6943864067	$2.25 \cdot 10^{-03}$	86.513	86.5233	0.01
AlF_3	-542.33395598	-542.3248079226	$1.69 \cdot 10^{-03}$	488.233	488.0676	0.03
GaF_3	-2224.91751150	-2224.9070758946	$4.69 \cdot 10^{-04}$	1617.604	1617.0729	0.03
InF_3	-6042.81651013	-6042.8084344755	$1.34 \cdot 10^{-04}$	3433.030	3431.9242	0.03
TlF_3	-16616.7182237358	-16616.7671781364	$2.95 \cdot 10^{-04}$	2301.619	2298.1168	0.15
CH_4	-40.52635795	-40.5263525545	$1.33 \cdot 10^{-05}$	189.467	189.5258	0.03
SiH_4	-291.89556183	-291.8945060369	$3.62 \cdot 10^{-04}$	430.765	430.9256	0.04
GeH_4	-2079.66951901	-2079.6671541974	$1.14 \cdot 10^{-04}$	1623.120	1623.6621	0.03
SnH_4	-6028.2573061	-6028.2571973643	$1.80 \cdot 10^{-06}$	3028.779	3029.3992	0.02
PbH_4	-16721.88466889	-16727.7633494616	$3.51 \cdot 10^{-02}$	361.777	1103.6348	67.22
NF_3	-354.26503202	-354.2573290195	$2.17 \cdot 10^{-03}$	-173.465	-173.3361	0.07
PF_3	-641.15763948	-641.1490942599	$1.33 \cdot 10^{-03}$	143.46	143.5681	0.08
AsF_3	-2535.91958150	-2535.9101010094	$3.74 \cdot 10^{-04}$	937.356	937.5547	0.02
SbF_3	-6616.25503242	-6616.2476280081	$1.12 \cdot 10^{-04}$	2311.996	2311.6912	$1.32 \cdot 10^{-02}$
BiF_3	-17444.102831772	-17444.1442276269	$2.37 \cdot 10^{-04}$	-88960.503	-88940.6025	0.02
NMe_3	-174.52764994	-174.5260034751	$9.43 \cdot 10^{-04}$	221.690	221.7584	0.03
PMe_3	-461.16274592	-461.1608857242	$4.03 \cdot 10^{-04}$	340.965	341.4433	0.14
$AsMe_3$	-2355.94255853	-2355.9394699665	$1.31 \cdot 10^{-04}$	1362.513	1363.7218	0.09
$SbMe_3$	-6436.24897594	-6436.2481839890	$1.23 \cdot 10^{-05}$	2480.758	2482.4593	0.07
$BiMe_3$	-17264.1419239911	-17264.1895221413	$2.76 \cdot 10^{-04}$	-2519.602	-1050.1272	139.93
H_2O	-76.45360529	-76.4520761878	$2.00 \cdot 10^{-03}$	333.238	333.2605	0.01
H_2S	-399.42119571	-399.420061074800	$2.84 \cdot 10^{-04}$	692.054	692.4586	0.06
H_2Se	-2403.03720579	-2403.0353483516	$7.73 \cdot 10^{-05}$	2064.058	2065.0663	0.05
H_2Te	-6616.03367973	-6616.0339387449	$3.91 \cdot 10^{-06}$	3528.554	3530.4475	0.05
H_2Po	-17569.66779886	-17569.6798147149	$6.84 \cdot 10^{-05}$	2340.202	2349.8693	0.41

Table A.5: Comparison of *ORCA* and *NWChem* in a DFT-calculation regarding the converged SCF energy and isotropic shielding. For the latter, the values for the heavy nuclei are listed.

Molecule	**last SCF Energy [E_h]**		**Deviation [%]**	**isotropic Shielding [ppm]**		**Deviation [%]**
	ORCA	***NWChem***		***ORCA***	***NWChem***	
HF	-100.47510740	-100.47293953066	$2.16 \cdot 10^{-03}$	412.608	412.5853	0.01
HCl	-460.83249973	-460.8310009755	$3.25 \cdot 10^{-04}$	928.161	928.8169	0.07
HBr	-2575.02815168	-2575.0263969722	$6.81 \cdot 10^{-05}$	2550.804	2551.4096	0.02
HI	-6921.69564787	-6921.6960788497	$6.23 \cdot 10^{-06}$	4401.406	4402.6465	0.03
HAt	-18001.86957406	-18001.8821303534	$6.97 \cdot 10^{-05}$	7791.358	7792.1769	0.01
NeF_2	-328.42411824	-328.3428043151	$2.48 \cdot 10^{-02}$	8718.697	92.7788	9297.29
ArF_2	-727.113209440	-727.1068697701	$8.72 \cdot 10^{-04}$	866.382	866.8026	0.05
KrF_2	-2953.65238915	-2953.6462099077	$2.09 \cdot 10^{-04}$	1823.945	1825.5101	0.09
XeF_2	-7434.94613622	-7434.9424414936	$4.97 \cdot 10^{-05}$	2287.564	2291.1641	0.16
RnF_2	-18645.98150881	-18645.9898288925	$4.46 \cdot 10^{-05}$	12133.654	12133.6483	$4.70 \cdot 10^{-05}$
ArF_4	-926.65530876	-926.6446889382	$1.15 \cdot 10^{-03}$	128.474	129.1338	0.51
KrF_4	-3153.24490728	-3153.234344023	$3.35 \cdot 10^{-04}$	215.884	217.7877	0.87
XeF_4	-7634.61085669	-7634.6026468746	$1.08 \cdot 10^{-04}$	-31.723	-27.9736	13.40
RnF_4	-18845.83147798	-18845.8445961906	$6.96 \cdot 10^{-05}$	-4143.039	-4141.2580	0.04
ArF_6	-1126.17847446	-1126.1635574077	$1.32 \cdot 10^{-03}$	-483.770	-482.7846	0.20
KrF_6	-3352.82528433	-3352.8103788330	$4.45 \cdot 10^{-04}$	-530.867	-528.8437	0.38
XeF_6	-7834.27095890	-7834.2582603722	$1.62 \cdot 10^{-04}$	276.934	279.0887	0.77
RnF_6	-19045.74825382	-19045.7702654827	$1.16 \cdot 10^{-04}$	-10814.108	-3719.0295	190.78

Table A.6: Comparison of *ORCA* and *NWChem* in a scalar relativistisc DFT-calculation with the ZORA-hamiltonian regarding the converged SCF energy and isotropic shielding. For the latter, the values for the heavy nuclei are listed.

Molecule	**last SCF Energy [E_h]**		**Deviation [%]**	**isotropic Shielding [ppm]**		**Deviation [%]**
	ORCA	***NWChem***		***ORCA***	***NWChem***	
BF_3	-325.14375033	-325.1038725559	$1.23 \cdot 10^{-02}$	86.377	86.3484	0.03
AlF_3	-543.46118302	-543.3859924959	$1.38 \cdot 10^{-02}$	487.231	486.0098	0.25
GaF_3	-2253.20842132	-2252.6241370946	$2.59 \cdot 10^{-02}$	1590.819	1577.1879	0.86
InF_3	-6228.39388090	-6226.7753581836	$2.60 \cdot 10^{-02}$	3383.044	3330.6144	1.57
TlF_3	-21173.65205748	-21190.3620949926	$7.89 \cdot 10^{-02}$	6626.540	6488.9073	2.12
CH_4	-40.55174712	-40.5490450312	$6.66 \cdot 10^{-03}$	189.360	189.3443	0.01
SiH_4	-292.85734909	-292.8114468815	$1.57 \cdot 10^{-02}$	429.888	428.8114	0.25
GeH_4	-2111.48524549	-2110.8889136436	$2.83 \cdot 10^{-02}$	1609.008	1594.4217	0.91
SnH_4	-6229.40002389	-6227.7845547936	$2.59 \cdot 10^{-02}$	3039.544	2986.7339	1.77
PbH_4	-21556.07035187	-21571.9357474374	$7.35 \cdot 10^{-02}$	5198.477	5140.2468	1.13
NF_3	-354.7448621	-354.7015862477	$1.22 \cdot 10^{-02}$	-174.078	-173.9762	0.06
PF_3	-642.88521044	-642.7893986614	$1.49 \cdot 10^{-02}$	143.29	142.0641	0.86
AsF_3	-2572.52490462	-2571.8359379692	$2.68 \cdot 10^{-02}$	949.422	933.5905	1.70
SbF_3	-6834.78720491	-6833.1187106506	$2.44 \cdot 10^{-02}$	2528.496	2473.5685	2.22
BiF_3	-22552.33016609	-22564.4988131519	0.05	3007.452	3251.6202	7.51
NMe_3	-174.65271635	-174.6385381513	$8.12 \cdot 10^{-03}$	221.181	221.1709	$4.57 \cdot 10^{-03}$
PMe_3	-462.53579021	-462.4696416915	$1.43 \cdot 10^{-02}$	339.444	338.6324	0.24
$AsMe_3$	-2392.19559781	-2391.5361645279	$2.76 \cdot 10^{-02}$	1362.586	1347.4576	1.12
$SbMe_3$	-6654.43875116	-6652.7996989365	$2.46 \cdot 10^{-02}$	2527.494	2480.0474	1.91
$BiMe_3$	-22371.98787397	-22384.1779520981	0.05	3291.524	3923.6158	16.11
H_2O	-76.54307504	-76.5318271665	0.01	332.793	332.6463	0.04
H_2S	-401.13593816	-407.065006192050	1.46	689.279	687.8733	0.20
H_2Se	-2444.2017345943	-2443.4908852800	0.03	2035.598	2018.5956	0.84
H_2Te	-6852.18143916	-6850.5406666904	0.02	3562.821	3504.6881	1.66
H_2Po	-22968.927134	-22975.7411229097	0.03	5057.567	5043.6337	0.28

Table A.7: Comparison of *ORCA* and *NWChem* in a scalar relativistisc DFT-calculation with the ZORA-hamiltonian regarding the converged SCF energy and isotropic shielding. For the latter, the values for the heavy nuclei are listed.

Molecule	**last SCF Energy [E_h]**		**Deviation [%]**	**isotropic Shielding [ppm]**		**Deviation [%]**
	ORCA	***NWChem***		***ORCA***	***NWChem***	
HF	-100.61826210	-100.6057409118	0.01	412.047	411.7519	0.07
HCl	-463.05985166	-462.9730425258	0.02	925.041	922.9944	0.22
HBr	-2621.26168677	-2620.4952912203	0.03	2501.362	2481.8349	0.79
HI	-7176.94897039	-7175.3137250384	0.02	4318.030	4252.4953	1.54
HAt	-23701.24348687	-23701.4926667122	$1.05 \cdot 10^{-03}$	7152.947	6920.8849	3.35
NeF_2	-328.93530332	-328.8932060479	$1.28 \cdot 10^{-02}$	8727.403	8665.4090	0.72
ArF_2	-730.249902060	-730.1200665889	$1.78 \cdot 10^{-02}$	866.033	863.4987	0.29
KrF_2	-3005.92540462	-3005.0739262689	$2.83 \cdot 10^{-02}$	1842.128	1821.7403	1.12
XeF_2	-7710.69551689	-7709.0628132302	$2.12 \cdot 10^{-02}$	2619.829	2559.5287	2.36
RnF_2	-24644.35013599	-24643.6643745996	$2.78 \cdot 10^{-03}$	1404.494	1122.842	25.08
ArF_4	-930.07987215	-929.9250637714	$1.66 \cdot 10^{-02}$	128.740	126.8044	1.53
KrF_4	-3205.80613869	-3204.9295988996	$2.73 \cdot 10^{-02}$	295.527	277.6495	6.44
XeF_4	-7910.65175134	-7908.9938427598	$2.10 \cdot 10^{-02}$	564.062	514.4568	9.64
RnF_4	-24844.32757300	-24843.6163994428	$2.86 \cdot 10^{-03}$	-4495.569	-3794.2920	18.48
ArF_6	-1129.89090706	-1129.7111085507	$1.59 \cdot 10^{-02}$	-483.977	-485.3985	0.29
KrF_6	-3405.67579055	-3404.774214749	$2.65 \cdot 10^{-02}$	-453.803	-469.7841	3.40
XeF_6	-8110.60650047	-8108.9233931362	$2.08 \cdot 10^{-02}$	554.155	507.4434	9.21
RnF_6	-25044.31764262	-25043.5809833794	$2.94 \cdot 10^{-03}$	-2581.581	-1999.5868	29.11

A.3. Grid dependency

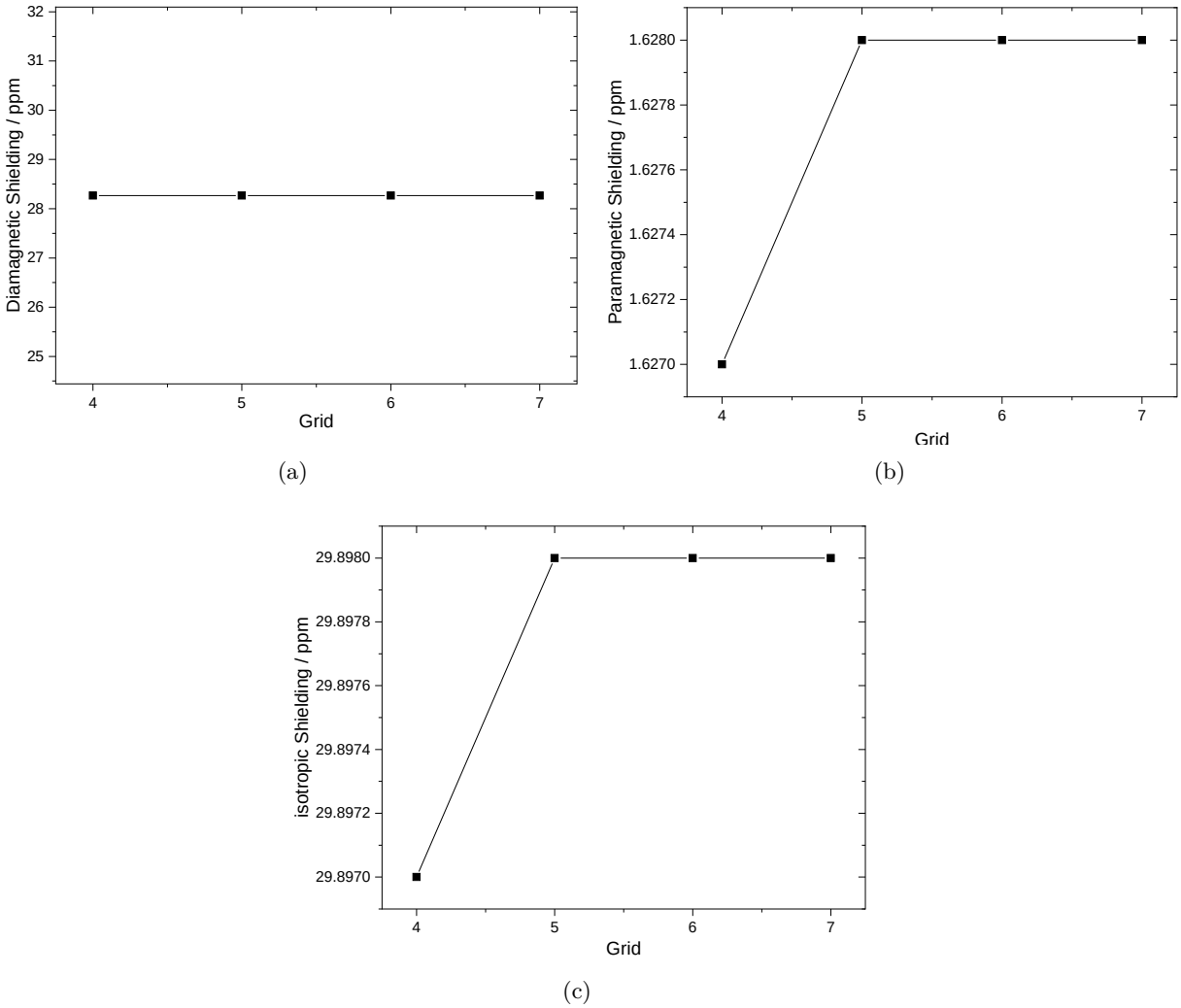

Figure A.1: Grid dependency of the NMR ZORA calculation of TeH_2. Shown are the isotropic shieldings of the H-atom: in a) the diamagnetic b) the paramagnetic contribution and in c) the total isotropic shielding.

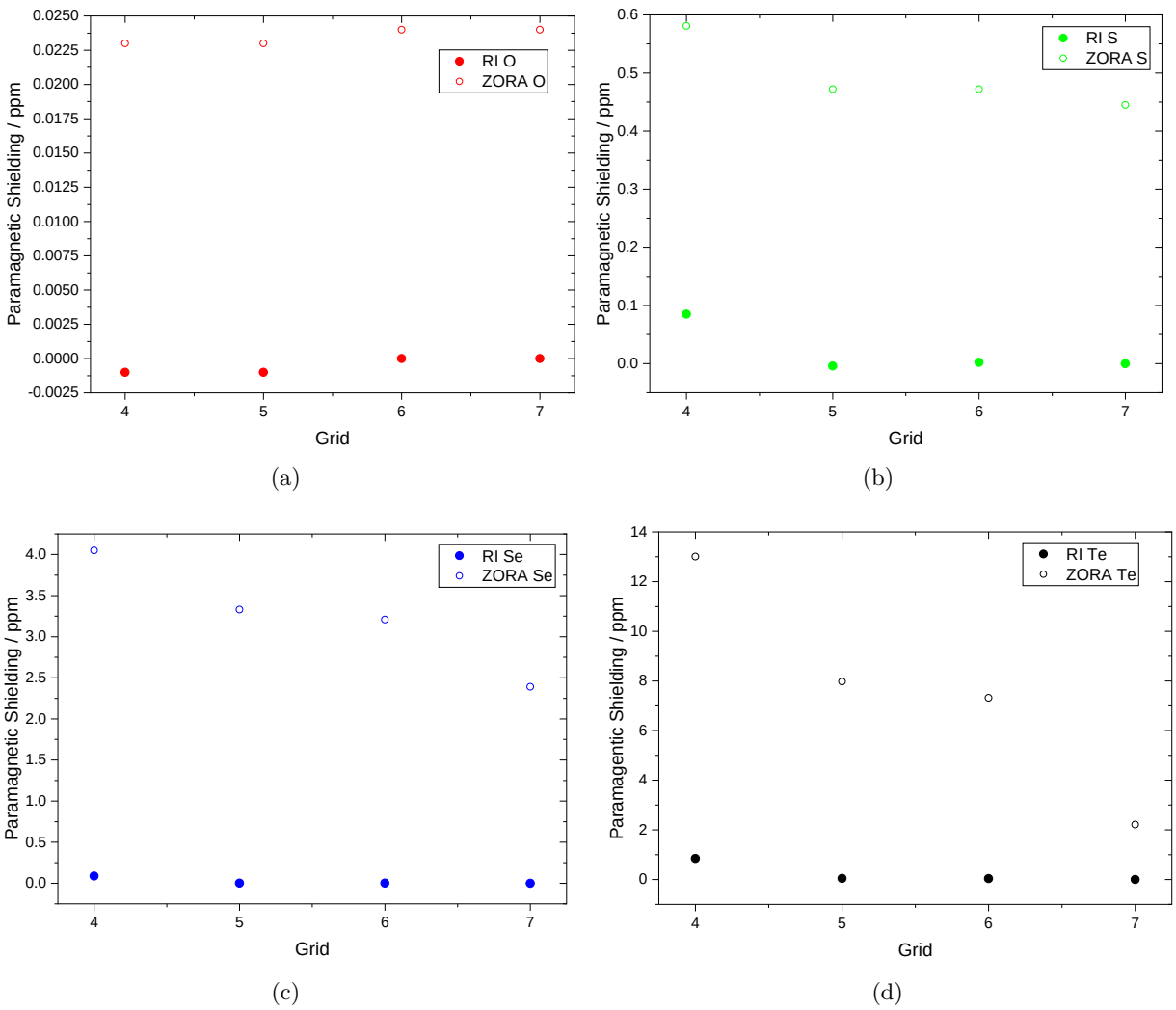

Figure A.2: Grid dependence of dioxo compounds of the 16th group. Comparison of the paramagnetic contribution with ZORA and RIZORA. The grid dependence is shown for a) the O-atom, b) the S-atom, c) the Se-atom and d) the Te-atom.

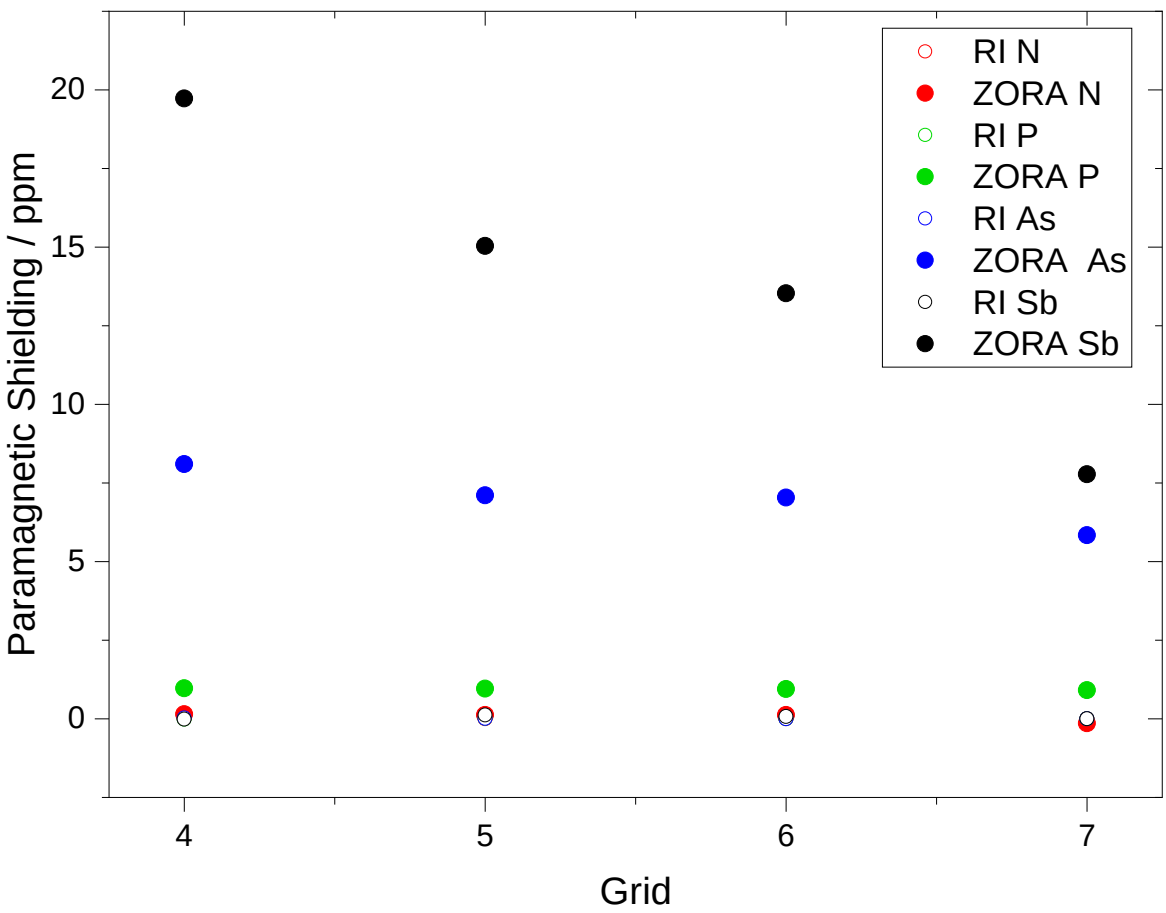

Figure A.3: Paramagnetic grid dependence of the trifluoride compounds of the 15th group. Shown for the heavy atom. Comparison of RIZORA (filled circles) and ZORA (rings). All values were normalized to Grid 7 from RIZORA for the individual compound.

Table A.8: Comparison of RIZORA and ZORA for the p-block: 13th-18th group. Including the isotropic paramagnetic shielding of the heavy atom and the computation time of the NMR calculation.

Molecule	**paramagnetic isotropic shielding**			**Time** [s]	
	RIZORA [ppm]	ZORA [ppm]	Deviation [%]	RIZORA	ZORA
BF_3	-111.384	-111.372	0.01	1267.805	262.14
AlF_3	-305.124	-304.88	0.08	1587.792	313.596
GaF_3	-1052.325	-1050.355	0.19	3130.713	608.213
InF_3	-1588.651	-1587.629	0.06	7193.239	348.601
TlF_3	-2170.661	-2900.881	25.17	3837.85	420.685
CH_4	-57.181	-57.169	0.02	753.706	102.764
SiH_4	-446.853	-446.42	0.10	1333.159	81.881
GeH_4	-1164.844	-1162.199	0.23	1609.755	175.587
SnH_4	-2168.713	-2165.684	0.14	2094.41	230.968
PbH_4	-4002.507	-4311.011	7.16	1507.577	148.889
NF_3	-471.057	-471.198	0.03	1266.654	130.645
PF_3	-808.498	-807.583	0.11	1733.795	180.995
AsF_3	-1996.632	-1990.796	0.29	3192.405	325.432
SbF_3	-3101.31	-3093.53	0.25	3761.314	377.017
BiF_3	-5642.47	-5839.307	3.37	4254.22	487.642
H_2O	-55.335	-55.311	0.04	121.005	16.367
H_2S	-361.345	-360.900	0.12	268.117	32.088
H_2Se	-975.089	-972.698	0.25	814.789	99.331
H_2Te	-1987.447	-1985.233	0.11	1110.57	130.15
H_2Po	-4097.247	-4485.596	8.66	1381.427	189.222
HF	-54.341	-54.314	0.05	57.678	7.301
HCl	-216.692	-216.395	0.14	148.932	15.347
HBr	-601.545	-600.1	0.24	509.803	59.401
HI	-1207.058	-1206.141	0.08	775.682	95.029
HAt	-2543.437	-2652.678	4.12	1060.687	151.837
NeF_2	7952.821	7948.414	0.06	328.844	31.534
ArF_2	-367.027	-366.497	0.14	1192.575	52.903
KrF_2	-1458.002	-1453.271	0.33	1727.228	130.83
XeF_2	-3555.144	-3543.65	0.32	1972.452	388.057
RnF_2	-7354.936	-7961.532	7.62	6346.532	698.774
ArF_6	-1704.898	-1702.088	0.17	6336.295	1675.912
KrF_6	-3942.638	-3928.266	0.37	10055.414	803.285
XeF_6	-5920.017	-5902.086	0.30	23359.981	2937.691
RnF_6	-10665.282	-11533.484	7.53	22592.638	1916.136

A.4. SOC Implementation

A.4.1. Basis Set convergence

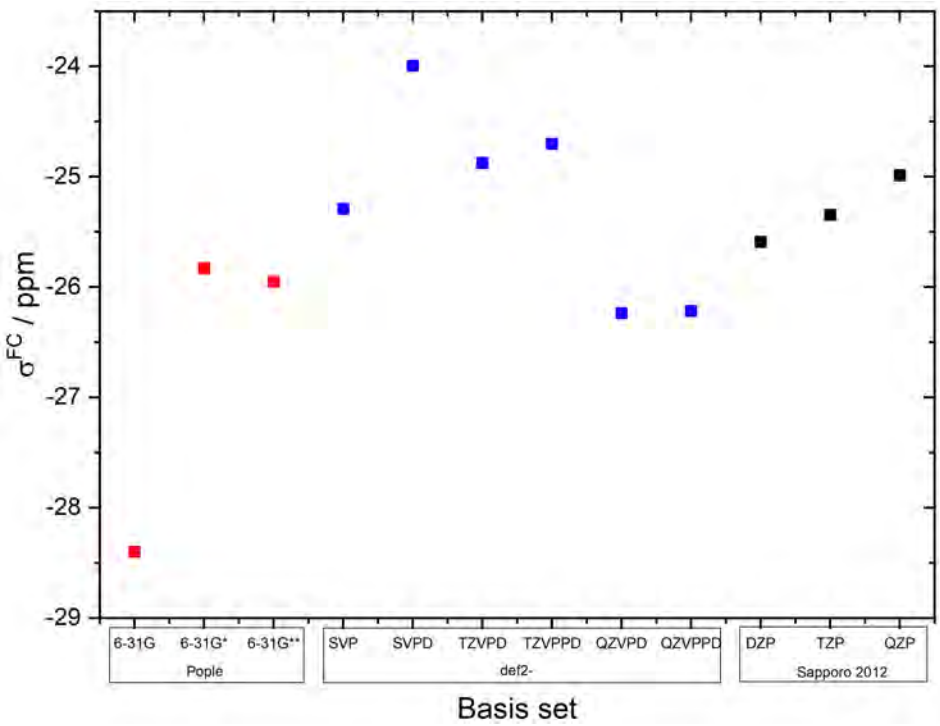

(a)

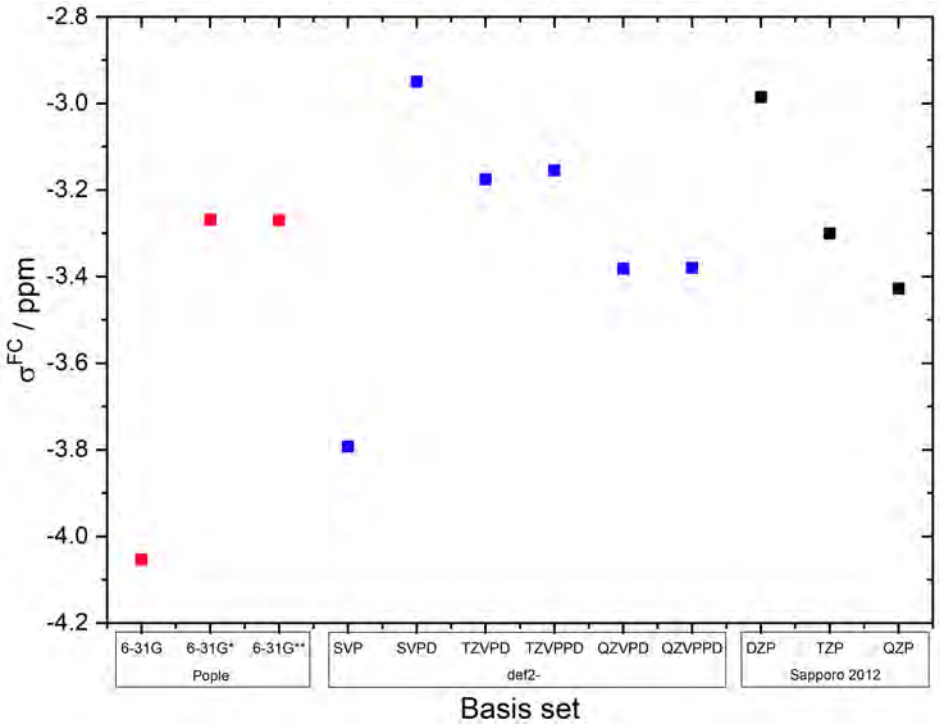

(b)

Figure A.4: Basis set convergence of the SOC Implementation of *ORCA*. The Pople, def2 of the Karlsruhe group and the Sapporo-2012 basis set were used. Shown are the SOC contribution for a) Br and b) H.

Table A.9: Values of the basis set convergence of the SOC approach in *ORCA* for H_2S. Shown are the results for the S-atom.

Basis set	**DSO**	**PSO**	**FC**	**Rel**	**NR**	**SOC** (Δ(Rel-NR))
sto-3g	1033	-490.594	-1.509872	540.896128	542.454	-1.557872
6-31G	1054.393	-516.779	-2.370303	535.243697	537.643	-2.399303
6-31G*	1054.393	-532.279	-2.100257	520.013743	522.141	-2.127257
6-31G**	1054.211	-520.619	-2.064141	531.527859	533.618	-2.090141
def2-SVP	1053.511	-511.609	-2.130333	539.771667	541.923	-2.151333
def2-SVPD	1052.069	-480.013	-1.980469	570.075531	572.08	-2.004469
def2-TZVPD	1057.634	-501.649	-2.113378	553.871622	556.016	-2.144378
def2-TZVPPD	1056.43	-498.291	-2.109371	556.029629	558.169	-2.139371
def2-QZVPD	1055.628	-500.523	-2.214196	552.890804	555.108	-2.217196
def2-QZVPPD	1054.86	-498.24	-2.194556	554.425444	556.668	-2.242556
Sapporo-DZP	1055.157	-507.165	-2.06529	545.92671	548.022	-2.09529
Sapporo-TZP	1057.933	-504.941	-2.079572	550.912428	553.022	-2.109572
Sapporo-QZP	1055.602	-500.117	-2.108652	553.376348	555.524	-2.147652

Table A.10: Values of the basis set convergence of the SOC approach in *ORCA* for H_2S. Shown are the results for the H-atom.

Basis set	**DSO**	**PSO**	**FC**	**Rel**	**NR**	**SOC** (Δ(Rel-NR))
sto-3g	27.449	1.992	-0.952237	28.488763	29.441	-0.952237
6-31G	27.043	2.042	-0.473033	28.611967	29.085	-0.473033
6-31G*	26.446	2.087	-0.47208	28.06092	28.534	-0.47308
6-31G**	26.399	1.413	-0.461892	27.350108	27.812	-0.461892
def2-SVP	26.606	1.631	-0.452115	27.784885	28.238	-0.453115
def2-SVPD	26.686	1.503	-0.422705	27.766295	28.189	-0.422705
def2-TZVPD	26.098	2.034	-0.459943	27.672057	28.133	-0.460943
def2-TZVPPD	26.35	1.604	-0.456692	27.497308	27.955	-0.457692
def2-QZVPD	26.363	1.562	-0.455669	27.469331	27.926	-0.456669
def2-QZVPPD	26.501	1.43	-0.465749	27.465251	27.932	-0.466749
Sapporo-DZP	26.789	1.28	-0.437212	27.631788	28.07	-0.438212
Sapporo-TZP	26.607	1.312	-0.48145	27.43755	27.92	-0.48245
Sapporo-QZP	26.371	1.524	-0.496176	27.398824	27.895	-0.496176

Table A.11: Basis set convergence for the SOC approach in *ORCA*, results for the Br-atom in HBr.

Basis set	**DSO**	**PSO**	**FC**	**Rel**	**NR**	**SOC** (Δ(Rel-NR))
sto-3g	3067.804	-607.892	-16.756619	2443.15538	2460.708	-17.552619
6-31G	3122.079	-634.261	-26.715824	2461.10218	2489.5	-28.397824
6-31G*	3121.732	-595.817	-24.277425	2501.63758	2527.468	-25.830425
6-31G**	3121.379	-592.502	-24.288854	2504.58815	2530.541	-25.952854
def2-SVP	3121.224	-593.439	-23.788411	2503.99659	2529.287	-25.290411
def2-SVPD	3123.03	-573.775	-22.653289	2526.60171	2550.596	-23.994289
def2-TZVPD	3123.198	-575.28	-23.538234	2524.37977	2549.256	-24.876234
def2-TZVPPD	3122.384	-570.246	-23.394787	2528.74321	2553.445	-24.701787
def2-QZVPD	3122.659	-573.553	-24.026522	2525.07948	2551.317	-26.237522
def2-QZVPPD	3122.584	-573.85	-24.006719	2524.72728	2550.943	-26.215719
Sapporo-DZP	3121.788	-581.835	-23.868537	2516.08446	2541.677	-25.592537
Sapporo-TZP	3121.517	-576.129	-23.576156	2521.81184	2547.16	-25.348156
Sapporo-QZP	3121.814	-573.465	-23.21174	2525.13726	2550.126	-24.98874

Table A.12: Values of the basis set convergence of the SOC approach in *ORCA*. The results for the H-atom in HBr are shown.

Basis set	**DSO**	**PSO**	**FC**	**Rel**	**NR**	**SOC** (Δ(Rel-NR))
sto-3g	30.65	3.605	-2.4032	31.8518	34.256	-2.4042
6-31G	29.806	3.244	-3.523414	29.526586	33.58	-4.053414
6-31G*	28.923	2.612	-3.260146	28.274854	31.544	-3.269146
6-31G**	29.01	2.55	-3.260672	28.299328	31.57	-3.270672
def2-SVP	28.883	2.787	-3.78332	27.88668	31.679	-3.79232
def2-SVPD	28.947	2.729	-2.940834	28.735166	31.685	-2.949834
def2-TZVPD	27.695	4.108	-3.164696	28.638304	31.814	-3.175696
def2-TZVPPD	28.33	3.165	-3.144243	28.350757	31.505	-3.154243
def2-QZVPD	28.71	2.735	-3.367307	28.077693	31.459	-3.381307
def2-QZVPPD	28.751	2.692	-3.366399	28.076601	31.456	-3.379399
Sapporo-DZP	29.673	2.013	-2.974824	28.711176	31.697	-2.985824
Sapporo-TZP	29.951	1.456	-3.289497	28.117503	31.418	-3.300497
Sapporo-QZP	29.085	2.328	-3.416789	27.996211	31.424	-3.427789

A.4.2. Functional dependence

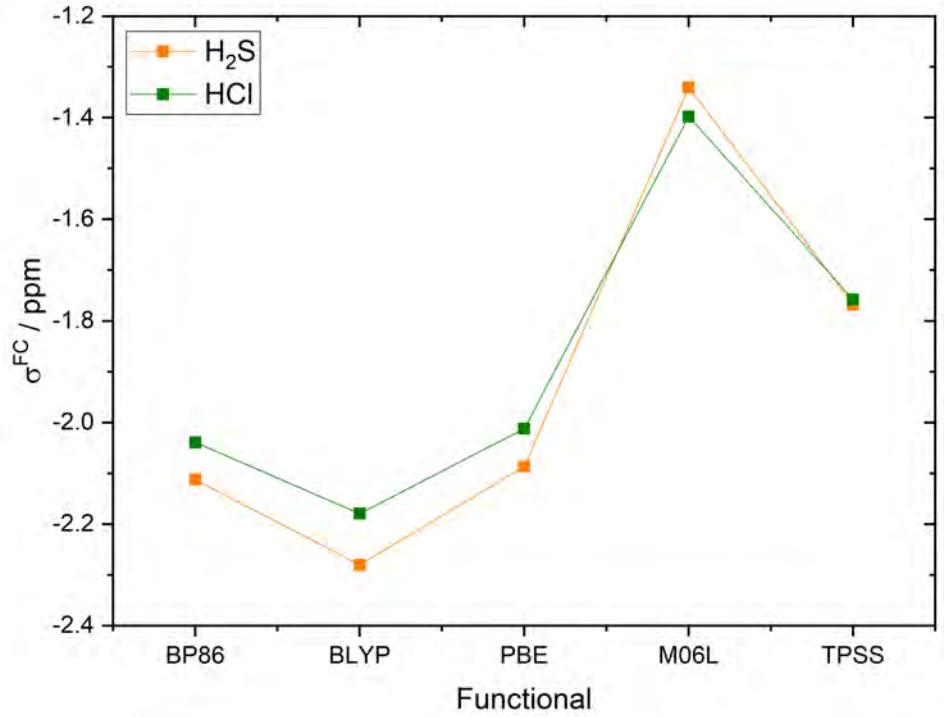

(a)

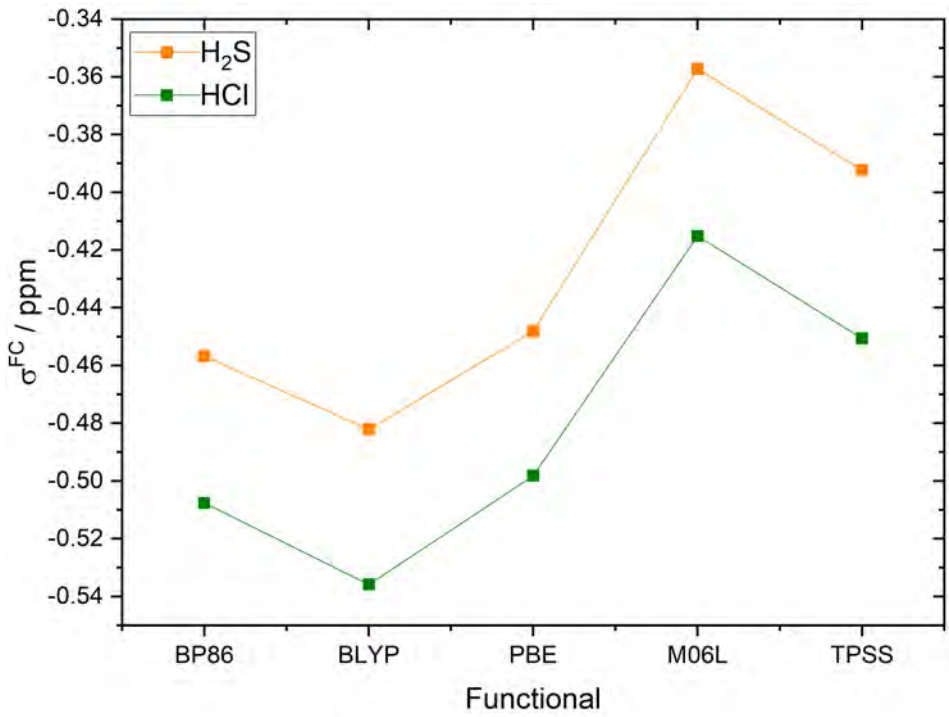

(b)

Figure A.5: Functional dependence of the SOC Implementation of *ORCA*. BP86, BLYP, PBE, M06L and TPSS functionals were used and the isotropic shielding are shown in a) for the heavy atoms and in b) for the H-atoms of H_2S and HCl.

Table A.13: Functional dependence of the SOC approach in *ORCA*, shown for H_2S and H_2Se. DSO, PSO, FC, and the resulting Rel, NR and the SOC contributions are shown.

		isotropic Shielding [ppm]					
Molecule / Atom	**Functional**	DSO	PSO	FC	Rel (DSO+PSO+FC)	NR	SOC (Δ(Rel-NR))
H_2S / S	BP86	1056.598	-500.151	-2.086278	554.360722	556.473	-2.112278
	BLYP	1056.906	-526.686	-2.254975	527.965025	530.245	-2.279975
	PBE	1056.789	-491.479	-2.060577	563.249423	565.336	-2.086577
	M06L	1055.556	-424.676	-1.321492	629.558508	630.899	-1.340492
	TPSS	1056.631	-472.026	-1.743483	582.861517	584.629	-1.767483
H_2S / H	BP86	26.779	1.215	-0.4568	27.5372	27.994	-0.4568
	BLYP	27.112	1.134	-0.482096	27.763904	28.246	-0.482096
	PBE	26.725	1.206	-0.448139	27.482861	27.931	-0.448139
	M06L	26.1	1.697	-0.357324	27.439676	27.797	-0.357324
	TPSS	27.074	0.994	-0.391401	27.676599	28.069	-0.392401
H_2Se / Se	BP86	2997.675	-932.278	-18.794679	2046.60232	2067.147	-20.544679
	BLYP	2997.747	-973.987	-20.154832	2003.60517	2025.562	-21.956832
	PBE	2998.01	-914.531	-18.527429	2064.95157	2085.183	-20.231429
	M06L	2995.362	-840.556	-12.539231	2142.26677	2156.283	-14.016231
	TPSS	2997.955	-892.847	-16.032619	2089.07538	2106.746	-17.670619
H_2Se / H	BP86	29.792	0.556	-2.001988	28.346012	30.373	-2.026988
	BLYP	30.207	0.42	-2.099278	28.527722	30.642	-2.114278
	PBE	29.864	0.457	-1.957405	28.363595	30.336	-1.972405
	M06L	29.689	0.924	-1.541332	29.071668	30.625	-1.553332
	TPSS	30.164	0.354	-1.743849	28.774151	30.532	-1.757849

Table A.14: Functional dependence of the SOC approach in *ORCA* for HCl and HBr. DSO, PSO, FC, and the resulting Rel, NR and the SOC contributions are shown.

		isotropic Shielding [ppm]					
Molecule / Atom	**Functional**	DSO	PSO	FC	Rel (DSO+PSO+FC)	NR	SOC (Δ(Rel-NR))
HCl / Cl	BP86	1148.491	-213.324	-2.017094	933.149906	935.189	-2.039094
	BLYP	1148.712	-223.883	-2.154188	922.674812	924.854	-2.179188
	PBE	1148.418	-209.557	-1.98884	936.87216	938.884	-2.01184
	M06L	1147.825	-184.182	-1.382599	962.260401	963.658	-1.397599
	TPSS	1148.494	-202.321	-1.737738	944.435262	946.193	-1.757738
HCl / H	BP86	29.104	2.284	-0.507572	30.880428	31.388	-0.507572
	BLYP	29.311	2.371	-0.534826	31.147174	31.683	-0.535826
	PBE	28.939	2.376	-0.498152	30.816848	31.315	-0.498152
	M06L	28.595	2.553	-0.415156	30.732844	31.148	-0.415156
	TPSS	29.398	2.02	-0.450602	30.967398	31.418	-0.450602
HBr / Br	BP86	3122.375	-571.275	-23.534376	2527.56562	2552.598	-25.032376
	BLYP	3122.4	-599.394	-25.085472	2497.92053	2524.605	-26.684472
	PBE	3122.05	-541.353	-20.725302	2559.9717	2582.042	-22.070302
	M06L	3120.85	-522.622	-16.71062	2581.51738	2599.299	-17.78162
	TPSS	3122.257	-560.066	-23.176486	2539.01451	2563.672	-24.657486
HBr / H	BP86	29.432	2.125	-3.146765	28.410235	31.567	-3.156765
	BLYP	29.798	2.137	-3.332528	28.602472	31.945	-3.342528
	PBE	29.75	1.861	-2.777648	28.833352	31.621	-2.787648
	M06L	29.267	2.421	-2.494492	29.193508	31.698	-2.504492
	TPSS	29.419	2.087	-3.078225	28.427775	31.515	-3.087225

A.4.3. Using of different SOC Hamiltonian

Table A.15: Results for using different SOC Hamiltonian in the SOC approach in *ORCA*. DSO, PSO, FC and the resulting Rel, NR and the SOC contribution for H_2S and HBr are shown

		isotropic shielding [ppm]					
Molecule	**SOC Hamiltonian**	DSO	PSO	FC	Rel (DSO+PSO+FC)	NR	SOC (Δ(Rel-NR))
H_2S/S	SOMF	1056.598	-500.151	-2.086278	554.360722	556.473	-2.112278
	AMFI	1056.599	-500.152	-2.106762	554.340238	556.473	-2.132762
	AMFI-A	1056.6	-500.153	-2.074023	554.372977	556.473	-2.100023
	VEFF-SOC	1056.599	-500.155	-2.310366	554.133634	556.473	-2.339366
H_2S / H	SOMF	26.779	1.215	-0.4568	27.5372	27.994	-0.4568
	AMFI	26.779	1.215	-0.460018	27.533982	27.994	-0.460018
	AMFI-A	26.779	1.215	-0.438744	27.555256	27.994	-0.438744
	VEFF-SOC	26.779	1.215	-0.509307	27.484693	27.994	-0.509307
HBr / Br	SOMF	3122.375	-571.275	-23.534376	2527.56562	2552.598	-25.032376
	AMFI	3122.381	-571.286	-23.983115	2527.11189	2552.598	-25.486115
	AMFI-A	3122.38	-571.287	-23.683868	2527.40913	2552.598	-25.188868
	VEFF-SOC	3122.405	-571.393	-24.556706	2526.45529	2552.598	-26.142706
HBr / H	SOMF	29.432	2.125	-3.146765	28.410235	31.567	-3.156765
	AMFI	29.423	2.134	-3.167807	28.389193	31.567	-3.177807
	AMFI-A	29.428	2.129	-3.153563	28.403437	31.567	-3.163563
	VEFF-SOC	29.431	2.125	-3.283433	28.272567	31.567	-3.294433

A.5. Dirac Calculations

Table A.16: Dirac results using the X2C Hamiltonian. Shown are the isotropic shieldings of the heavy atoms of the 13th-16th group. The full relativistic effect was obtained by $Rel - NR$, the ScR contribution by $Rel - ScR$ and the SOC contribution by $Rel - ScR$.

Molecule	**isotropic shielding** [%]			**relativistic contribution** [ppm]			**relativistic contribution** [%]		
	NR	ScR	Rel	full relativistic	ScR	SOC	full relativistic	ScR	SOC
BF_3	133.9586	133.9565	133.8733	-0.09	$-2.10 \cdot 10^{-03}$	-0.08	0.06	$1.57 \cdot 10^{-03}$	0.06
AlF_3	768.609	776.1203	773.9543	5.35	7.51	-2.17	0.69	0.97	0.28
GaF_3	1788.9338	1750.3994	1750.6389	-38.29	-38.53	0.24	2.19	2.20	0.01
InF_3	4460.5099	4691.3266	4673.728	213.22	230.82	-17.60	4.56	4.92	0.38
TlF_3	10012.1546	10587.9596	10086.4211	74.27	575.81	-501.54	0.74	5.44	4.97
CH_4	399.9761	400.1023	400.1337	0.16	0.13	0.03	0.04	0.03	0.01
SiH_4	961.9986	962.2643	961.3649	-0.63	0.27	-0.90	0.07	0.03	0.09
GeH_4	2527.6101	2463.8873	2438.6341	-88.98	-63.72	-25.25	3.65	2.59	1.04
SnH_4	4556.6252	4419.4512	4274.2084	-282.42	-137.17	-145.24	6.61	3.10	3.40
PbH_4	8638.3956	6088.4061	4912.8609	-3725.53	-2549.99	-1175.55	75.83	41.88	23.93
NF_3	-2.1995	-1.4714	1.4276	3.63	0.73	2.90	254.07	49.48	203.07
PF_3	133.946	124.6362	129.9005	-4.05	-9.31	5.26	3.11	7.47	4.05
AsF_3	857.5441	801.619	807.7114	-49.83	-55.93	6.09	6.17	6.98	0.75
SbF_3	2311.3888	2062.3099	2004.8929	-306.50	-249.08	-57.42	15.29	12.08	2.86
BiF_3	6242.8974	6347.1829	5024.8746	-1218.02	104.29	-1322.31	24.24	1.64	26.32
NMe_3	4025.0163	4324.7591	4351.3257	326.31	299.74	26.57	7.50	6.93	0.61
PMe_3	1511.152	1522.8531	1522.6434	11.49	11.70	-0.21	0.75	0.77	0.01
$AsMe_3$	4025.0163	4324.7591	4351.3257	326.31	299.74	26.57	7.50	6.93	0.61
$SbMe_3$	5565.3278	6663.7099	6776.9158	1211.59	1098.38	113.21	17.88	16.48	1.67
$BiMe_3$	6903.5976	12741.7902	14453.1201	7549.52	5838.19	1711.33	52.23	45.82	11.84
H_2O	612.3129	615.5812	615.2811	2.97	3.27	-0.30	0.48	0.53	0.05
H_2S	1398.3847	1426.7125	1428.8592	30.47	28.33	2.15	2.13	1.99	0.15
H_2Se	3574.6502	3875.7982	3905.4095	330.76	301.15	29.61	8.47	7.77	0.76
H_2Te	5685.6212	6813.9348	6949.9193	1264.30	1128.31	135.98	18.19	16.56	1.96
H_2Po	10294.9379	16485.0748	16993.3901	6698.45	6190.14	508.32	39.42	37.55	2.99

Table A.17: Dirac results using the X2C Hamiltonian. Shown are the isotropic shieldings of the heavy atom of the 17th-18th group.

Molecule	**isotropic shielding** [%]			**relativistic contribution** [ppm]			**relativistic contribution** [%]		
	NR	ScR	Rel	full relativistic	scalar relativistic	SOC	full relativistic	scalar relativistic	SOC
HF	903.3107	909.2732	818.6825	-84.63	5.96	-90.59	10.34	0.66	11.07
HCl	1871.3165	1913.8307	1909.5189	38.20	42.51	-4.31	2.00	2.22	0.23
HBr	4607.4004	5020.6621	4979.0782	371.68	413.26	-41.58	7.46	8.23	0.84
HI	7386.1651	8916.6308	8768.2265	1382.06	1530.47	-148.40	15.76	17.16	1.69
HAt	13167.3153	21282.0864	20006.9547	6839.64	8114.77	-1275.13	34.19	38.13	6.37
ArF_2	1533.007	1578.27	1579.6037	46.60	45.26	1.33	2.95	2.87	0.08
KrF_2	3053.9719	3423.0993	3472.7863	418.81	369.13	49.69	12.06	10.78	1.43
XeF_2	3859.6065	5071.9089	5357.4975	1497.89	1212.30	285.59	27.96	23.90	5.33
RnF_2	6363.5314	12435.5623	14861.7706	8498.24	6072.03	2426.21	57.18	48.83	16.33
ArF_6	4140.2837	4217.5611	4221.0000	80.72	77.28	3.44	1.91	1.83	0.08
KrF_6	9391.9617	10179.6580	10193.4181	801.46	787.70	13.76	7.86	7.74	0.13
XeF_6	12248.5165	14611.5908	14786.7432	2538.23	2363.07	175.15	17.17	16.17	1.18
RnF_6	19526.3304	33270.3133	35313.9003	15787.57	13743.98	2043.59	44.71	41.31	5.79

Table A.18: Dirac results using the X2C Hamiltonian. Shown are the isotropic shieldings of the light atoms of the 13th-15th group. The full relativistic effect was obtained by $Rel - NR$, the ScR contribution by $Rel - ScR$ and the SOC contribution by $Rel - ScR$.

Molecule	**isotropic shielding** [%]			**relativistic contribution** [ppm]			**relativistic contribution** [%]		
	NR	ScR	Rel	full relativistic	ScR	SOC	full relativistic	ScR	SOC
BF_3	123.7957	127.5613	127.1653	3.37	3.77	-0.40	2.65	2.95	0.31
AlF_3	201.2572	206.2851	205.6273	4.37	5.03	-0.66	2.13	2.44	0.32
GaF_3	236.0435	240.5762	240.9002	4.86	4.53	0.32	2.02	1.88	0.13
InF_3	291.9623	295.1671	296.1416	4.18	3.20	0.97	1.41	1.09	0.33
TlF_3	306.6437	239.6412	243.6878	-62.96	-67.00	4.05	25.83	27.96	1.66
CH_4	42.8216	42.8260	42.7401	-0.08	0.00	-0.09	0.19	0.01	0.20
SiH_4	34.2405	34.3066	34.6226	0.38	0.07	0.32	1.10	0.19	0.91
GeH_4	33.8787	34.1919	36.4581	2.58	0.31	2.27	7.07	0.92	6.22
SnH_4	28.4043	29.1072	34.4166	6.01	0.70	5.31	17.47	2.41	15.43
PbH_4	25.5488	27.6257	44.2169	18.67	2.08	16.59	42.22	7.52	37.52
NF_3	371.8814	374.5739	375.427	3.55	2.69	0.85	0.94	0.72	0.23
PF_3	268.8326	270.0015	270.3147	1.48	1.17	0.31	0.55	0.43	0.12
AsF_3	383.0255	385.9145	386.6852	3.66	2.89	0.77	0.95	0.75	0.20
SbF_3	431.0802	437.873	439.0552	7.98	6.79	1.18	1.82	1.55	0.27
BiF_3	457.1899	473.4307	483.5113	26.32	16.24	10.08	5.44	3.43	2.08
NMe_3 (C)	331.5794	331.5750	331.6045	0.03	0.00	0.03	0.01	0.00	0.01
NMe_3 (H)	23.8758	23.8973	23.7227	-0.15	0.02	-0.17	0.65	0.09	0.74
PMe_3 (C)	395.8296	395.8526	397.4587	1.63	0.02	1.61	0.41	0.01	0.40
PMe_3 (H)	21.9073	21.9488	21.7915	-0.12	0.04	-0.16	0.53	0.19	0.72
$AsMe_3$ (C)	406.4875	405.8707	415.9656	9.48	-0.62	10.09	2.28	0.15	2.43
$AsMe_3$ (H)	24.2972	24.3963	24.1062	-0.191	0.0991	-0.2901	0.79	0.41	1.20
$SbMe_3$ (C)	432.7647	430.8487	454.8731	22.1084	-1.916	24.0244	4.86	0.44	5.28
$SbMe_3$ (H)	25.3453	25.6286	25.0151	-0.3302	0.2833	-0.6135	1.32	1.11	2.45
$BiMe_3$ (C)	440.9365	439.7887	510.7276	69.7911	-1.1478	70.9389	13.67	0.26	13.89
$BiMe_3$ (H)	24.1126	24.7388	23.0334	-1.0792	0.6262	-1.7054	4.69	2.53	7.40

Table A.19: Dirac results using the X2C Hamiltonian. Shown are the isotropic shieldings of the light atoms of the 16th-18th group.

Molecule	**isotropic shielding** [%]			**relativistic contribution** [ppm]			**relativistic contribution** [%]		
	NR	ScR	Rel	full relativistic	scalar relativistic	SOC	full relativistic	scalar relativistic	SOC
H_2O	37.2368	37.2158	37.2061	-0.03	-0.02	-0.01	0.08	0.06	0.03
H_2S	32.0315	31.9736	32.3827	0.35	-0.06	0.41	1.08	0.18	1.26
H_2Se	28.4408	28.0728	30.4979	2.06	-0.37	2.43	6.75	1.31	7.95
H_2Te	25.0528	23.8891	29.8377	4.78	-1.16	5.95	16.04	4.87	19.94
H2Po	22.4183	19.06	23.6959	1.28	-3.36	4.64	5.39	17.62	19.56
HF	18.8062	18.7896	29.7936	10.99	-0.02	11.00	36.88	0.09	36.93
HCl	17.3234	17.298	17.0462	-0.28	-0.03	-0.25	1.63	0.15	1.48
HBr	18.2922	18.1747	17.4132	-0.88	-0.12	-0.76	5.05	0.65	4.37
HI	20.0910	19.8608	19.2629	-0.83	-0.23	-0.60	4.30	1.16	3.10
HAt	19.965	19.4202	17.3613	-2.60	-0.54	-2.06	15.00	2.81	11.86
ArF_2	861.1182	867.8308	866.6562	5.54	6.71	-1.17	0.64	0.77	0.14
KrF_2	1157.6835	1164.0989	1152.6155	-5.07	6.42	-11.48	0.44	0.55	1.00
XeF_2	1355.2678	1369.8673	1338.1335	-17.13	14.60	-31.73	1.28	1.07	2.37
RnF_2	1506.8003	1537.0831	1389.3868	-117.41	30.28	-147.70	8.45	1.97	10.63
ArF_6	1080.3546	1082.7698	1092.4739	12.12	2.42	9.70	1.11	0.22	0.89
KrF_6	1094.4448	1096.4426	1103.6553	9.21	2.00	7.21	0.83	0.18	0.65
XeF_6	794.2045	814.6557	817.0813	22.88	20.45	2.43	2.80	2.51	0.30
RnF_6	684.6814	753.4988	756.4547	71.77	68.82	2.96	9.49	9.13	0.39

Table A.20: Dirac results using the BSS Hamiltonian. Shown are the isotropic shieldings of the heavy atoms of the 13th-16th group. The full relativistic effect was obtained by $Rel - NR$, the ScR and the SOC contribution by $ScR - NR$, $Rel - ScR$.

Molecule	**isotropic shielding** [%]			**relativistic contribution** [ppm]			**relativistic contribution** [%]		
	NR	ScR	Rel	full relativistic	ScR	SOC	full relativistic	ScR	SOC
BF_3	84.7821	86.4584	87.1726	2.39	1.68	0.71	2.74	1.94	0.82
AlF_3	491.1349	517.4228	518.0997	26.96	26.29	0.68	5.20	5.08	0.13
GaF_3	1604.3127	1977.6954	1992.9253	388.61	373.38	15.23	19.50	18.88	0.76
InF_3	3414.9467	4964.7197	4988.5691	1573.62	1549.77	23.85	31.54	31.22	0.48
TlF_3	7296.7448	16234.6347	16004.5886	8707.84	8937.89	-230.05	54.41	55.05	1.44
CH_4	188.9552	191.8887	191.8316	2.88	2.93	-0.06	1.50	1.53	0.03
SiH_4	440.1033	472.3942	471.6758	31.57	32.29	-0.72	6.69	6.84	0.15
GeH_4	1611.5863	2024.7513	2015.3885	403.80	413.17	-9.36	20.04	20.41	0.46
SnH_4	3009.0606	4641.1523	4588.8923	1579.83	1632.09	-52.26	34.43	35.17	1.14
PbH_4	6456.981	15524.3669	15050.2676	8593.29	9067.39	-474.10	57.10	58.41	3.15
NF_3	-178.8472	-175.5085	-170.6662	8.18	3.34	4.84	4.79	1.90	2.84
PF_3	161.8425	201.1285	200.5308	38.69	39.29	-0.60	19.29	19.53	0.30
AsF_3	925.9623	1352.9941	1289.8074	363.85	427.03	-63.19	28.21	31.56	4.90
SbF_3	2241.3492	3856.5479	3489.4501	1248.10	1615.20	-367.10	35.77	41.88	10.52
BiF_3	5343.8152	14215.0614	9673.8604	4330.05	8871.25	-4541.20	44.76	62.41	46.94
NMe_3	224.4709	228.9969	229.4986	5.03	4.53	0.50	2.19	1.98	0.22
PMe_3	384.5475	424.9112	424.8333	40.29	40.36	-0.08	9.48	9.50	0.02
$AsMe_3$	1366.3784	1790.2177	1782.063	415.68	423.84	-8.15	23.33	23.68	0.46
$SbMe_3$	2480.8977	4142.987	4055.1618	1574.26	1662.09	-87.83	38.82	40.12	2.17
$BiMe_3$	5420.9195	14522.6395	13419.4911	7998.57	9101.72	-1103.15	59.60	62.67	8.22
H_2O	325.424	331.6309	332.0511	6.63	6.21	0.42	2.00	1.87	0.13
H_2S	708.3019	756.8291	758.9547	50.65	48.53	2.13	6.67	6.41	0.28
H_2Se	2072.3459	2559.8729	2589.8584	517.51	487.53	29.99	19.98	19.04	1.16
H_2Te	3536.8153	5339.7015	5450.2322	1913.42	1802.89	110.53	35.11	33.76	2.03
H_2Po	7052.818	16606.9966	17166.5513	10113.73	9554.18	559.55	58.92	57.53	3.26

Table A.21: Dirac results using the BSS Hamiltonian. Shown are the isotropic shieldings of the heavy atoms of the 13th-16th group.

Molecule	**isotropic shielding** [%]			**relativistic contribution** [ppm]			**relativistic contribution** [%]		
	NR	ScR	Rel	full relativistic	scalar relativistic	SOC	full relativistic	scalar relativistic	SOC
HF	407.9006	416.4254	417.1288	9.23	8.52	0.70	2.21	2.05	0.17
HCl	938.588	998.1839	1001.966	63.38	59.60	3.78	6.33	5.97	0.38
HBr	2557.5080	3103.593	3150.0791	592.57	546.09	46.49	18.81	17.60	1.48
HI	4419.2303	6398.7214	6598.6969	2179.47	1979.49	199.98	33.03	30.94	3.03
HAt	8635.4473	19100.4832	20336.7773	11701.33	10465.04	1236.29	57.54	54.79	6.08
ArF_2	863.174	936.4159	938.7297	75.56	73.24	2.31	8.05	7.82	0.25
KrF_2	1761.4573	2355.6459	2443.9332	682.48	594.19	88.29	27.93	25.22	3.61
XeF_2	2547.9142	4556.6357	4894.3475	2346.43	2008.72	337.71	47.94	44.08	6.90
RnF_2	4798.891	15280.824	17720.9674	12922.08	10481.93	2440.14	72.92	68.60	13.77
ArF_6	221.1544	289.3886	291.9609	70.81	68.23	2.57	24.25	23.58	0.88
KrF_6	211.497	719.2750	784.0184	572.52	507.78	64.74	73.02	70.60	8.26
XeF_6	202.2089	1942.7223	2117.5248	1915.32	1740.51	174.80	90.45	89.59	8.26
RnF_6	2196.224	10832.5613	8169.415	5973.19	8636.34	-2663.15	73.12	79.73	32.60

Table A.22: Dirac results using the BSS Hamiltonian. Shown are the isotropic shieldings of the light atoms of the 13th-15th group. The full relativistic effect was obtained by $Rel - NR$, the ScR and the SOC contribution by $ScR - NR$, $Rel - ScR$.

Molecule	**isotropic shielding** [%]			**relativistic contribution** [ppm]			**relativistic contribution** [%]		
	NR	ScR	Rel	full relativistic	ScR	SOC	full relativistic	ScR	SOC
BF_3	294.7953	301.3845	301.9275	7.13	6.59	0.54	2.36	2.19	0.18
AlF_3	384.8866	391.6631	392.1771	7.29	6.78	0.51	1.86	1.73	0.13
GaF_3	344.94	340.4314	342.3711	-2.57	-4.51	1.94	0.75	1.32	0.57
InF_3	357.8467	329.3532	332.9752	-24.87	-28.49	3.62	7.47	8.65	1.09
TlF_3	369.9357	181.1255	186.9726	-182.96	-188.81	5.85	97.86	104.24	3.13
CH_4	31.4017	31.3823	31.4072	0.01	-0.02	0.02	0.02	0.06	0.08
SiH_4	27.8479	27.8428	27.8826	0.03	-0.01	0.04	0.12	0.02	0.14
GeH_4	27.5982	27.4435	27.8059	0.21	-0.15	0.36	0.75	0.56	1.30
SnH_4	27.4046	27.0185	27.4558	0.05	-0.39	0.44	0.19	1.43	1.59
PbH_4	27.9645	26.6526	25.7624	-2.20	-1.31	-0.89	8.55	4.92	3.46
NF_3	-1.9967	3.7298	6.6159	8.61	5.73	2.89	130.18	153.53	43.62
PF_3	186.5833	191.5444	193.7387	7.16	4.96	2.19	3.69	2.59	1.13
AsF_3	173.8849	172.7159	179.8074	5.92	-1.17	7.09	3.29	0.68	3.94
SbF_3	194.5155	184.873	199.1909	4.68	-9.64	14.32	2.35	5.22	7.19
BiF_3	197.4755	153.2747	183.4959	-13.98	-44.20	30.22	7.62	28.84	16.47
NMe_3 (C)	138.5168	141.0287	141.1756	2.66	2.51	0.15	1.88	1.78	0.10
NMe_3 (H)	29.2791	29.2514	29.26	-0.02	-0.03	0.01	0.07	0.09	0.03
PMe_3 (C)	167.5075	170.3989	171.2481	3.74	2.89	0.85	2.18	1.70	0.50
PMe_3 (H)	30.681	30.6532	30.649	-0.03	-0.03	0.00	0.10	0.09	0.01
$AsMe_3$ (C)	169.1579	171.2091	175.5866	6.43	2.05	4.38	3.66	1.20	2.49
$AsMe_3$ (H)	30.8532	30.8044	30.7023	-0.1509	-0.0488	-0.10	0.49	0.16	0.33
$SbMe_3$ (C)	177.3708	176.8856	185.8627	8.4919	-0.4852	8.98	4.57	0.27	4.83
$SbMe_3$ (H)	31.6437	31.58	31.3151	-0.3286	-0.0637	-0.26	1.05	0.20	0.85
$BiMe_3$ (C)	181.4688	175.7203	188.0725	6.6037	-5.7485	12.35	3.51	3.27	6.57
$BiMe_3$ (H)	31.7568	31.5416	30.9832	-0.7736	-0.2152	-0.56	2.50	0.68	1.80

Table A.23: Dirac results using the BSS Hamiltonian. Shown are the isotropic shieldings of the light atoms of the 16th-18th group.

Molecule	**isotropic shielding** [%]			**relativistic contribution** [ppm]			**relativistic contribution** [%]		
	NR	ScR	Rel	full relativistic	scalar relativistic	SOC	full relativistic	scalar relativistic	SOC
H_2O	31.0597	31.0401	31.0511	-0.01	-0.02	0.01	0.03	0.06	0.04
H_2S	30.8172	30.8345	31.4213	0.60	0.02	0.59	1.92	0.06	1.87
H_2Se	30.3034	30.288	33.5066	3.20	-0.02	3.22	9.56	0.05	9.61
H_2Te	29.7592	29.6371	38.4912	8.73	-0.12	8.85	22.69	0.41	23.00
H_2Po	30.0695	29.5611	41.2324	11.16	-0.51	11.67	27.07	1.72	28.31
HF	29.6007	29.5783	29.778	0.18	-0.02	0.20	0.60	0.08	0.67
HCl	31.2762	31.313	32.248	0.97	0.04	0.93	3.01	0.12	2.90
HBr	31.4423	31.4775	36.5937	5.15	0.04	5.12	14.08	0.11	13.98
HI	31.8027	31.7578	46.2884	14.49	-0.04	14.53	31.29	0.14	31.39
HAt	32.1752	31.8948	62.8412	30.67	-0.28	30.95	48.80	0.88	49.25
ArF_2	-322.2122	-315.557	-314.106	8.11	6.66	1.45	2.58	2.11	0.46
KrF_2	36.4722	39.6099	19.6615	-16.81	3.14	-19.95	85.50	7.92	101.46
XeF_2	320.2995	320.0188	80.2304	-240.07	-0.28	-239.79	299.22	0.09	298.87
RnF_2	435.1973	415.1942	319.9638	-20.00	-20.00	-95.23	36.01	4.82	29.76
ArF_6	-931.4376	-926.9832	-910.8143	20.62	4.45	16.17	2.26	0.48	1.78
KrF_6	-297.9643	-302.2050	-289.0183	8.95	-4.24	13.19	3.10	1.40	4.56
XeF_6	-17.877	-18.6547	-3.1034	14.77	-0.78	15.55	476.05	4.17	501.11
RnF_6	47.1031	49.1327	45.7714	-1.33	2.03	-3.36	2.91	4.13	7.34

Table A.24: Four-Component calculation using *DIRAC*. Shown are the isotropic shielding of the heavy atoms. The Dirac-Coloumb Hamiltonian was used. The relativistic contribution was obtained by $Rel - NR$.

Molecule	**isotropic shielding**[ppm]		**rel. contribution**	**rel. contribution**
	NR	Rel	[ppm]	[%]
H_2O	325.8743	327.3762	1.50	0.46
H_2S	724.1133	731.3631	7.25	0.99
H_2Se	2120.0339	2323.4665	203.43	8.76
H_2Te	5253.3009	6478.1638	1224.86	18.91
NF_3	-175.7083	-173.8404	1.87	1.07
PF_3	210.8643	176.8363	-34.03	19.24
AsF_3	1059.7291	1050.3227	-9.41	0.90
HF	407.8568	410.8857	3.03	0.74
HCl	938.265	968.3777	30.11	3.11
HBr	3085.0332	3399.3599	314.33	9.25
HI	5395.8280	6695.1859	1299.36	19.41

Table A.25: Four-Component calculation using *DIRAC*. Shown are the isotropic shielding of the light atom. The Dirac-Coloumb Hamiltonian was used. The relativistic contribution was obtained by $Rel - NR$.

Molecule	**isotropic shielding**[ppm]		**rel. contribution**	**rel. contribution**
	NR	Rel	[ppm]	[%]
H_2O	31.0629	30.9534	-0.11	0.35
H_2S	30.8123	31.1795	0.37	1.18
H_2Se	30.2918	33.1297	2.84	8.57
H_2Te	65.5323	67.1055	1.57	2.34
NF_3	-0.1251	1.611	1.74	107.77
PF_3	187.6896	189.8779	2.19	1.15
AsF_3	175.2365	176.2265	0.99	0.56
HF	29.6001	29.4855	-0.11	0.39
HCl	31.2717	31.9126	0.64	2.01
HBr	71.2230	70.6295	-0.59	0.84
HI	67.3819	68.8383	1.46	2.12

A.6. HALA Effect

Table A.26: Calculated HALA contributions using the BSS Hamiltonian in *DIRAC* of the hydrogen compounds of the 13th-17th group. The isotropic shieldings of the hydrogens are shown. The full relativistic effect was obtained by $Rel - NR$, the ScR and SOC contribution by $ScR - NR$, $Rel - ScR$.

Molecule	**isotropic shielding [ppm]**			**relativistic contributions [ppm]**		
	NR	ScR	R	full relativistic	ScR	SOC
BH_3	23.064	23.0627	23.0249	-0.0391	-0.0013	-0.0378
AlH_3	25.7727	25.7772	25.4866	-0.2861	0.0045	-0.2906
GaH_3	24.4686	24.2985	22.4198	-2.0488	-0.1701	-1.8787
InH_3	24.9134	24.4555	18.4141	-6.4993	-0.4579	-6.0414
TlH_3	25.1488	23.6137	0.9446	-24.2042	-1.5351	-22.6691
CH_4	31.4017	31.3823	31.4072	0.0055	-0.0194	0.0249
SiH_4	27.8479	27.8428	27.8826	0.0347	-0.0051	0.0398
GeH_4	27.5982	27.4435	27.8059	0.2077	-0.1547	0.3624
SnH_4	27.4046	27.0185	27.4558	0.0512	-0.3861	0.4373
PbH_4	27.9645	26.6526	25.7624	-2.2021	-1.3119	-0.8902
NH_3	31.6498	31.6281	31.6785	0.0287	-0.0217	0.0504
PH_3	29.5526	29.563	29.8217	0.2691	0.0104	0.2587
AsH_3	28.9245	28.8852	30.1939	1.2694	-0.0393	1.3087
SbH_3	28.0717	27.9044	30.7524	2.6807	-0.1673	2.848
BiH_3	27.8268	27.3323	27.5744	-0.2524	-0.4945	0.2421
H_2O	31.0597	31.0401	31.0511	-0.0086	-0.0196	0.011
H_2S	30.8172	30.8345	31.4213	0.6041	0.0173	0.5868
HS_2e	30.3034	30.288	33.5066	3.2032	-0.0154	3.2186
H_2Te	29.7592	29.6371	38.4912	8.732	-0.1221	8.8541
H_2Po	30.0695	29.5611	41.2324	11.1629	-0.5084	11.6713
HF	29.6007	29.5783	29.778	0.1773	-0.0224	0.1997
HCl	31.2762	31.313	32.248	0.9718	0.0368	0.935
HBr	31.4423	31.4775	36.5937	5.1514	0.0352	5.1162
HI	31.8027	31.7578	46.2884	14.4857	-0.0449	14.5306
HAt	32.1752	31.8948	62.8412	30.666	-0.2804	30.9464

Table A.27: Calculated HALA contributions using the X2C Hamiltonian in *DIRAC* of the hydrogen compounds of the 13th-17th group. The isotropic shielding of the hydrogen is shown. The full relativistic effect was obtained by $Rel - NR$, the ScR and SOC contribution by $ScR - NR$, $Rel - ScR$.

Molecule	**isotropic shielding [ppm]**			**relativistic contributions [ppm]**		
	NR	ScR	R	full relativistic	ScR	SOC
BH_3	33.227	33.2375	33.2007	-0.0263	0.0105	-0.0368
AlH_3	34.6976	34.7984	34.6162	-0.0814	0.1008	-0.1822
GaH_3	37.3379	37.9148	36.7527	-0.5852	0.5769	-1.1621
InH_3	32.0916	33.6118	29.6204	-2.4712	1.5202	-3.9914
TlH_3	30.3628	35.0434	20.7878	-9.575	4.6806	-14.2556
CH_4	42.8216	42.826	42.7401	-0.0815	0.0044	-0.0859
SiH_4	34.2405	34.3066	34.6226	0.3821	0.0661	0.316
GeH_4	33.8787	34.1919	36.4581	2.5794	0.3132	2.2662
SnH_4	28.4043	29.1072	34.4166	6.0123	0.7029	5.3094
PbH_4	25.5488	27.6257	44.2169	18.6681	2.0769	16.5912
NH_3	44.1009	44.0947	44.045	-0.0559	-0.0062	-0.0497
PH_3	29.8646	29.7979	30.315	0.4504	-0.0667	0.5171
AsH_3	24.5775	24.013	27.4253	2.8478	-0.5645	3.4123
SbH_3	18.868	16.9822	25.7645	6.8965	-1.8858	8.7823
BiH_3	15.5728	9.8112	36.4411	20.8683	-5.7616	26.6299
H_2O	37.2368	37.2158	37.2061	-0.0307	-0.021	-0.0097
H_2S	32.0315	31.9736	32.3827	0.3512	-0.0579	0.4091
H_2Se	28.4408	28.0728	30.4979	2.0571	-0.368	2.4251
H_2Te	25.0528	23.8891	29.8377	4.7849	-1.1637	5.9486
H_2Po	22.4183	19.06	23.6959	1.2776	-3.3583	4.6359
HF	18.8062	18.7896	29.7936	10.9874	-0.0166	11.004
HCl	17.3234	17.298	17.0462	-0.2772	-0.0254	-0.2518
HBr	18.2922	18.1747	17.4132	-0.879	-0.1175	-0.7615
HI	20.091	19.8608	19.2629	-0.8281	-0.2302	-0.5979
HAt	19.965	19.4202	17.3613	-2.6037	-0.5448	-2.0589

Table A.28: HALA contributions of the hydrogen compounds of the 13th-17th group. Calculated by using the a-posteriori approach in *ORCA*. The isotropic shieldings of the hydrogen are shown. Note that ScR effects are neglected. The SOC contribution was obtained by the FC term.

Molecule	**isotropic shielding [ppm]**		**rel. contributions [ppm]**
	NR	NR+SOC	SOC
BH_3	23.107	23.060158	-0.046842
AlH_3	25.789	25.758452	-0.030548
GaH_3	24.508	25.569654	1.061654
InH_3	24.972	28.022112	3.050112
CH_4	31.703	32.356102	0.653102
SiH_4	27.878	27.57674	-0.30126
GeH_4	27.677	27.411587	-0.265413
SnH_4	27.473	26.97179	-0.50121
NH_3	31.818	31.98342	0.16542
PH_3	29.513	29.385308	-0.127692
AsH_3	28.935	28.8083952	-0.1266048
SbH_3	28.088	25.786258	-2.301742
H_2O	30.117	31.292636	1.175636
H_2S	31.388	30.517658	-0.870342
H_2Se	31.567	28.356012	-3.210988
H_2Te	31.855	23.388915	-8.466085
HF	30.117	30.041815	-0.075185
HCl	31.388	30.880428	-0.507572
HBr	31.567	28.410235	-3.156765
HI	31.855	22.088857	-9.766143

A.7. HALA Application

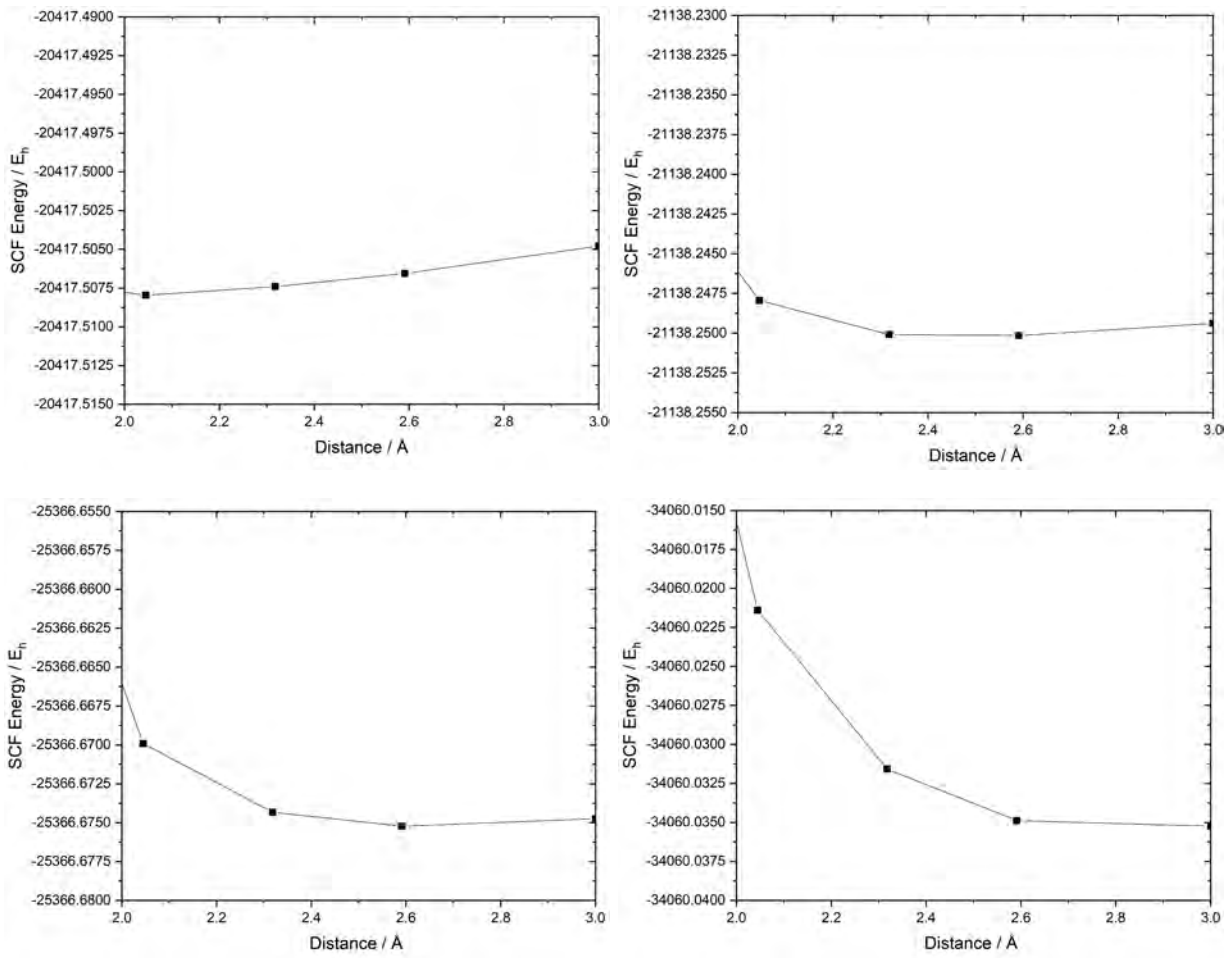

Figure A.6: Distance dependence of the SCF energy for different halides F (a), Cl (b), Br (c) and I (d). Illustrated are the SCF energies in Hartree of the systems.

Table A.29: Isotropic shieldings of the distance variation between H_2O and $MeBiX_2$. Shown for X = F, Cl, Br, I. The distances refers to the *-marked atoms.

		Distance [Å]					
Halide	**Atom**	1.5	1.636	2.045	2.318	2.591	3
F	Bi	4067.216	4089.739	4137.395	4156.491	4165.165	4168.344
	C	159.716	160.143	160.284	160.356	160.347	160.498
	H	30.712	30.742	30.749	30.768	30.788	30.771
	H	30.217	30.301	30.417	30.473	30.518	30.532
	H	30.254	30.287	30.362	30.386	30.394	30.410
	F	258.150	262.520	266.572	268.230	270.176	268.951
	F*	274.440	283.961	299.293	304.556	306.921	304.191
	O	250.735	259.855	274.597	281.379	287.668	290.641
	H	29.532	29.599	29.666	29.758	29.897	29.973
	H*	23.012	25.202	28.568	29.386	29.727	29.888
Cl	Bi	4010.013	4019.889	4003.481	4007.360	4011.849	4013.028
	C	155.534	156.726	157.460	157.693	157.681	157.657
	H	30.153	30.291	30.370	30.370	30.366	30.367
	H	30.120	30.139	30.249	30.322	30.366	30.401
	H	29.729	29.777	29.875	29.898	29.922	29.940
	Cl	686.599	726.141	767.151	744.265	778.038	782.515
	Cl*	705.671	740.263	795.188	813.718	825.258	832.603
	O	157.249	189.972	249.997	268.325	280.233	290.753
	H	28.267	28.791	29.547	29.731	29.853	29.992
	H*	14.917	18.498	25.762	27.913	29.019	29.697
Br	Bi	3669.145	3697.927	3852.002	3854.141	3856.909	3860.832
	C	156.932	157.175	156.549	156.380	156.433	156.386
	H	30.225	30.221	30.249	30.230	30.228	30.226
	H	30.052	29.998	30.096	30.200	30.254	30.312
	H	29.723	29.728	29.738	29.767	29.786	29.808
	Br	2263.810	2276.539	2211.875	2228.912	2242.016	2255.601
	Br*	2454.557	2379.857	2270.699	2313.831	2337.147	2365.001
	O	123.606	187.845	231.308	257.016	272.172	285.700
	H	28.206	29.470	29.331	29.625	29.799	29.980
	H*	21.283	22.198	24.417	27.083	28.530	29.519
I	Bi	3812.627	3830.015	3789.148	3793.590	3784.366	3785.569
	C	159.931	159.646	157.275	157.528	157.570	157.746
	H	30.195	30.196	30.164	30.190	30.213	30.216
	H	29.983	30.014	30.065	30.069	30.099	30.124
	H	29.618	29.621	28.164	28.263	28.235	28.406
	I	4130.688	4133.867	4118.357	4118.420	4124.056	4134.090
	I*	4451.691	4354.487	4128.106	4137.281	4152.306	4166.970
	O	4.203	85.418	220.262	259.757	280.568	299.804
	H	25.983	27.541	29.828	30.197	30.368	30.540
	H*	20.536	22.203	24.373	27.286	28.901	30.018

*Distance variation

A.8. Geometries

A.8.1. p-Block Geometries

BiF3

B	0.00000000	-0.00000000	0.00000000
F	0.00289295	-1.31591125	0.00000000
F	1.13816610	0.66046100	0.00000000
F	-1.14105905	0.65545026	0.00000000

AlF3

Al	0.00000000	0.00000000	0.00000000
F	1.57889829	-0.42306452	0.00000000
F	-0.42306452	1.57889829	0.00000000
F	-1.15583377	-1.15583377	0.00000000

GaF3

Ga	0.00000000	0.00000000	0.00000000
F	1.67525832	-0.44888411	0.00000000
F	-0.44888411	1.67525832	0.00000000
F	-1.22637420	-1.22637420	0.00000000

InF3

In	0.00000000	-0.00000000	0.00000000
F	0.03988030	-1.93220582	0.00000000
F	1.65339918	1.00064026	0.00000000
F	-1.69327948	0.93156556	0.00000000

TlF3

Tl	0.00000000	-0.00000000	-0.00000000
F	0.01295730	-2.01234265	0.00000000
F	1.73626120	1.01739268	0.00000000
F	-1.74921851	0.99494997	0.00000000

BH3

B	-0.00000000	-0.00000000	0.00000000
H	0.84134514	0.84134514	0.00000000
H	-1.14929883	0.30795369	0.00000000
H	0.30795369	-1.14929883	0.00000000

AlH3

Al	0.00000000	0.00000000	0.00000000
H	1.11787168	1.11787168	0.00000000
H	-1.52704112	0.40916943	0.00000000
H	0.40916943	-1.52704112	0.00000000

GaH3

Ga	0.00000000	0.00000000	0.00000000
H	1.11057972	1.11057972	0.00000000
H	-1.51708010	0.40650039	0.00000000
H	0.40650039	-1.51708010	0.00000000

InH3

In	-0.00000000	-0.00000000	0.00000000
H	1.22434620	1.22434620	0.00000000
H	-1.67248801	0.44814181	0.00000000
H	0.44814181	-1.67248801	0.00000000

TlH3

Tl	0.00000000	0.00000000	0.00000000
H	-1.59617785	0.71463924	0.00000000
H	0.17919319	-1.73965019	0.00000000
H	1.41698466	1.02501095	0.00000000

CH4

C	0.00000000	0.00000000	0.00000050
H	1.08954600	0.00000000	0.00000050
H	-0.36318100	-0.22433300	-1.00243950
H	-0.36318200	0.98030500	0.30693950
H	-0.36318300	-0.75597200	0.69549650

SiH4

Si	0.00000000	-0.00000006	0.00000000
H	1.48094400	-0.00000006	0.00000400
H	-0.49364300	-0.63083006	-1.24561800
H	-0.49364900	1.39414994	0.07649100
H	-0.49365200	-0.76331906	1.16912300

GeH4

Ge	0.00000017	-0.00000003	-0.00000003
H	1.53652617	0.00000197	-0.00000103
H	-0.51217583	-0.73698103	1.24717597
H	-0.51217783	-0.71159603	-1.26183203
H	-0.51217783	1.44857597	0.01465797

SnH4

Sn	0.00000002	-0.00000009	0.00000000
H	1.06620602	1.30081691	0.30534000
H	-1.59250898	0.59695391	-0.17237400
H	0.46909202	-0.79564609	-1.43842000
H	0.05721002	-1.10212009	1.30545400

PbH4

Pb	-0.00000005	-0.00000001	0.00000005
H	1.06247095	-0.73001901	1.19987805
H	-1.16041805	-1.19890201	-0.56350495
H	0.95867095	0.57417799	-1.36115895
H	-0.86072005	1.35474399	0.72478205

NF3

N	0.00000000	0.00000000	-0.48287777
F	0.87468896	0.87468896	0.12519053
F	-1.19484734	0.32015838	0.12519053
F	0.32015838	-1.19484734	0.12519053

PF3

P	-0.00000000	-0.00000000	-0.50318039
F	0.97167975	0.97167975	0.27954466
F	-1.32733922	0.35565947	0.27954466
F	0.35565947	-1.32733922	0.27954466

AsF3

As	-0.00000000	-0.00000000	-0.39897546
F	1.05038104	1.05038104	0.48763667
F	-1.43484718	0.38446614	0.48763667
F	0.38446614	-1.43484718	0.48763667

SbF3

Sb	-0.00000000	-0.00000000	-0.34512025
F	1.14600102	1.14600102	0.65189380
F	-1.56546651	0.41946549	0.65189380
F	0.41946549	-1.56546651	0.65189380

BiF3

Bi	-0.00000000	0.00000000	-0.25343619
F	1.21572319	1.21572319	0.77908161
F	-1.66070876	0.44498557	0.77908161
F	0.44498557	-1.66070876	0.77908161

NH3

N	0.00000000	0.00000000	-0.11172960
H	0.66677285	0.66677285	0.26070240
H	-0.91082865	0.24405580	0.26070240
H	0.24405580	-0.91082865	0.26070240

PH3

P	-0.00000000	-0.00000000	-0.12823605
H	0.84327353	0.84327353	0.64118027
H	-1.15193306	0.30865953	0.64118027
H	0.30865953	-1.15193306	0.64118027

AsH3

As	-0.00000000	0.00000000	-0.07075525
H	0.89640271	0.89640271	0.77830773
H	-1.22450887	0.32810616	0.77830773
H	0.32810616	-1.22450887	0.77830773

SbH3

Sb	0.00000000	-0.00000000	-0.05360270
H	1.00216723	1.00216723	0.91124596
H	-1.36898589	0.36681866	0.91124596
H	0.36681866	-1.36898589	0.91124596

BiH3

Bi	0.00000000	0.00000000	-0.03585773
H	1.04260515	1.04260515	0.99206376
H	-1.42422512	0.38161997	0.99206376
H	0.38161997	-1.42422512	0.99206376

NMe3

N	-0.00000000	0.00000000	-0.36456054
C	1.37561004	0.18843454	0.05926538
C	-0.85099411	1.09709597	0.05926538
C	-0.52461592	-1.28553051	0.05926538
H	-0.46286819	2.04006284	-0.33081081
H	-0.92263390	1.18745935	1.15935691
H	-1.86010606	0.95762541	-0.33349715
H	0.10072509	-2.08971181	-0.33349715
H	-1.53531215	-1.42088703	-0.33081081
H	-0.56705301	-1.39275407	1.15935691
H	1.99818034	-0.61917581	-0.33081081
H	1.48968691	0.20529472	1.15935691
H	1.75938096	1.13208639	-0.33349715

PMe3

P	0.00000000	0.00000000	-0.59622333
C	0.48348515	1.56161346	0.27650481
C	-1.59413950	-0.36209631	0.27650481
C	1.11065435	-1.19951715	0.27650481
H	-2.34688314	0.37021970	-0.02165119
H	-1.49202259	-0.33876974	1.36520345
H	-1.95648328	-1.34786053	-0.02146448
H	2.14552310	-1.02043396	-0.02146448
H	0.85282191	-2.21757027	-0.02165119
H	1.03939449	-1.12274460	1.36520345
H	1.49406124	1.84735057	-0.02165119
H	0.45262810	1.46151434	1.36520345
H	-0.18903982	2.36829449	-0.02146448

AsMe3

As	0.00000000	-0.00000000	-0.47274985
C	1.60479839	0.62164783	0.51985508
C	-1.34076201	1.07897226	0.51985508
C	-0.26403638	-1.70062009	0.51985508
H	-1.23331977	2.12778467	0.24151902
H	-1.21441431	0.97680209	1.59867518
H	-2.34232865	0.75021366	0.24092368
H	0.52146024	-2.40362295	0.24092368
H	-1.22605569	-2.13197859	0.24151902
H	-0.23872827	-1.54011469	1.59867518
H	2.45937546	0.00419392	0.24151902
H	1.45314258	0.56331260	1.59867518
H	1.82086842	1.65340929	0.24092368

SbMe3

Sb	0.00000000	0.00000000	-0.41806963
C	1.68375775	0.78804803	0.72726437
C	-1.52434849	1.06415297	0.72726437
C	-0.15940926	-1.85220100	0.72726437
H	-1.49451803	2.12413723	0.47474665
H	-1.34904475	0.94027164	1.79591862
H	-2.50926943	0.67240498	0.47293216
H	0.67231492	-2.50929356	0.47293216
H	-1.09229779	-2.35635919	0.47474665
H	-0.13977675	-1.63844285	1.79591862
H	2.58681582	0.23222197	0.47474665
H	1.48882151	0.69817120	1.79591862
H	1.83695451	1.83688858	0.47293216

BiMe3

Bi	0.00000000	0.00000000	-0.31741527
C	-1.87457025	0.44243407	0.91247137
C	0.55412598	-1.84464249	0.91247137
C	1.32044427	1.40220843	0.91247137
H	-0.13101680	-2.65547020	0.66758977
H	0.48331513	-1.60690600	1.97266347
H	1.57227635	-2.14433644	0.66674094
H	1.07091165	2.43379948	0.66674094
H	2.36521305	1.21427122	0.66758977
H	1.14996385	1.22201618	1.97266347
H	-2.23419625	1.44119898	0.66758977
H	-1.63327898	0.38488982	1.97266347
H	-2.64318800	-0.28946305	0.66674094

H2O

O	0.00000000	0.00000000	-0.11692647
H	0.76517934	0.00000000	0.46770588
H	-0.76517934	0.00000000	0.46770588

H2S

S	0.00000000	0.00000000	-0.10314543
H	0.97057123	0.00000000	0.82516344
H	-0.97057123	0.00000000	0.82516344

H2Se

Se	0.00000000	0.00000000	0.05712194
H	-1.05181900	0.00000000	-0.97107306
H	1.05181900	0.00000000	-0.97107306

H2Te

Te	0.00000000	0.00000000	0.04334615
H	-1.17972600	0.00000000	-1.12699985
H	1.17972600	0.00000000	-1.12699985

H2Po

Po	0.00000000	0.00000000	-0.02882794
H	-1.23543124	0.00000000	1.21077348
H	1.23543124	0.00000000	1.21077348

HF

F	0.00000000	0.00000000	-0.09247220
H	0.00000000	0.00000000	0.83224980

HCl

Cl	0.00000000	0.00000000	-0.07124189
H	0.00000000	0.00000000	1.21111211

HBr

Br	0.00000000	0.00000000	-0.03958967
H	0.00000000	0.00000000	1.38563833

HI

I	0.00000000	0.00000000	-0.02992500
H	0.00000000	0.00000000	1.58602500

HAt

At	0.00000000	0.00000000	-0.01985840
H	0.00000000	0.00000000	1.68796360

ArF2				XeF2			
Ar	0.00000000	0.00000000	0.00000000	Xe	0.00000000	0.00000000	0.00000000
F	0.00000000	0.00000000	1.80983800	F	0.00000000	0.00000000	2.00581900
F	0.00000000	0.00000000	-1.80983800	F	0.00000000	0.00000000	-2.00581900

KrF2				RnF2			
Kr	0.00000000	0.00000000	0.00000000	Rn	0.00000000	0.00000000	0.00000000
F	0.00000000	0.00000000	1.89679600	F	0.00000000	0.00000000	2.08571000
F	0.00000000	0.00000000	-1.89679600	F	0.00000000	0.00000000	-2.08571000

ArF4				XeF4			
Ar	0.00000000	0.00000000	0.00000000	Xe	0.00000000	0.00000000	0.00000000
F	-1.27343881	-1.27343881	0.00000000	F	-1.41736828	-1.35941707	0.00000000
F	1.27343881	1.27343881	0.00000000	F	1.41736828	1.35941707	0.00000000
F	-1.27343881	1.27343881	0.00000000	F	-1.35941707	1.41736828	0.00000000
F	1.27343881	-1.27343881	0.00000000	F	1.35941707	-1.41736828	0.00000000

KrF4				RnF4			
Kr	0.00000000	0.00000000	0.00000000	Rn	0.00000000	0.00000000	0.00000000
F	-1.86929654	-0.00846857	0.00000000	F	-1.43930270	-1.43930270	0.00000000
F	1.86929654	0.00846857	0.00000000	F	1.43930270	1.43930270	0.00000000
F	-0.00846857	1.86929654	0.00000000	F	-1.43930270	1.43930270	0.00000000
F	0.00846857	-1.86929654	0.00000000	F	1.43930270	-1.43930270	0.00000000

ArF6				KrF6			
Ar	0.00000000	0.00000000	0.00000000	Kr	0.00000000	0.00000000	0.00000000
F	0.43747065	-0.28487012	-1.73160495	F	0.14132741	0.21157010	-1.84467844
F	-0.43747065	0.28487012	1.73160495	F	-0.14132741	-0.21157010	1.84467844
F	-0.41461267	-1.75095785	0.18328104	F	-1.85647915	-0.01831115	-0.14432653
F	0.41461267	1.75095785	-0.18328104	F	1.85647915	0.01831115	0.14432653
F	1.70527762	-0.35263876	0.48878668	F	0.03453482	-1.85015956	-0.20951492
F	-1.70527762	0.35263876	-0.48878668	F	-0.03453482	1.85015956	0.20951492

XeF6

Xe	0.00000000	0.00000000	0.00000000
F	1.65412547	0.68198953	-0.76329046
F	-1.65412547	-0.68198953	0.76329046
F	-0.05545839	-1.38873682	-1.36095392
F	0.05545839	1.38873682	1.36095392
F	1.02207965	-1.17907969	1.16145731
F	-1.02207965	1.17907969	-1.16145731

RnF6

Rn	0.00000000	0.00000000	0.00000000
F	0.61108712	1.54143505	-1.11745377
F	-0.61108712	-1.54143505	1.11745377
F	0.48197380	-1.26071695	-1.47522755
F	-0.48197380	1.26071695	1.47522755
F	1.84187459	-0.18150995	0.75677391
F	-1.84187459	0.18150995	-0.75677391

A.8.2. Bismuth Compounds - Molecule model

Model F

C	-3.26329	-0.23548	3.03839
C	-2.03377	-0.00257	3.65684
H	-3.94462	-0.96605	3.45750
Bi	-1.53819	-1.07277	5.60905
C	-0.33377	-2.75495	4.69409
C	-0.46069	-3.14644	3.36092
F	-3.33304	-2.07754	5.49358
H	0.11373	-3.92119	2.99372
H	-1.12898	-2.66126	2.74204
H	0.34187	-3.25678	5.29133
H	-3.60805	0.51942	2.38367
H	-1.34668	0.74790	3.34759

Model Br

C	-3.28944	-0.20181	3.02482
C	-2.06086	-0.00112	3.65450
H	-3.99899	-0.91073	3.43360
Bi	-1.50221	-1.02792	5.63211
C	-0.31171	-2.72056	4.70644
C	-0.39463	-3.07262	3.35978
Br	-3.79054	-2.38505	5.86145
H	-3.64828	0.14119	2.00814
H	-1.31768	0.78299	3.33120
H	0.17255	-3.85372	2.99477
H	-1.02317	-2.55210	2.72810
H	0.32541	-3.25910	5.31395

Model Cl

C	-3.28678	-0.20733	3.02626
C	-2.05807	-0.00198	3.65430
H	-3.99181	-0.91999	3.43626
Bi	-1.51232	-1.03822	5.62677
C	-0.31656	-2.72724	4.70309
C	-0.41587	-3.09453	3.36151
H	-1.08004	-2.55965	2.69374
Cl	-3.67416	-2.30628	5.76333
H	0.13100	-3.69992	2.78420
H	0.40167	-2.97921	5.34361
H	-3.78034	0.14685	2.13789
H	-1.40503	0.85583	3.51582

Model I

C	-3.28409	-0.19124	3.04513
C	-2.05285	0.00880	3.67016
H	-3.99542	-0.89592	3.45839
Bi	-1.47010	-1.00272	5.65314
C	-0.30291	-2.71045	4.72076
C	-0.38293	-3.05087	3.37112
H	-1.02662	-2.49448	2.70101
I	-3.92685	-2.45945	6.03915
H	0.26062	-3.83021	3.12594
H	0.26711	-3.31695	5.33210
H	-3.53880	0.71151	2.49796
H	-1.23435	0.46967	3.35394

A.8.3. Bismuth Compounds - Distance model

F - 1.500 Å

Bi	-2.02682854505117	0.49732100420407	0.59055777353456
C	-3.72446848806117	-0.83595347544692	-0.04582523313005
H	-4.42399841055660	-0.95046799981436	0.79109790564748
H	-3.32520476963352	-1.80319489471662	-0.36696095725788
H	-4.21302931397283	-0.31439499712208	-0.87661928740417
F	-3.22872534974082	2.15545789793804	0.59937526753762
F	-1.42527882363815	0.83491214231794	-1.40412187533419
O	-0.40616672326917	-1.28436859400633	-0.79958632223302
H	0.55710660427206	-1.25780922771289	-0.68642947028067
H	-0.65763618034856	-0.45118185564082	-1.32234780107968

F - 1.636 Å

Bi	-2.04175375809965	0.52834433311234	0.57254091722878
C	-3.73112365336688	-0.82208309729721	-0.04851249103147
H	-4.39198943819303	-0.99147293301821	0.81062636687671
H	-3.31842835400803	-1.76887389609765	-0.41222313456870
H	-4.27202218239766	-0.29756112197580	-0.84356045002668
F	-3.25388766614414	2.17613163240731	0.61016550101746
F	-1.46165337310175	0.87551778901396	-1.41006364601005
O	-0.38125262398068	-1.30556630851854	-0.78199849532741
H	0.58167919242345	-1.28735397801721	-0.66544395362726
H	-0.60379814313153	-0.51676241960898	-1.35239061453136

2.045 ÅF

Bi	-2.04469182854884	0.60482162468641	0.53461039726884
C	-3.70165381311232	-0.80197209951742	-0.05384163080749
H	-4.39118006141649	-0.91170330149100	0.79209725057611
H	-3.28346769278765	-1.77123054140403	-0.34439538185583
H	-4.21483451643441	-0.32807773769136	-0.89790583555645
F	-3.37584481091174	2.14708215696434	0.75397180139457
F	-1.58182587425068	1.04692000093296	-1.43293967190578
O	-0.37152001609368	-1.33320384234375	-0.76290237795078
H	0.58777853378078	-1.37603187210007	-0.62168041105407
H	-0.49698992022484	-0.68628438803605	-1.48787414010911

F - 2.318 Å

Bi	-2.05935390002345	0.65901283177564	0.50548102274536
C	-3.69017306508495	-0.78632858094703	-0.06451524768791
H	-4.32531780407048	-0.96788931966920	0.81114529409311
H	-3.25171234429524	-1.72236602322406	-0.42562138096578
H	-4.26983959730542	-0.29358384462036	-0.85291128280096
F	-3.43329932278882	2.15216170443136	0.78952779943395
F	-1.65017093386709	1.14418383978079	-1.45385360492161
O	-0.35980348366879	-1.34591985188720	-0.72593873425274
H	0.59284010182259	-1.42584704024116	-0.55770691849164
H	-0.42739965071820	-0.82310371539874	-1.54646694715178

F - 2.591 Å

Bi	-2.07487798723632	0.70016528752304	0.48121898006410
C	-3.68877956069440	-0.77329908624851	-0.07058201459965
H	-4.27692627935786	-1.00699915317016	0.82540560390318
H	-3.23913098611928	-1.68253641913215	-0.48314991041703
H	-4.31910838527655	-0.27285995558776	-0.81382618700898
F	-3.46915466513404	2.16271252526390	0.82190196022090
F	-1.72571956972244	1.23323231753304	-1.47052264709651
O	-0.33838912954504	-1.34422644358375	-0.71026229155192
H	0.60035318998626	-1.47224541872465	-0.49950542540738
H	-0.34249662690016	-0.95362365387297	-1.60153806810670

F - 3.000 Å

Bi	-2.06193269413726	0.70896389287567	0.41624514379567
C	-3.69585688811556	-0.75893448478130	-0.09444016273510
H	-4.32512161798638	-0.90120199614853	0.79244333886566
H	-3.26270410003885	-1.71160009203406	-0.41768996380067
H	-4.27934492083178	-0.30125181995814	-0.90106785100217
F	-3.43686130147429	2.11638674319257	0.99836489796491
F	-1.90074852988562	1.36391755089232	-1.51789514279973
O	-0.28960607759322	-1.36708778280265	-0.70671725921664
H	0.64188202941498	-1.41229079610984	-0.43715001069128
H	-0.26393589935180	-1.14658121512601	-1.65295299038062

Cl - 1.500 Å

Bi	-2.08279548509163	0.78507204924120	0.52442502648335
C	-3.56399522990479	-0.75038580405731	-0.23410013417149
H	-4.35529300677700	-0.84695575829279	0.51732564847829
H	-3.04731445806346	-1.70353343028948	-0.39247866505323
H	-3.98170637241243	-0.37405046036623	-1.17355278870153
Cl	-3.93762251234466	2.31505942464922	1.25497279943071
Cl	-1.71299145135854	1.94855322177312	-1.78128739888466
O	-0.38360709256737	-0.17847356918507	-1.19089173548775
H	-0.61203658496273	-0.96497285143288	-1.71286702998906
H	-0.86359780651733	0.71707717796021	-1.67175572210462

Cl - 1.636 Å

C	-3.60111632363384	-0.72370289052280	-0.23186997719823
H	-4.29341063428205	-0.94189106105122	0.58936910655369
H	-3.05729421041494	-1.62370644913289	-0.53789420297217
H	-4.14549488373462	-0.28928282354964	-1.07642937168923
Cl	-3.98714999252546	2.33966236873621	1.25810539450978
Cl	-1.76745436301318	1.91686039910771	-1.79229661525450
O	-0.30194189558914	-0.19802372276056	-1.18857169017786
H	-0.47733706824527	-0.98546245443753	-1.72903526244740
H	-0.77686082395920	0.62073379731714	-1.66397634142286

Cl - 2.045 Å

Bi	-2.20336507922200	0.92128271598115	0.47025200317902
C	-3.64642919524239	-0.67944508673248	-0.23363414705878
H	-4.19622822934700	-1.04057724198082	0.64341658670387
H	-3.08578614001382	-1.49411464179112	-0.70413961942666
H	-4.33445105991695	-0.21417424608475	-0.94646965360764
Cl	-4.05733955197147	2.35562189037927	1.32580627736862
Cl	-1.94716955938814	1.98530360078444	-1.81292522179380
O	-0.19693330919606	-0.26308736854020	-1.17397168128986
H	-0.28309219752716	-1.08010245086766	-1.69140387792900
H	-0.59016567817491	0.45668282885217	-1.73714066614574

Cl - 2.318 Å

Bi	-2.23112312362336	0.96874412655053	0.43369302866798
C	-3.65981622591712	-0.65487796436118	-0.24663092810499
H	-4.09528063971770	-1.11637001603649	0.64748431694077
H	-3.11356149146379	-1.39598856002406	-0.83991883863566
H	-4.44132744035209	-0.17452330872654	-0.84346306076540
Cl	-4.08731568076533	2.35160926465079	1.36742249007459
Cl	-2.06247336512615	2.04928454193977	-1.83571958955814
O	-0.16875122757248	-0.29621313174595	-1.14233514601860
H	-0.21422240275693	-1.15201971815175	-1.59875298360500
H	-0.46708840270493	0.36774476590488	-1.80198928899553

Cl - 2.591 Å

Bi	-2.25122598495702	1.00939848680684	0.39610110007846
C	-3.66999011404239	-0.63309901867533	-0.26218922094553
H	-4.02769834218932	-1.15361164043318	0.63410866587197
H	-3.14145046499333	-1.32320382036279	-0.92872327684645
H	-4.50562931792087	-0.15270230838526	-0.78008046538412
Cl	-4.10010583859394	2.33686652290075	1.42460886524856
Cl	-2.18284513093377	2.11459235335304	-1.85516580859379
O	-0.15496690920719	-0.31645247897939	-1.12092796782977
H	-0.15037293162222	-1.21113894528192	-1.49813210551311
H	-0.35667496553978	0.27674084905722	-1.86980978608619

Cl - 3.000 Å

Bi	-2.27456608805308	1.06881104531395	0.34155888130437
C	-3.67071423234310	-0.60637854100145	-0.28290597011912
H	-3.96045513711939	-1.16573904211872	0.61453985643018
H	-3.15813672728562	-1.25642004523153	-1.00038401431712
H	-4.54899046627248	-0.13993486235625	-0.73917292182591
Cl	-4.11023208932716	2.30028150979951	1.50764237658047
Cl	-2.36351262337741	2.21454850239738	-1.87766847748903
O	-0.14541449088897	-0.34821915977618	-1.10616330104653
H	-0.13014958150395	-1.27895919093815	-1.38215442842274
H	-0.17878856382864	0.15939978391144	-1.93550200109453

Br - 1.500 Å

Bi	-2.75388256229314	0.95125092713076	0.92603791811509
C	-4.10383601365975	-0.70577412350315	0.16724112979875
H	-4.72393821212145	-1.05170990272461	1.00239734057022
H	-3.47310735897894	-1.51778172760229	-0.21222857210359
H	-4.72967584236777	-0.29625154969489	-0.63144343626591
Br	-4.68002406182059	2.71919602080879	1.12997572864269
Br	-1.77138296622959	1.49774365628485	-1.52416791037396
O	-0.21061445386752	0.81729491467831	-3.45622581294376
H	-0.79628639248773	0.75074700745803	-4.22913787803859
H	-0.86942213617350	1.01751477716419	-2.62227850740093

Br - 1.636 Å

Bi	-2.75243862308563	1.00712275543667	0.97257584893410
C	-3.98207021646627	-0.64889057485550	0.03090894578798
H	-4.62629406393171	-1.07886705475847	0.80701054985484
H	-3.29535455449102	-1.40414033906003	-0.36844219237542
H	-4.58459253642650	-0.21075922840978	-0.77010011699305
Br	-4.77246987841947	2.66163551545275	1.22414780484213
Br	-1.71761466090005	1.79772084063543	-1.36470769979895
O	-0.40639413195196	0.55674309103728	-3.33388563479008
H	-1.00714201196560	0.54560441743325	-4.09642960656928
H	-0.96779932236174	0.95606057708840	-2.55090789889223

Br - 2.045 Å

Bi	-2.33679535918441	0.90546419959899	0.23206959569328
C	-3.96588940324190	-0.43210999854858	-0.61004225194134
H	-4.30625522251570	-1.09071001256600	0.19786739362012
H	-3.55410633134687	-1.01486525240574	-1.44087670468430
H	-4.78626154804594	0.20749446702972	-0.94853245063820
Br	-4.01648545385217	2.12329153230274	1.88675156492279
Br	-2.38844717569502	2.63904866601909	-1.82983094571249
O	-0.69557489397196	0.21438566141571	-1.99166420330013
H	-0.90633840666106	-0.43490307830938	-2.68239333533558
H	-1.15601620548482	1.06513381546344	-2.26317866262407

Br - 2.318 Å

Bi	-2.37001782126092	0.96981540190568	0.21524162708683
C	-3.97765910563278	-0.40174176450121	-0.61671104074296
H	-4.17529580745600	-1.18221258041819	0.12772183432679
H	-3.61911788218364	-0.83857103352462	-1.55431200258357
H	-4.87599974038864	0.19973187903772	-0.78295709130241
Br	-4.04432921638370	2.12570473542747	1.92006620822664
Br	-2.50797932130033	2.70615740885264	-1.82312366195291
O	-0.65819039397939	0.16236893134443	-1.96707941818239
H	-0.83015481683050	-0.53967477917446	-2.61557942490256
H	-1.05342589458391	0.98065180105052	-2.35309702997338

Br - 2.591 Å

Bi	-2.39088255466988	1.02197969539250	0.19584806586250
C	-3.97981188379372	-0.37860975287158	-0.62602327775856
H	-4.13456349341571	-1.18337480845718	0.10239597359630
H	-3.63394396496142	-0.77991206246783	-1.58409004733417
H	-4.89948624838311	0.19955424580008	-0.75394329592391
Br	-4.04884597820504	2.08835172316163	1.97490796936941
Br	-2.62688705802878	2.78787905869783	-1.79570495297314
O	-0.64442143972223	0.13044831488461	-1.95768396758433
H	-0.79416517424587	-0.62036331976274	-2.55514913941041
H	-0.95916220457403	0.91627690562265	-2.45038732784360

Cl - 3.000 Å

Bi	-2.27456608805308	1.06881104531395	0.34155888130437
C	-3.67071423234310	-0.60637854100145	-0.28290597011912
H	-3.96045513711939	-1.16573904211872	0.61453985643018
H	-3.15813672728562	-1.25642004523153	-1.00038401431712
H	-4.54899046627248	-0.13993486235625	-0.73917292182591
Cl	-4.11023208932716	2.30028150979951	1.50764237658047
Cl	-2.36351262337741	2.21454850239738	-1.87766847748903
O	-0.14541449088897	-0.34821915977618	-1.10616330104653
H	-0.13014958150395	-1.27895919093815	-1.38215442842274
H	-0.17878856382864	0.15939978391144	-1.93550200109453

I - 1.500 Å

Bi	-2.87480682844902	1.18564061146883	0.92790029499103
C	-3.91579496025025	-0.73786067972955	0.29197857109604
H	-4.41266039688553	-1.15920814841139	1.17311137781603
H	-3.14439531252162	-1.41847237935676	-0.08656384922812
H	-4.64955106097536	-0.50407998908755	-0.48471146887324
I	-5.25032244496487	2.67985756527268	1.28562569074101
I	-2.09667892075602	1.91392329636869	-1.78912790783432
O	-1.82286338145988	1.53513420878938	-4.36359695285770
H	-2.30126758720785	2.28893842862702	-4.75003119234523
H	-2.07568910652951	1.58900708605865	-3.25336456350545

I - 1.636 Å

Bi	-2.87682534592164	1.18015854996361	0.95680047454749
C	-3.90933322869108	-0.73462638561762	0.28830223408487
H	-4.47163349396194	-1.12767029722727	1.14310217621918
H	-3.13477707591148	-1.44293588085549	-0.02772808417779
H	-4.58149652177399	-0.50169161309367	-0.54211063554468
I	-5.25853351639672	2.67674725443673	1.27397121272089
I	-2.03055021038914	1.90919611147020	-1.71050745270661
O	-1.86955113972157	1.53145294606109	-4.37229230577069
H	-2.35651003823635	2.28784412495326	-4.74219388803612
H	-2.05481942899597	1.59440518990913	-3.31612373133649

I - 2.045 Å

Bi	-2.85300985173850	1.20132267147980	0.93508328381414
C	-3.62408863457264	-0.52548294996391	-0.32085287701896
H	-4.57481805632445	-0.84780476474312	0.11840236601850
H	-2.87931929523110	-1.32967951523630	-0.27396566465820
H	-3.75377359964817	-0.17730425727751	-1.35262505970962
I	-5.18079807544844	2.78904277632703	0.65343107295409
I	-1.17053503480620	2.27615264705797	-1.12979367839974
O	-2.86720270954023	0.93040729621489	-3.27753805146387
H	-3.31963796914120	1.61253233118464	-3.79882359706311
H	-2.32084677354881	1.44369376495646	-2.60209779447312

I - 2.318 Å

Bi	-2.86058789044419	1.18345355326695	0.99702987929980
C	-3.61631454370434	-0.51046622282798	-0.31429205787932
H	-4.58193273455144	-0.82856075224009	0.09461715956764
H	-2.88278617305875	-1.32448130798329	-0.26204144627151
H	-3.71835561575384	-0.14816845701845	-1.34364866327212
I	-5.17050636979400	2.79584182151335	0.69421153711535
I	-1.10686609707436	2.31471179282215	-0.97128875777108
O	-2.89346553495102	0.89957193371967	-3.35636577734732
H	-3.34065393469431	1.57297257565570	-3.89295366781111
H	-2.37256110597342	1.41800506309193	-2.69404820563019

I - 2.591 Å

Bi	-2.88923390986420	1.17070094002200	1.05166136825483
C	-3.60989315963451	-0.48722441639655	-0.32160707002155
H	-4.56327401254702	-0.84614106175682	0.08306604000547
H	-2.85572376529362	-1.28361307314648	-0.30568842093549
H	-3.73174403071566	-0.09212306165578	-1.33641059779871
I	-5.17408289941297	2.81379337146368	0.70643149641973
I	-1.03628740833749	2.33793458016912	-0.79776189742567
O	-2.92633870173410	0.85637321616864	-3.40548551716243
H	-3.42528367866932	1.52686467853491	-3.89820852352760
H	-2.33216843379072	1.37631482659719	-2.82477687780845

I - 3.000 Å

Bi	-2.94302235114875	1.16099102298261	1.14043589834003
C	-3.57797980789217	-0.47594836309363	-0.29965365990977
H	-4.53786607263178	-0.86317730800093	0.06206764462725
H	-2.80899743250401	-1.25769389955835	-0.27236988184307
H	-3.67586538061616	-0.06661155648973	-1.31089877134888
I	-5.17085326873540	2.85037992042533	0.65256858145015
I	-0.91754955964614	2.28774554951263	-0.53329332271118
O	-3.00282956618720	0.84913775291163	-3.50680462690095
H	-3.54155953291731	1.50193970512621	-3.98082219719712
H	-2.36750702772060	1.38611717618414	-3.00000966450630

A.9. Inputfiles

A.9.1. Geometry optimization

NWChem

```
start nwchem
memory global 2400 mb stack 800 mb heap 100 mb noverify
charge 0
geometry units an
END

basis
END

ECP
END

dft
direct
mult 1
xc becke88 perdew86
grid fine
convergence energy 1d-10
decomp
end

task dft optimize
task dft freq
task dft energy
```

ORCA

```
! BP86 def2-TZVP tightscf grid7 opt freq

*xyz 0 1
*
```

A.9.2. Property Calculation - Comparison to *NWChem*

NWChem

```
start nwchem
memory global 2400 mb stack 800 mb heap 100 mb noverify
charge 0
geometry units an
END

basis spherical
END

dft
mult 1
xc becke88 perdew86
direct
grid treutler #GaussChebychev
Grid lebedev 14 #angulargrid
grid fine
tol2e 1d-10
convergence energy 1e-9
convergence density 1e-8
convergence gradient 1e-6
end

relativistic
zora on
end

task dft

property
shielding
end

task dft property
```

ORCA

```
! BP86 grid6 def2-TZVP NMR nofinalgrid conv

%method
RI off
end

%scf
TolE 1e-9
TolMaxP 1e-8
TolG 1e-6
end

%eprnmr
GIAO_1el = giao_1el_analytic
GIAO_2el = giao_2el_analytic
end

%basis
DelECP
NewGTO "Sapporo-TZP-2012" end
end

* xyz 0 1
*
```

A.9.3. Dirac - BSS

NR	ScR	Rela
**DIRAC	**DIRAC	**DIRAC
.WAVE FUNCTION	.WAVE FUNCTION	.WAVE FUNCTION
.PROPERTIES	.PROPERTIES	.PROPERTIES
**GENERAL	**MOLECULE	**MOLECULE
.CVALUE	*BASIS	*BASIS
2000	.DEFAULT	.DEFAULT
**MOLECULE	aug-cc-pVQZ	aug-cc-pVQZ
*BASIS	**INTEGRALS	**INTEGRALS
.DEFAULT	*READIN	*READIN
aug-cc-pVQZ	.UNCONTRACT	.UNCONTRACT
**INTEGRALS	**HAMILTONIAN	**HAMILTONIAN
*READIN	.SPINFREE	.BSS
.UNCONTRACT	.BSS	099
**HAMILTONIAN	109	.DFT
.BSS	.DFT	BP86
099	BP86	**WAVE FUNCTION
.DFT	**WAVE FUNCTION	.SCF
BP86	.SCF	**PROPERTIES
**WAVE FUNCTION	**PROPERTIES	.SHIELDING
.SCF	.SHIELDING	*NMR
**PROPERTIES	*NMR	.LONDON
.SHIELDING	.LONDON	**END OF
*NMR	**END OF	
.LONDON		
**END OF		

A.9.4. Dirac - X2C

NR

```
**DIRAC
.WAVE FUNCTION
.PROPERTIES
**WAVE FUNCTION
.SCF
*SCF
.MAXITR
200
**GENERAL
.CVALUE
2000
**MOLECULE
*BASIS
.DEFAULT
dyall.ae2z
**INTEGRALS
*READIN
.UNCONTRACT
**HAMILTONIAN
.X2C
.DFT
BP86
*AMFI
.MXITER
200
**Properties
.SHIELDING
*NMR
.LONDON
**END oF
```

ScR

```
**DIRAC
.WAVE FUNCTION
.PROPERTIES
**WAVE FUNCTION
.SCF
**MOLECULE
*BASIS
.DEFAULT
dyall.ae2z
**INTEGRALS
*READIN
.UNCONTRACT
**HAMILTONIAN
.X2C
.SPINFREE
.DFT
BP86
**Properties
.SHIELDING
*NMR
.LONDON
**END oF
```

Rela

```
**DIRAC
.WAVE FUNCTION
.PROPERTIES
**WAVE FUNCTION
.SCF
*SCF
.MAXITR
200
**MOLECULE
*BASIS
.DEFAULT
dyall.ae2z
**INTEGRALS
*READIN
.UNCONTRACT
**HAMILTONIAN
.X2C
.DFT
BP86
*AMFI
.MXITER
200
**Properties
.SHIELDING
*NMR
.LONDON
**END oF
```

A.9.5. Dirac - four-Component

SCF Calculation

```
**DIRAC
.WAVE FUNCTION
**MOLECULE
*BASIS
.DEFAULT
aug-cc-pVQZ
**INTEGRALS
*READIN
.UNCONTRACT
**HAMILTONIAN
.DFT
BP86
**WAVE FUNCTION
.SCF
*SCF
.CLOSED SHELL
18
**END OF
```

NMR Calculation

```
**DIRAC
.PROPERTIES
**GENERAL
.RKBIMP
**MOLECULE
*BASIS
.DEFAULT
aug-cc-pVQZ
**INTEGRALS
*READIN
.UNCONTRACT
**HAMILTONIAN
.URKBAL
.DFT
BP86
**WAVE FUNCTION
.SCF
*SCF
.CLOSED SHELL
18
**PROPERTIES
.SHIELDING
*NMR
.LONDON
**END OF
```

A.10. Derivations

A.10.1. Derivation of the CPHF formalism

The HF-energy ca be expressed as a sum of one-electron integrals H, two-electron integrals and the nuclear-repulsion energy $\mathcal{V}_{KK}$.

$$E^{HF} = \sum_{\mu\nu} P_{\mu\nu} H_{\mu\nu} + \frac{1}{2} \sum_{\lambda\sigma} P_{\sigma\lambda} (\mu\lambda||\nu\sigma) + \mathcal{V}_{KK} \tag{A.1}$$

The first derivative with respect to an arbitrary parameter x yields

$$\begin{aligned} \frac{\partial E^{HF}}{\partial x} &= \sum_{\mu\nu} P_{\mu\nu} \frac{\partial H_{\mu\nu}}{\partial x} + \frac{1}{2} \sum_{\mu\nu\lambda\sigma} P_{\mu\nu} P_{\lambda\omega} \frac{\partial}{\partial x} (\mu\lambda||\nu\sigma) \\ &+ \frac{\partial V_{nuc}}{\partial x} + \sum_{\mu\nu} \frac{\partial P_{\mu\nu}}{\partial x} H_{\mu\nu} + \sum_{\mu\nu\lambda\omega} \frac{\partial P_{\mu\nu}}{\partial x} P_{\lambda\sigma} (\mu\lambda||\nu\sigma) \end{aligned} \tag{A.2}$$

The last two terms (red) contain the derivative of the density matrix P which requires the derivative of the coefficients c. These terms have to be transformed into coefficient-free terms. By using the definition of the density matrix P (2.36) and the Fock matrix $F_{\mu\nu}$ (2.32), the transformation can be carry out and yields an expression (A.4) using the overlap matrix $\mathbf{S}$.

$$\sum_{\mu\nu} \frac{\partial P_{\mu\nu}}{\partial x} H_{\mu\nu} + \sum_{\mu\nu\lambda\sigma} \frac{\partial P_{\mu\nu}}{\partial x} (\mu\lambda||\nu\sigma) \tag{A.3}$$

$$= \sum_{\mu\nu\lambda\sigma} \sum_{j=1}^{N} \frac{\partial c^*_{\mu j}}{\partial x} c_{\nu j} \epsilon_j S_{\mu\nu} + \sum_{\mu\nu\lambda\sigma} \sum_{i=1}^{N} c^*_{\mu j} \frac{\partial c_{\nu j}}{\partial x} \epsilon_j S_{\mu\nu} \tag{A.4}$$

The complete transformation is shown below (A.10.2).

Using the fact that the rearranged Fock equation and its derivative is zero, the relation A.5 can be used.

$$\sum_{\mu\nu\lambda\sigma} \sum_{j=1}^{N} \frac{\partial c^*_{\mu j}}{\partial x} c_{\nu j} \epsilon_j S_{\mu\nu} + \sum_{\mu\nu\lambda\sigma} \sum_{j=1}^{N} c^*_{\mu j} \frac{\partial c_{\nu j}}{\partial x} \epsilon_j S_{\mu\nu} = - \sum_{\mu\nu} \sum_{j=1}^{n} c^*_{\mu j} \epsilon_j \frac{\partial S_{\mu\nu}}{\partial x} c_{\nu j} \tag{A.5}$$

Introducing the energy-weighted density matrix W

$$W_{\mu\nu} = \sum_j \epsilon_j c^*_{\mu j} c_{\nu j} \tag{A.6}$$

the complete transformation of the first derivative of the HF energy A.2 is resulting. The derivative of the coefficient is replaced by the derivative of the overlapping matrix S.

$$\begin{aligned}\frac{\partial E^{HF}}{\partial x} &= \sum_{\mu\nu} P_{\mu\nu} \frac{\partial H_{\mu\nu}}{\partial x} + \frac{1}{2} \sum_{\mu\nu\lambda\sigma} P_{\mu\nu} P_{\lambda\omega} \frac{\partial}{\partial x} (\mu\lambda||\nu\sigma) \\ &+ \frac{\partial V_{nuc}}{\partial x} - \sum_{\mu\nu} W_{\mu\nu} \frac{\partial S_{\mu\nu}}{\partial x}\end{aligned} \tag{A.7}$$

Based on the current result, the second derivative with respect to a second arbitrary parameter y of the HF energy ca be written as

$$\begin{aligned}\frac{\partial^2 E^{HF}}{\partial x \partial y} &= \sum_{\mu\nu} P_{\mu\nu} \frac{\partial^2 H_{\mu\nu}}{\partial x \partial y} + \frac{1}{2} \sum_{\mu\nu\lambda\sigma} P_{\mu\nu} P_{\lambda\omega} \frac{\partial^2}{\partial x \partial y} (\mu\lambda||\nu\sigma) \\ &+ \frac{\partial^2 V_{nuc}}{\partial x \partial y} - W_{\mu\nu} \frac{\partial^2 S_{\mu\nu}}{\partial x \partial y} \\ &+ \sum_{\mu\nu} \frac{\partial P_{\mu\nu}}{\partial y} \frac{\partial H_{\mu\nu}}{\partial x} + \frac{1}{2} \sum_{\mu\nu\lambda\sigma} \frac{\partial P_{\mu\nu}}{\partial y} P_{\lambda\omega} \frac{\partial}{\partial x} (\mu\lambda||\nu\sigma) \\ &- \frac{\partial W_{\mu\nu}}{\partial y} \frac{\partial S_{\mu\nu}}{\partial x}\end{aligned} \tag{A.8}$$

The first two lines contain the the second derivative of the Hamiltonian, which is easy to obtain. The last two lines include the derivative of the coefficients by P and W. Because of this it has to be calculated the perturbed wave function or rather a perturbed density. The perturbed HF equation by the perturbation y in matrix form can be written as

$$\mathbf{F}(y)\mathbf{C}(y) = \mathbf{S}(y)\mathbf{C}(y)\mathbf{E}(y) \tag{A.9}$$

It is still required that the spin orbitals are orthonormal in spite of a

perturbation, thus the condition can be formulated

$$(\mathbf{C}(y))^{\dagger}\mathbf{S}(y)\mathbf{C}(y) = \mathbf{1} \tag{A.10}$$

The perturbed coefficients $c(y)$ are transformed to a basis of the unperturbed spin orbitals. Note that greek letters imply unperturbed while roman letters define perturbed factors. In this case it is possible to write the perturbed coefficient $c(y)$ as the unperturbed coefficients C in basis of a transformation perturbation matrix U

$$c_{\mu p}(y) = \sum_{q} c_{\mu q} u_p(y) \tag{A.11a}$$

$$\text{in matrix form: } \mathbf{C}(y) = \mathbf{C}\mathbf{U}(y) \tag{A.11b}$$

The perturbed spin orbitals $\chi(y)$ expand in perturbed basis functions $\omega(y)$.

$$\chi_p(y) = \sum_{\mu} c_{\mu p}(y)\omega_{\mu}(y) = \sum_{\mu}\sum_{q} c_{\mu q} u_p(y)\omega_{\mu}(y) \tag{A.12}$$

Inserting (A.11b) into (A.9), multipying with the complex conjugate $C^{\dagger}$ from the left and use of the definitions

$$\tilde{\mathbf{F}}(y) = \mathbf{C}^{\dagger}\mathbf{F}(y)\mathbf{C} \tag{A.13}$$

$$\tilde{\mathbf{S}}(y) = \mathbf{C}^{\dagger}\mathbf{S}(y)\mathbf{C} \tag{A.14}$$

yields the perturbed Fock equation under elimination of the perturbed coefficients $\mathbf{C}(y)$.

$$\tilde{\mathbf{F}}(y)\mathbf{U}(y) = \tilde{\mathbf{S}}(y)\mathbf{U}(y)\mathbf{E}(y) \tag{A.15}$$

The various contributions are expanded in powers of the perturbation y

and are terminated after the first order.

$$\begin{aligned}\tilde{\mathbf{F}}(y) &= \mathbf{E} + y\tilde{\mathbf{F}}^{(1)} \\ \tilde{\mathbf{S}}(y) &= \mathbf{1} + y\tilde{\mathbf{S}}^{(1)} \\ \mathbf{U}(y) &= \mathbf{1} + y\mathbf{U}^{(1)} \\ \mathbf{E}(y) &= \mathbf{1} + y\mathbf{E}^{(1)}\end{aligned} \tag{A.16}$$

Note that the superscript index *(1)* denotes perturbation in first order and without superscript the zeroth order. Introducing the expansion (A.16) into (A.15) and the orthonormatily condition (A.17) of the perturbated overlap matrix the perturbed Fock equation can be written as in A.18 and A.19.

$$(\mathbf{U}(y))^{\dagger}\tilde{\mathbf{S}}(y)\mathbf{U}(y) = \mathbf{1} \tag{A.17}$$

$$\tilde{\mathbf{F}}^{(1)} + \mathbf{E}\mathbf{U}^{(1)} = \tilde{\mathbf{S}}^{(1)}\mathbf{E} + \mathbf{U}^{(1)}\mathbf{E} + \mathbf{E}^{(1)} \tag{A.18}$$

$$(\mathbf{U}^{(1)})^{\dagger} + \mathbf{U}^{(1)} + \tilde{\mathbf{S}}^{(1)} = 0 \tag{A.19}$$

The resulting expression of (A.18) and (A.19) can be spitted into diagonal and off-diagonal cases in matrix element formulation.

$$u_{pp}^{(1)} = -\frac{1}{2}\tilde{S}_{pp}^{(1)} \tag{A.20}$$

$$u_{pq}^{(1)} = \frac{\tilde{F}_{pq}^{(1)} - \tilde{S}_{pp}^{(1)}\epsilon_p}{\epsilon_p - \epsilon_q} \tag{A.21}$$

$$\text{with } \epsilon_p^{(1)} = \tilde{F}_{pp}^{(1)} - \tilde{S}_{pp}^{(1)}\epsilon_p \tag{A.22}$$

These equations are the central result of the CPHF-approach for solving the derivatives of W and P of A.8.

Now it is shown how exactly $\mathbf{U}$ is looks like. Therefore the perturbed first-order $\tilde{\mathbf{F}}^{(1)}$ and $\tilde{\mathbf{S}}^{(1)}$ must be further defined. The overlap matrix $\mathbf{S}$ is

handle easy with equation (A.14) and the condition of (A.16) it is possible to write

$$\begin{aligned} \tilde{S}^{(1)}_{qp} &= \sum_{\mu\nu} c^*_{\mu q} S^{(1)}_{\mu\nu} c_{\nu p} = \sum_{\mu\nu} c^*_{\mu q} \frac{\partial S^{(1)}_{\mu\nu}}{\partial y} c_{\nu p} \\ \text{in matrix form: } \tilde{\mathbf{S}}^{(1)} &= \mathbf{C}^\dagger \mathbf{S}^{(1)} \mathbf{C} \end{aligned} \tag{A.23}$$

However, the description of the first-order Fock matrix is more complex since $\tilde{\mathbf{F}}^{(1)}$ can be written as

$$\tilde{F}^{(1)}_{qp} = \tilde{H}^{(1)}_{qp} + \tilde{G}^{(1)}_{qp} \tag{A.24}$$

The Fock matrix contains the one-electron part $\tilde{\mathbf{H}}^{(1)}$ (A.25) and the first-order term of the two-electron part $\tilde{\mathbf{G}}^{(1)}$ (A.26).

$$\tilde{H}^{(1)}_{qp} = \sum_{\mu\nu} c^*_{\mu q} H^{(1)}_{\mu\nu} c_{\nu p} \tag{A.25}$$

$$\tilde{G}^{(1)}_{qp} = \sum_i \sum_{rs} u^*_{ri}(y) u_{si}(y) [(qr||ps)]^{trans}_y \tag{A.26}$$

$[(qr||ps)]^{trans}_y$ indicate, that this integral is transformed and a derivation in respect to y. Because of that the integral may be written as

$$[(qr||ps)]^{trans}_y = \sum_{\mu\nu\lambda\sigma} c^*_{\mu q} c^*_{\lambda r} c_{\nu p} c_{\sigma s} \Big((\mu\lambda||\nu\sigma) \Big)_{y=0} \tag{A.27}$$

This depends on y only through the original two-electron integral.[21] With A.26 and A.27 the first-order of the two-electron integral is

$$\begin{aligned} \tilde{G}^{(1)}_{qp} = \sum_i \sum_{rs} & [u^{(1)*}_{ri}(qr||pi) + u^{(1)}_{ri}(qi||pr)] \\ & + \sum_{\mu\nu\lambda\sigma} c^*_{\mu q} c_{\nu p} P_{\lambda\sigma} \Big((\mu\lambda||\nu\sigma) \Big)_{y=0} \end{aligned} \tag{A.28}$$

By collecting terms to compile the expression of the first-order Fock matrix (**??**), it is possible to split the sum over r in A.28 into an occupied

$(r = j)$ and virtual $(r = a = n + 1)$ part. The obtained occupied part can further simplified by using A.20 or rather A.19 to replace the transformations into overlap matrix elements S.

$$\tilde{F}_{ai}^{(1)} = \tilde{H}_{ai}^{(1)} + \sum_i \sum_j \Big(- \tilde{S}_{ji}^{(1)}(qj||pi)\Big) + \sum_i \sum_a [u_{ra}^{(1)*}(qa||pi) + u_{ra}^{(1)}(qi||pa)] + \sum_{\mu\nu\lambda\sigma} c_{\mu q}^* c_{\nu p} P_{\lambda\sigma}\Big((\mu\lambda||\nu\sigma)\Big)_{y=0} \tag{A.29}$$

Substituting A.29 into A.21 it is possible to write down the whole expression of the transformation perturbation matrix $\mathbf{U}$ as a product of the energy difference (A.30).

$$\begin{aligned}(\epsilon_i - \epsilon_a) \cdot U_{ai}^{(1)} = \tilde{H}_{ai}^{(1)} &+ \sum_i \sum_j \Big(- \tilde{S}_{ji}^{(1)}(qj||pi)\Big) \\ &+ \sum_i \sum_a [u_{ra}^{(1)*}(qa||pi) + u_{ra}^{(1)}(qi||pa)] \\ &+ \sum_{\mu\nu\lambda\sigma} c_{\mu q}^* c_{\nu p} P_{\lambda\sigma}\Big((\mu\lambda||\nu\sigma)\Big)_{y=0} \\ &- \tilde{S}_{ai}^{(1)} \epsilon_i\end{aligned} \tag{A.30}$$

This expression helps to determine the derivatives of $\mathbf{P}$ and $\mathbf{W}$. Similar to the unperturbed definition of $\mathbf{P}$ it is possible to formulate a perturbed density matrix $\tilde{\mathbf{P}}$ in the basis of the perturbed spin orbitals with the perturbed coefficients as

$$\tilde{P}_{rs}(y) = \sum_i u_{ri}^*(y) u_{si} y) \tag{A.31}$$

The same expansion as before into the first order in y and adding the relation A.20 yields

$$\tilde{P}_{rs}^{(1)} = u_{ri}^{(1)*}(y) + u_{si}^{(1)}(y) \tag{A.32}$$

With these it is possible to write down the derivation of the density matrix

as

$$\Big(\frac{\partial P_{\mu\nu}}{\partial y}\Big)_{y=0} = \sum_{rs}^{2N} \tilde{P}_{rs}^{(1)} c_{\mu r}^{*} c_{\nu s} \tag{A.33}$$

The same procedure to generate the derivation of $\mathbf{W}$ has to be done. As the unperturbed definition of $\mathbf{W}$ in A.6 it is possible to define a new perturbed $\mathbf{W}(y)$ in the basis of the perturbed coefficients $u(y)$ (A.34).

$$W_{\mu\nu}(y) = \sum_{i} \epsilon_i(y) u_{ri}^{*}(y) u_{si}(y) \tag{A.34}$$

Again an expansion in power of y until the first order and using of A.22 and A.21 yields the first order energy-weighted matrix $\tilde{\mathbf{W}}^{(1)}$ as a sum of the first order Fock $\tilde{F}_{ij}^{(1)}$ and overlap matrix $\tilde{S}_{ji}^{(1)}$.

$$\tilde{W}_{ij}^{(1)} = \tilde{F}_{ij}^{(1)} - (\epsilon_i - \epsilon_j)\tilde{S}_{ji}^{(1)} \tag{A.35}$$

With the first order energy-weighted matrix the derivation of the $\mathbf{W}$ can be written in the basis of the unperturbated coefficients.[21]

$$\Big(\frac{\partial W_{\mu\nu}}{\partial y}\Big)_{y=0} = \sum_{rs}^{2N} \tilde{W}_{rs}^{(1)} c_{\mu r}^{*} c_{\nu s} \tag{A.36}$$

A.10.2. Obtaining of equation A.4

Complete transformation of equation A.3 to A.4 in section A.10.1.

$$\begin{aligned}
\sum_{\mu\nu} \frac{\partial P_{\mu\nu}}{\partial x} H_{\mu\nu} + \sum_{\mu\nu\lambda\sigma} \frac{\partial P_{\mu\nu}}{\partial x} (\mu\lambda||\nu\sigma) \\
&= \sum_{\mu\nu} \sum_{i=1}^{n} \frac{\partial c^*_{\mu i}}{\partial x} H_{\mu\nu} c_{\nu i} + \sum_{\mu\nu\lambda\sigma} \sum_{i=1}^{n} \frac{\partial c^*_{\mu i}}{\partial x} c_{\nu i} (\mu\lambda||\nu\sigma) && \text{(A.37)} \\
&\quad + \sum_{\mu\nu} \sum_{i=1}^{n} c^*_{\mu i} H_{\mu\nu} \frac{c_{\nu i}}{\partial x} + \sum_{\mu\nu\lambda\sigma} \sum_{i=1}^{n} c^*_{\mu i} \frac{\partial c_{\nu i}}{\partial x} (\mu\lambda||\nu\sigma) \\
&= \sum_{\mu\nu\lambda\sigma} \sum_{i=1}^{n} \frac{\partial c^*_{\mu i}}{\partial x} c_{\nu i} F_{\mu\nu} + \sum_{\mu\nu\lambda\sigma} \sum_{i=1}^{n} c^*_{\mu i} \frac{\partial c_{\nu i}}{\partial x} F_{\mu\nu} && \text{(A.38)} \\
&= \sum_{\mu\nu\lambda\sigma} \sum_{i=1}^{n} \frac{\partial c^*_{\mu i}}{\partial x} c_{\nu i} \epsilon_i S_{\mu\nu} + \sum_{\mu\nu\lambda\sigma} \sum_{i=1}^{n} c^*_{\mu i} \frac{\partial c_{\nu i}}{\partial x} \epsilon_i S_{\mu\nu} && \text{(A.39)}
\end{aligned}$$

A.10.3. Derivation of the Pauli Hamiltonian

In the Pauli-Approximation the small component ψ^S is eliminated.[35] The starting point of this approach is rearranging of 2.89b to relate ψ^S to ψ^L by A.40

$$\begin{aligned}
\psi^S &= X \cdot \psi^L \\
with\ X &= \frac{c\vec{\sigma}\vec{p}}{E - V + 2mc^2}
\end{aligned} \tag{A.40}$$

Using the relation, the two-component eigenvalue equation of the large component is obtained (A.41).

$$(V + c\vec{\sigma}\vec{p}X)\Psi^L = E\Psi^L \tag{A.41}$$

The relation factor X is modified by some mathematics steps to obtain

$$X = \left(\frac{E - V + 2c^2}{c}\right)^{-1} \cdot \vec{\sigma}\vec{p} \tag{A.42}$$

First the fraction of X in A.40 is split and then extent by $2c$ to obtain

A.43.

$$\left(\frac{(E-V)2c}{2mc^2}+2c\right)^{-1}\cdot\vec{\sigma}\vec{p} \tag{A.43}$$

In the next step $(2c)^{-1}$ is excluded.

$$\frac{1}{2c}\cdot\left(\frac{(E-V)}{2mc^2}+1\right)^{-1}\cdot\vec{\sigma}\vec{p} \tag{A.44}$$

To simplyfy the obtained equation a geometric series is used and is subsequently truncates after the first two terms (k = 0, 1).[31] This is guilty for $|V-E|<1$.

$$\begin{aligned} X &= \frac{1}{2c^2}\cdot w\cdot\vec{\sigma}\vec{p} \\ \text{with } w = \left(1-\frac{(V-E)}{2mc^2}\right)^{-1} &= \sum_{k=0}\left(\frac{V-E}{2mc^2}\right)^k \end{aligned} \tag{A.45}$$

Carried out the transformations the two-component eigenvalue equation with the Pauli approximation (A.46) is obtained by including A.45 in A.41.

$$(V+\frac{1}{2mc^2}\cdot\left[c\vec{\sigma}\vec{p}\left(1+\frac{V-E}{2mc^2}\right)c\vec{\sigma}\vec{p}\right]\Psi^L = E\Psi^L \tag{A.46}$$

Note that the potential energy operator V is already completely preserved in (A.41). To obtain the kinetic energy operator, the expression in the square brackets with the prefactor must be further transformed. Therefore, it is first expanded and applied by the Dirac's relation[33], then the factor $\frac{1}{2c^2}$ is excluded to obtain

$$\frac{1}{2mc^2}\cdot\left[c\vec{\sigma}\vec{p}\left(1+\frac{V-E}{2mc^2}\right)c\vec{\sigma}\vec{p}\right] = \frac{\vec{p}^2}{2m}+\frac{\vec{\sigma}\vec{p}V\vec{\sigma}\vec{p}}{4m^2c^2}-\frac{Ep^2}{4m^2c^2} \tag{A.47}$$

The first part of is add to the Pauli Hamiltonian. The second part needs further simplifications. In the following steps the factor of $\frac{1}{4c^2}$ is neglected

and will be added later.

Using Dirac's relation it is obtained

$$\vec{\sigma}\vec{p}V\vec{\sigma}\vec{p} = \vec{p}V\vec{p} + i\vec{\sigma}\left(\vec{p}V \times \vec{p}\right) \tag{A.48}$$

The right term is added to the Pauli Hamiltonian with the previously neglected prefactor while the left term is transformed in further steps. The left term can alternatively be written as in equation A.49a. This is extended by zero, in this case it means concrete that $-\vec{p}^2 + \vec{p}^2$ is added to obtained equation A.49c.

$$\vec{p}V\vec{p} = \frac{1}{2} \cdot (\vec{p}V\vec{p} + \vec{p}V\vec{p}) \tag{A.49a}$$

$$= \frac{1}{2} \cdot \left((\vec{p}V)\vec{p} + V\vec{p}^2 + (\vec{p}V)\vec{p} + V\vec{p}^2\right) \tag{A.49b}$$

$$= \frac{1}{2} \cdot \left((\vec{p}V)\vec{p} + V\vec{p}^2 + (\vec{p}V)\vec{p} + V\vec{p}^2 - \vec{p}^2V + \vec{p}^2V\right) \tag{A.49c}$$

The term p^2V in A.49c is transformed in A.50, indicate by square brackets.

$$\begin{aligned}
&= \frac{1}{2} \cdot \left((\vec{p}V)\vec{p} + V\vec{p}^2 + (\vec{p}V)\vec{p} + V\vec{p}^2 - \vec{p}^2V + [\vec{p}\vec{p}V]\right) \\
&= \frac{1}{2} \cdot \left((\vec{p}V)\vec{p} + V\vec{p}^2 + (\vec{p}V)\vec{p} + V\vec{p}^2 - \vec{p}^2V + [\vec{p}(\vec{p}V) + \vec{p}(V\vec{p})]\right) \\
&= \frac{1}{2} \cdot \left((\vec{p}V)\vec{p} + V\vec{p}^2 + (\vec{p}V)\vec{p} + V\vec{p}^2 - \vec{p}^2V + \left[\vec{p}^2V + 2(\vec{p}V)\vec{p} + V\vec{p}^2\right]\right) \\
&= \frac{1}{2} \cdot \left(V\vec{p}^2 + \vec{p}^2V - \vec{p}^2V\right)
\end{aligned} \tag{A.50}$$

In the resulting expression $\vec{p}^2$ is replaced by the Laplace operator Δ shown in atomic units in A.51.

$$\vec{p}^2 = \vec{p}\vec{p} = (-i\vec{\nabla})(-i\vec{\nabla}) = -\vec{\nabla}^2 = -\Delta \tag{A.51}$$

Add A.51 to A.50 results

$$\frac{1}{2} \cdot \left(V\vec{p}^2 + \vec{p}^2 V\right) + \frac{1}{2}\Delta V \tag{A.52}$$

The right term is multiplied by the previously neglected prefactor and added to the Pauli Hamiltonian. The left term is further transformed with the non-relativistic Schrödinger equation for hydrogen like orbitals (A.53).

$$(V + \frac{\vec{p}^2}{2m})\Psi^{NR} = E^{NR}\Psi^{NR} \tag{A.53}$$

Rearranged to V and adding of the anticommutator relation (left term in A.52) yields

$$\frac{1}{2} \cdot \left(V\vec{p}^2 + \vec{p}^2 V\right) = \frac{1}{2} \cdot \left([E^{NR} - \frac{\vec{p}^2}{2m}] \cdot \vec{p}^2 + \vec{p}^2 \cdot [E^{NR} - \frac{\vec{p}^2}{2m}]\right) \tag{A.54a}$$

$$= E^{NR}\vec{p}^2 - \frac{\vec{p}^4}{2m} \tag{A.54b}$$

The right term of A.54b is multiplied by the neglected factor and added to the Pauli Hamiltonian.

A.10.4. mathematics step to obtain 2.104 for the ZORA derivation

The rewriting of the relation between the small and large component starts with the known relation shown in 2.90. First the prefactor is written into the fraction and multiplied out.

$$X_{new} = \frac{1}{2c \cdot [\frac{E-V}{2c^2} + 1]} \cdot \vec{\sigma}\vec{p} \tag{A.55}$$

Next c is excluded and extended by $2c^2$.

$$X_{new} = c \cdot \left[\frac{1}{E - V + 2c^2}\right] \cdot \vec{\sigma}\vec{p} \tag{A.56}$$

Now each Term in the brackets is divided by E.

$$X_{new} = c \cdot \Big[\frac{1}{E + E \cdot (\frac{2c^2 - V}{E})}\Big] \cdot \vec{\sigma}\vec{p} \tag{A.57}$$

Finally $\frac{1}{2c^2-V}$ is pulled out and the reciprocal value is formed in the square bracktes.

$$\begin{aligned} X_{new} &= \frac{c}{2c^2 - V} \cdot \Big[\frac{E + E \cdot (\frac{2c^2 - V}{E})}{2c^2 - V}\Big]^{-1} \cdot \vec{\sigma}\vec{p} \\ &= \frac{c}{2c^2 - V} \cdot \Big[1 + \frac{E}{2c^2 - V}\Big]^{-1} \cdot \vec{\sigma}\vec{p} \end{aligned} \tag{A.58}$$